Reviews

Proton Conductivity: Materials and Applications

Klaus-Dieter Kreuer

Max-Planck-Institut für Festkörperforschung, Heisenbergstrasse 1, D-70569 Stuttgart, Germany

Received April 28, 1995. Revised Manuscript Received January 19, 1996[⊗]

In this review the phenomenon of proton conductivity in materials and the elements of proton conduction mechanisms—proton transfer, structural reorganization and diffusional motion of extended moieties—are discussed with special emphasis on proton chemistry. This is characterized by a strong proton localization within the valence electron density of electronegative species (e.g., oxygen, nitrogen) and self-localization effects due to solvent interactions which allows for significant proton diffusivities only when assisted by the dynamics of the proton environment in Grotthuss and vehicle type mechanisms. In systems with high proton density, proton/proton interactions lead to proton ordering below first-order phase transition rather than to coherent proton transfers along extended hydrogen-bond chains as is frequently suggested in textbooks of physical chemistry. There is no indication for significant proton tunneling in fast proton conduction phenomena for which almost barrierless proton transfer is suggested to occur. Models of proton conductivity are applied to specific compounds comprising oxides, phosphates, sulfates, and water-containing systems. The importance of proton conductivity is emphasized for biological systems and in devices such as fuel cells, electrochemical sensors, electrochemical reactors, and electrochromic devices.

1. Introduction

Proton conductivity plays a key role in important processes as diverse as the photosynthesis in green plants and the production of electricity in a hydrogen fuel cell. Consequently, proton-transport and -transfer phenomena have been studied extensively from rather different points of view by material scientists, chemists, physicists, and biologists. Unfortunately, the abundant data are rather heterogeneous, and the current understanding of the underlying elementary steps including their mutual interdependence is still in its infancy.

It is beyond the scope of this review to address all systems for which proton conductivity has been reported. The interested reader may be referred to a number of general articles and reviews[1−18] and, in particular, to a comprehensive book edited by Colomban.[19] It is the aim of this article to present a detailed introduction into the main aspects of proton conductivity for all those with a scientific or engineering background. A selection of experimental findings that have not been discussed in the same context up to now help to illuminate various general aspects of proton-conduction phenomena.

After a brief introduction to some specific features of the proton chemistry in condensed matter (section 2), typical members of the families of compounds that have attracted major attention will be addressed (section 4). In section 4, common aspects of models on proton conductivity in condensed matter will be outlined before applying them to some specific compounds in section 5. Finally, recent technological applications of proton-conducting materials are summarized (section 6). This discussion generally refers to selected publications, in which references to further reading may be found. Some recent, as yet unpublished, work is also included.

For the experimental techniques which are of particular interest for the characterization of proton conductors (e.g., dielectric spectroscopy, neutron scattering, NMR techniques) the reader is referred to the corresponding chapters in ref 19.

[⊗] Abstract published in *Advance ACS Abstracts,* February 15, 1996.

(1) Nagle, J. F. *NATO ASI Ser. B* **1994**, *291*, 17.
(2) Kreuer, K. D.; Dippel, Th.; Hainovsky, N. G.; Maier, J. *Ber. Bunsen-Ges. Phys. Chem.* **1992**, *96*, 1736.
(3) Clearfield, A. *Solid State Ionics* **1991**, *46*, 35.
(4) Chandra, S. In *Superionic Solid Electrolytes*; Laskar, A., Chandra, S., Eds.; Academic Press: Boston, 1990; p 185.
(5) Goodenough, J. B. *NATO ASI Ser. B* **1990**, *217*, 195.
(6) Kreuer, K. D. *J. Mol. Struct.* **1988**, *177*, 265.
(7) Colomban, Ph.; Novak, A. *J. Mol. Struct.* **1988**, *177*, 277.
(8) Poulsen, F. W. In *High Conductivity Solid Ionic Conductors*; Takahashi, T., Ed.; World Publishing Co.: Singapore, 1988; p 166.
(9) Potier, A. *Opt. Pura Apl.* **1988**, *21*, 7.
(10) Goodenough, J. B. *Methods Enzymol.* **1986**, *127*, 263.
(11) Chandra, S.; Singh, N.; Hashmi, S. H. *Proc. Indian Natl. Sci. Acad.* **1986**, *52A*, 338.
(12) Wheat, T. A.; Ahmad, A.; Kuriakase, A. K.; Canaday, J. D. *J. Can. Ceram. Soc.* **1985**, 54, 32.
(13) Chandra, C. *Mater. Sci. Forum* **1984**, *1*, 153.
(14) Ernsberger, F. M. *J. Am. Ceram. Soc.* **1983**, *66*, 747.
(15) Jensen, J., Kleitz, M., Eds. *Solid State Protonic Conductors for Fuel Cells and Sensors*; Odense University Press: Odense, 1982; p 339.
(16) England, W. A.; Cross, M. G.; Hamnett, A.; Wiseman, P. J.; Goodenough, J. B. *Solid State Ionics* **1980**, *1*, 231.
(17) Glasser, L. *Chem. Rev.* **1975**, *75*, 21.
(18) Bruinink, J. *J. Appl. Electrochem.* **1972**, *2*, 33.
(19) Colomban, Ph., Ed.; *Proton Conductors: Solids, membranes and gels—materials and devices*; Cambridge University Press: Cambridge, 1992.

0897-4756/96/2808-0610$12.00/0

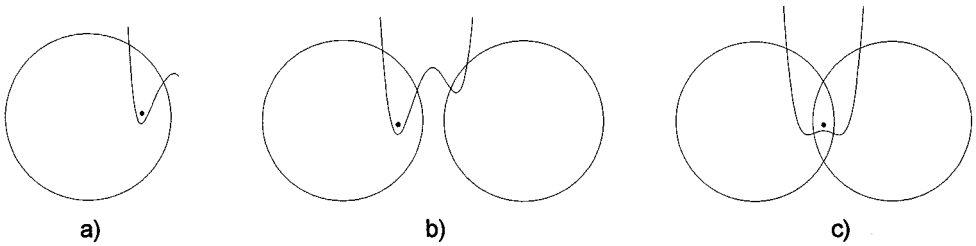

Figure 1. Schematic representation of different cases of proton binding in a nonmetallic environment where the proton is coordinated to one or two preferentially basic species. Note that the given potential surfaces correspond to the electronic structure of the indicated proton positions. They do not reflect the potential of adiabatic proton transfer which is accompanied by an electronic relaxation (see Figure 9).

All considerations are restricted to proton-transport phenomena close to thermodynamic equilibrium. Irreversible proton transport in high electrochemical potential gradients or in electronically excited states of the proton host, which are relevant in many biochemical reactions, has been omitted.

Any detailed mathematical treatment is avoided in this review. This may be found in the given references.

2. Some Remarks on Proton Chemistry and Proton Conduction Mechanisms

The proton is the only ion which has no electron shell of its own. Therefore, it strongly interacts with the electron density of its environment, which then takes on some H1s character (e.g., refs 5 and 10).

In metals this environment is the delocalized electron density of the conduction band, where the proton is considered to be a part of a hydrogen with some protonic or hydridic character depending on whether the energy of the H1s state is higher or lower than the Fermi energy of the pure metal. Only in metals may the "proton" (hydrogen) have a high coordination number, typically four or six on a tetrahedral or octahedral site (e.g., refs 2 and 6).

In nonmetallic compounds, however, the proton strongly interacts with the valence electron density of only one or two nearest neighbors. If this is a single oxygen, being well separated from other electronegative species, this results in the formation of an O−H bond which is less than 100 pm in length compared to ∼140 pm for the ionic "radius" of the oxide ion. The proton finds its equilibrium position deeply embedded in the valence electron density of the oxygen (Figure 1a). For medium distances of the oxygen from, e.g., another oxygen (∼250−280 pm), the proton may be involved in two bonds: a short, strong bond with the so-called proton donor and a longer, weak bond with a proton acceptor. This is the case of an asymmetrical hydrogen bond (O−H···O) which is directional in character (Figure 1b). For very short oxygen separations (∼240 pm) even a symmetrical hydrogen bond may be formed, i.e., the proton is involved in two equivalent bonds (Figure 1c). For details the reader is referred to the classical monograph on hydrogen bonding edited by Schuster, Zundel, and Sandorfy.[20]

It is interesting to note that electronically conducting oxides as a host for protons seem to represent a transition between these limiting cases of proton bonding. Whereas the proton forms a hydroxyl ion with one oxygen in electronically insulating oxides, the presence of a high concentration of conduction electrons leads to a breaking of the OH bond as indicated by the disappearance of the OH stretching vibration measured by inelastic neutron-scattering experiments.[21,22]

We focus herein on compounds with a low concentration of electronic charge carriers, where the proton is well confined within the valence electron density of either one species (in most cases oxygen or nitrogen) or the electron density of a hydrogen bond between two electronegative species.

For a rigid array of host species this restriction allows some local motion but no significant translational motion (diffusion) of protons, which may lead to proton conductivity. In the late 1960s, however, Fischer, Hofacker, and Rathner recognized that proton−phonon coupling may assist proton diffusivity,[22a−d] i.e., the dynamics of the proton environment is involved in proton conductivity. Two principal mechanisms describe proton diffusion in such a way that the proton remains shielded by some electron density along the entire diffusion path, i.e., not even the momentary existence of a free proton is required.

The most trivial case is the assistance of proton migration by the translational dynamics of bigger species (vehicle mechanism[23]). The proton diffuses together with a vehicle (e.g., as H_3O^+) where the counterdiffusion of unprotonated vehicles (e.g., H_2O) allows the net transport of protons. The relevant rate for the observed conductivity is that of the vehicle (molecular) diffusion Γ_D (Figure 2).

In the other principal case the "vehicles" show pronounced local dynamics but reside on their sites, the protons being transferred within hydrogen bonds from one "vehicle" to the other. Additional reorganization of the proton environment, which comprises, e.g., reorientation of individual species or even more extended ensembles, then results in the formation of an uninterrupted trajectory for proton migration. This mechanism is frequently termed the Grotthuss mechanism[24] in

(20) Schuster, P., Zundel, G., Sandorfy, C., Eds.; *The Hydrogen Bond*; North-Holland: Amsterdam, 1976.
(21) Fillaux, F.; Ouboumour, H.; Tomkinson, J.; Yu, L. T. *Chem. Phys.* **1991**, *149*, 459.
(22) Fillaux, F.; Ouboumour, H.; Cachet, C. H.; Tomkinson, J.; Levy-Clement, C.; Yu, L. T. *J. Electrochem. Soc.* **1983**, 140, 592. (a) Fischer, S. F.; Hofacker, G. L.; Rathner, M. A. *J. Chem. Phys.* **1970**, *52*, 1934. (b) Sabin, J. R.; Fischer, S. F.; Hofacker, G. L. *Int. J. Quantum Chem.* **1969**, *3* (Pt. 1), 257. (c) Fischer, S. F.; Hofacker, G. L. *Phys. Ice, Proc. Int. Symp.* **1969**, *369*. (d) Fischer, S. F.; Hofacker, G. L.; Sabin, J. R. *Phys. Kondens. Mater.* **1969**, *8*, 268.
(23) Kreuer, K. D.; Weppner, W.; Rabenau, A. *Angew. Chem., Int. Ed. Engl.* **1982**, 21, 208.
(24) van Grotthuss, C. J. D. *Ann. Chim.* **1806**, *58*, 54.
(25) Campbell, A. N.; Ross, L. *Can. J. Chem.* **1956**, *34*, 566.
(26) Haase, R.; Sauermann, P. F.; Dücker, K. H. *Z. Phys. Chem. N.F.* **1965**, *47*, 224.
(27) Dippel, Th.; Kreuer, K. D. *Solid State Ionics* **1991**, *46*, 3.
(28) Tuckermann, M.; Laasonen, L.; Sprik, M.; Parrinello, M. *J. Phys. Codens. Matter* **1994**, *6* (Supl. 23A), A99.

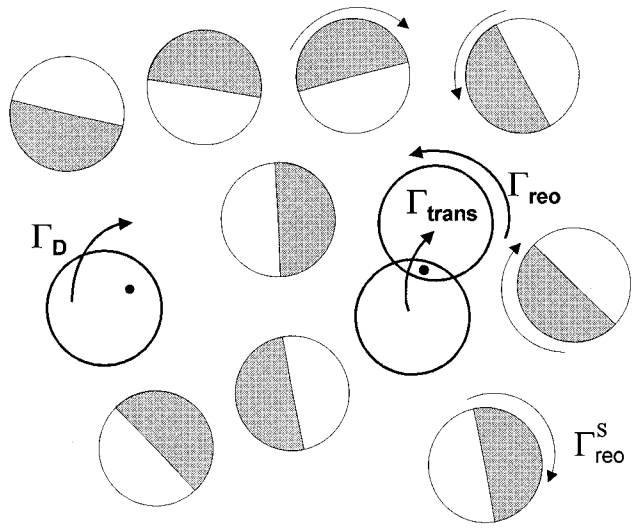

Figure 2. Schematic illustration of the modes involved in proton conduction phenomena. The species being a physical part of the proton diffusion trajectory are set off with respect to those which only accompany the primary steps of proton diffusion. In real systems, full frequency-dependent excitation and relaxation processes of complex structures have to be considered.

textbooks of electrochemistry or structure diffusion in order to indicate that the reorganization of the structural pattern is an inherent part of the proton diffusion path. The reorganization is frequently established by the reorientation of solvent dipoles (e.g., H_2O) which is thus part of the proton diffusion trajectory. The relevant rates for this mechanism are the ones of proton transfer Γ_{trans} and reorganization of its environment Γ_{reo}. All rates directly connected with the diffusion of protons (Γ_D, Γ_{trans}, Γ_{reo}) are schematically illustrated in Figure 2. It also shows the reorganization of the solvent (Γ^S_{reo}), which is not a physical part of the proton diffusion trajectory but accompanies the primary steps of proton diffusion. In many cases Grotthuss-type mechanisms are progressively dominated by vehicle-type mechanisms with increasing temperature. The parameters controlling the relevant rates for both proton conduction mechanisms will be discussed in section 4.

3. Compounds

It is the purpose of this section to give a survey of the proton-conducting compounds which have gained a major interest. They are separated into four families which represent the majority of all known fast proton conductors. Figures show the proton conductivities of some typical compounds and tables give access to the available literature. The citations are chosen in such a way that the reader finds a great part of the literature on proton conductivity as references therein.

3.1. Water-Containing Systems. As a consequence of the early interest in the physical chemistry of aqueous solutions, the high equivalent conductivity of excess protons in this environment had already been recognized in the past century. Since then proton conductivity in solid water, i.e., ice, has occasionally been studied. But neither pure nor doped ice has been found to be good proton conductors (Figure 3).

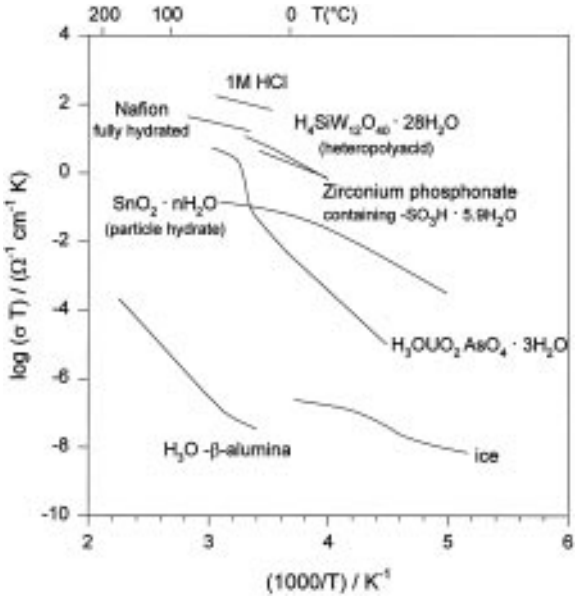

Figure 3. Proton conductivity of some representative water containing compounds. For references see Table 1.

The need for cation-conducting separator materials for the industrial chlor/alkali electrolysis stimulated the development of chemically resistant cation-exchange membranes in the late 1960s. These membranes are also good proton conductors in their hydrated protonic form. The polymer NAFION, having a perfluorinated backbone and side chains terminated by strongly acidic $-SO_3H$ groups

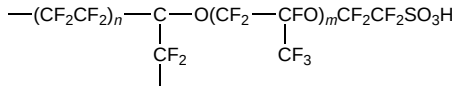

is still one of the technologically most attractive membrane materials and is commercialized by the company DuPont de Nemour.

With the rapidly increasing interest in fast ion-conducting phenomena in solids there had also been an increasing search for solid proton conductors in the early 1970s. Again, water containing compounds, i.e., hydrates, were the first known solid proton conductors. The layered compound $H_3OUO_2XO_4 \cdot 3H_2O$ (X = P (HUP), X = As (HUAs)), in which fast proton conductivity was first confirmed by Shilton and Howe in 1976 served as a model compound for proton conductivity in acidic hydrates for many research groups. Thus a comprehensive set of data on transport, local dynamics, structure, and thermodynamics is available in the literature. The high proton conductivity is observed above a phase transition (Figure 3) within the water layer of the structure which also contains the excess protons.

(29) Tuckermann, M.; Laasonen, L.; Sprik, M.; Parrinello, M. *J. Chem. Phys.*, in press.
(30) van Hippel, A. *J. Chem. Phys.* **1971**, *54*, 134.
(31) van Hippel, A. *J. Chem. Phys.* **1971**, 54, 145.
(32) Maidique, M. A.; von Hippel, A.; Westphal, W. B. *J. Chem. Phys.* **1971**, *54*, 150.
(33) Petrenko, V. F.; Maeno, N. *J. Phys.* **1987**, *48C*, 1.
(34) Fletcher, N. H. *The Chemical Physics of Ice*; Cambridge University Press: Cambridge, 1970.
(35) Ryzhkin, I. A. In ref 19, p 158.
(36) van Hippel, A.; Farrell, E. F. *Mater. Res. Bull.* **1973**, *8*, 127.
(37) Hobbs, P. V. *Ice Physics*; Clarendon Press: Oxford, 1974.
(38) Colomban, Ph.; Novak, A. In ref 19, p 254.
(39) Howe, A. T.; Shilton, M. G. *Mater. Res. Bull.* **1977**, *12*, 701.
(40) Howe, A. T.; Shilton, M. G. *J. Solid State Chem.* **1979**, *28*, 345; **1980**, *31*, 393; **1980**, *34*, 137; **1980**, *34*, 149; **1980**, *34*, 341; **1981**, *37*, 37.
(41) Mercier, R.; Pham-Thi, M.; Colomban, Ph. *Solid State Ionics* **1985**, *15*, 113.

Table 1. References to Water-Containing Proton Conductors

	transport and dynamics	structure and thermodynamics
acidic aqueous solution	25−29	28, 29
ice	30−35	36, 37
$H_3OUO_2XO_4 \cdot 3H_2O$ (X = P, As)	38−45	46−49
acidic phosphates and phosphonates	50−56	50, 57
heteropolyacids	58−64	62, 63, 65, 66
particle hydrates and xerogels	16, 67−74	68
protonic β-aluminas	75−84	84−87
hydrated acidic polymers	88−92	88, 89, 93−95

Other layered acidic phosphates and phosphonates of zirconium have been investigated in their hydrated and dry form. In contrast to HUP and HUAs, these compounds show some residual conductivity even after dehydration. The modification of such compounds by the introduction of $-SO_3H$ containing groups in between the hydrated layers has recently led to conductivities close to that of NAFION (Figure 3).

Very high three-dimensional proton conductivity has been observed in heteropolyacid hydrates (Figure 3) built out of Keggin anions which are held together by acidified hydrogen-bonded water structures. Also, highly dispersed systems, such as structures built out of hydrated acidic particles or xerogels, may show high proton conductivity (Figure 3). The high sodium ion conductivities of the β-aluminas inspired the preparation and characterization of proton-containing analogues. Whereas for β''-alumina only the mixed NH_4^+/H_3O^+ form is available, β-alumina may be prepared in its pure H_3O^+ form. However, the proton conductivity in the latter is rather low (Figure 3). References to the above-mentioned compounds are compiled in Table 1.

There are a huge number of additional proton-conducting hydrates. They all have in common that the conductivity is highly related to the presence of water and that the host acts as a Bronsted acid toward the water of hydration, which is generally loosely bound in the structure. This retains the water of hydration only up to temperatures not significantly higher than the boiling point of water.

3.2. Oxo Acids and Their Salts (Sulfates, Selenates, Phosphates, Arsenates). Oxo acids such as phosphoric acid (H_3PO_4), sulfuric acid (H_2SO_4), or perchloric acid ($HClO_4$) dissociate in aqueous solution according to their pK_A, generating hydrated protons and thus proton conductivity. But also in the absence of water, i.e., in the anhydrous state, such acids may show appreciable proton conductivity (e.g., H_3PO_4,[96] H_3OClO_4[98]) which is due to their self-dissociation[97] and conduction mechanisms discussed in section 5.2.

(42) Colomban, Ph.; Pham-Thi, M.; Novak, A. *Solid State Commun.* **1985**, *53*, 747.
(43) Pham-Thi, M.; Colomban, Ph. *Solid State Ionics* **1985**, *17*, 295.
(44) Kreuer, K. D.; Rabenau, A.; Messer, R. *Appl. Phys.* **1983**, *A32*, 45.
(45) Badot, J. C.; Fourrier-Lamer, A.; Baffier, N.; Colomban, Ph. *J. Phys.* **1987**, *48*, 1325.
(46) Morosin, B. *Acta Crystallogr.* **1978**, *B34*, 3732.
(47) Fitch, A. N.; Bernard, L.; Howe, A. T.; Wright, A. F.; Fender, B. E. F. *Acta Crystallogr.* **1983**, *C39*, 156.
(48) Fitch, A. N.; Wright, A. F.; Fender, B. E. F. *Acta Crystallogr.* **1982**, *B38*, 2546.
(49) Mercier, R.; Pham-Thi, M.; Colomban, Ph. *Solid State Ionics* **1985**, *15*, 113.
(50) Alberti, G.; Casciola, M. In ref 19, p 238.
(51) Casciola, M.; Bianchi, D. *Solid State Ionics* **1985**, *17*, 287.
(52) Sadaoka, Y.; Matsuguchi, M.; Sakai, Y.; Mitsui, S. *J. Mater. Sci.* **1987**, *22*, 2975.
(53) Alberti, G.; Casciola, M.; Palombari, R.; Peraio, A. *Solid State Ionics* **1992**, *58*, 339.
(54) Alberti, G.; Casciola, M.; Costantino, U.; Peraio, A.; Montoneri, E. *Solid State Ionics* **1992**, *50*, 315.
(55) Alberti, G.; Casciola, M.; Palombari, R.; Peraio, A. *Solid State Ionics* **1992**, *58*, 339.
(56) Casciola, M.; Marmottini, F.; Peraio, A. *Solid State Ionics* **1993**, *61*, 125.
(57) Clearfield, A.; Smith, G. D. *Inorg. Chem.* **1969**, *8*, 431.
(58) Fusin, L. A.; Pak, V. N. *Zh. Prikl. Khim.* **1992**, *65*, 260.
(59) Slade, R. C. T.; Omana, M. J. *Solid State Ionics* **1992**, *58*, **195**.
(60) Azuma, N.; Ohtsuka, R.; Morioka, Y.; Kosugi, H.; Kobayashi, J. *J. Mater. Chem.* **1991**, *1*, 989.
(61) Chuvaev, V. F.; Yaroslavtsev, A. B.; Yaroslavtseva, E. M.; Oniani, A. S. *Zh. Neorg. Kim.* **1991**, *36*, 2101.
(62) Mioc, U.; Davidovic, M.; Tjapkin, N.; Colomban, Ph.; Novak, A. *Solid State Ionics* **1991**, *46*, 103.
(63) Nakamura, O. *Kikan Kagaku Sosetsu* **1993**, *20*, 177.
(64) Kreuer, K. D.; Hampele, M.; Dolde, K.; Rabenau, A. *Solid State Ionics* **1988**, *28−30*, 589.
(65) Spirlet, M. R.; Busing, W. R. *Acta Crystallogr.* **1976**, *B32*, 1545.
(66) Clark, C. J.; Hall, D. *Acta Crystallogr.* **1976**, *B32*, 1545.
(67) Vaivars, G.; Kleperis, J.; Lusis, A. *Solid State Ionics* **1993**, *61*, 317.
(68) Polevoi, B. G.; Burmistrov, V. A.; Burmakin, E. I. *Neorg. Mater.* **1991**, *27*, 2584.
(69) Knudsen, N.; Krogh Andersen, E.; Krogh Andersen, I. G.; Norby, P.; Skou, E. *Solid State Ionics* **1993**, *61*, 153.
(70) Feng, S., Greenblatt, M. *Chem. Mater.* **1993**, *5*, 1277.
(71) Yoshiro, S. *Nippon Kinzoku Gakkai Kaiho* **1990**, *29*, 649.
(72) Colomban, Ph.; Novack, A. In ref 19, p 272.
(73) Ozawa, Y.; Miura, N.; Yamazoe, N.; Seiyama, T. *Chem. Lett.* **1983**, 1569.
(74) Badot, J. C.; Baffier, N. *J. Mater. Chem.* **1992**, *2*, 1167.
(75) Nicholson, P. In ref 19, p 499.
(76) Schäfer, G.; Kim, H. J.; Aldinger, F. *Solid State Ionics* **1995**, *77*, 234.
(77) Farrington, G. C.; Briant, J. L. *Mater. Res. Bull.* **1978**, *13*, 763.
(78) Roth, W. L.; Anne, M.; Tranqui, D. *Rev. Chim. Miner.* **1980**, *17*, 379.
(79) Lassègues, J. C.; Fouassier, M.; Baffier, N.; Colomban, Ph. *J. Phys.* **1980**, *41*, 273.
(80) Baffier, N.; Badot, J. C.; Colomban, Ph. *Solid State Ionics* **1984**, *13*, 233.
(81) De Nuzzio, J. D.; Farrington, G. C. *J. Solid State Chem.* **1989**, *79*, 65.
(82) Smoot, S. W.; Whitmore, D. H.; Halperin, W. P. *Solid State Ionics* **1986**, *18/19*, 687.
(83) Frase, K. G.; Thomas, J. O.; McGhie, A. G.; Farrington, G. C. *Solid State Chem.* **1986**, *62*, 297.
(84) Frase, K. G.; Farrington, G. C. *Annu. Rev. Mater. Sci.* **1984**, *14*, 279.
(85) Thomas, J. O.; Farrington, G. C. *Acta Crystallogr.* **1983**, *B39*, 227.
(86) Colomban, Ph.; Lucazeau, G.; Mercier, R.; Novak, A. *J. Chem. Phys.* **1977**, *67*, 5244.
(87) Colomban, Ph.; Novak, A. *Solid State Commun.* **1979**, *32*, 467.
(88) Eisenberg, A., Yeager, H. L., Eds. *Perfluorinated Ionomer Membranes*; ACS Symposium Series 180; American Chemical Society: Washington, DC, 1982.
(89) Gavach, C.; Pourcelly, G. In ref 19, p 487.
(90) Zawodzinski, T. A.; Derouin, Ch; Radzinski, S.; Gottesfeld, Sh. *J.E.C.S.* **1993**, *140*, 1041.
(91) Kreuer, K. D.; Dippel, Th.; Meyer, W.; Maier, J. *Mater. Res. Soc. Symp. Proc.* **1993**, *293*, 273.
(92) Scherer, G. G.; Gupta, B. *Polym. Mater. Sci. Eng.* **1993**, *68*, 114.
(93) Gierke, T. D.; Munn, G. E.; Wilson, F. C. *J. Polym. Sci.* **1981**, *19*, 1687.
(94) Yeo, R. S. *J.E.C.S.* **1983**, *130*, 533.
(95) Falk, M. *Can. J. Chem.* **1980**, *58*, 1495.
(96) Dippel, Th.; Kreuer, K. D.; Lassègues, J. C.; Rodriguez, D. *Solid State Ionics* **1993**, *61*, 41.
(97) Munson, R. A. *J. Phys. Chem.* **1964**, *68*, 3374.
(98) Potier, A.; Rousselet, D. *J. Chim. Phys. (Paris)* **1973**, *70*, 873.
(99) Baranov, A. I.; Dobrzhanskii, G. F.; Ilyukhin, V. V.; Ryabkin, V. S.; Sokolov, Yu. N.; Sorokina, N. I.; Shuvalov, L. A. *Sov. Phys. Crystallogr.* **1981**, *26*, 717.
(100) Barnov, A. I.; Shuvalov, L. A.; Schagina, N. M. *JETP Lett.* **1982**, *36*, 459.
(101) Sinitsyn, V. V.; Ponyatovskii, E. G.; Baranov, A. I.; Tregubchenko, A. V.; Shuvalov, L. A. *Sov. Phys. JETP* **1991**, *73*, 386.
(102) Hainovsky, N. G.; Pavlukhin, Yu. T.; Hairetdinov, E. F. *Solid State Ionics* **1986**, *20*, 249.
(103) Hainovsky, N. G.; Hairetdinov, E. F. *Izv. Sib. Otd. Akad. Nauk., SSSR, Ser. Khim. Nauk.* **1985**, *V4*, 33.

Despite investigations of numerous acidic salts of oxo acids, for a long time the proton conductivities observed were small. Especially for compounds of the KDP family (KH_2PO_4 and $NH_4H_2PO_4$) and $KHSO_4$ comprehensive data are available. Their intrinsic conductivities are small with high activation enthalpies and some increase at low temperature upon doping. For details see early reviews[17,18] and refs 182−185.

It was in the early 1980s when the systematic search for fast proton conductivity in this family of compounds led Baranov et al. to the discovery of the rather high conductivities of acidic iodates[99] and then to the discovery of the very high proton conductivity of $CsHSO_4$ above a first-order improper ferroelastic phase transition around 412 K.[100] This leads to the formation of a plastic phase characterized by a high degree of dynamic reorientational disorder of the sulfate tetrahedra. Since this discovery, similar phase transitions have only been

(104) Belushkin, A. V.; Carlile, C. J.; Shuvalov, L. A. *J. Phys.: Condens. Matter* **1992**, *4*, 389.
(105) Moskvich, Yu. N.; Polyakov, A. M.; Sukhovskii, A. A. *Sov. Phys.: Solid State* **1988**, *30*, 24.
(106) Blinc, R.; Dolinsek, J.; Lahajnar, G.; Zupancic, I.; Shuvalov, L. A.; Baranov, A. I. *Phys. Status Solidi* **1984**, *123*, K83.
(107) Belushkin, A. V.; Carlile, C. J.; David, W. I. F.; Ibberson, R. M.; Shuvalov, L. A.; Zajac, W. *Physica* **1991**, *B174*, 268.
(108) Belushkin, A. V.; David, W. I. F.; Ibberson, M.; Shuvalov, L. A. *Acta Crystallogr.* **1991**, *B47*, 161.
(109) Shakhmatov, V. S. *Sov. Phys. Crystallogr.* **1991**, *36*, 575.
(110) Komikae, M.; Tanaka, M.; Osaka, T.; Makita, Y.; Kozawa, K.; Uchida, T. *Ferroelectrics* **1989**, *96*, 199.
(111) Balagarov, A. M.; Belushkin, A. V.; Dutt, I. D.; Natkaniec, I.; Plakida, N. M.; Savenko, B. N.; Shuvalov, L. A.; Wasicki, J. *Ferroelectrics* **1985**, *63*, 59.
(112) Badot, J. C.; Colomban, Ph. *Solid State Ionics* **1989**, *35*, 143.
(113) Dimitriev, V. P.; Loshkarev, V. V.; Rabkin, L. M.; Shuvalov, L. A.; Shagina, N. M. *Sov. Phys. Crystallogr.* **1988**, *33*, 87.
(114) Pham-Thi, M.; Colomban, Ph.; Novak, A.; Blinc, R. *J. Raman Spectrosc.* **1987**, *18*, 185.
(115) Baran, J. *J. Mol. Struct.* **1987**, *162*, 229.
(116) Belushkin, A. V.; Natkaniec, I.; Pakida, N. M.; Shuvalov, L. A.; Wasicki, J. *J. Phys.* **1987**, *C20*, 671.
(117) Döbler, U.; Happ, H. *Phys. Status Solidi* **1987**, *144*, 853.
(118) Colomban, Ph.; Pham-Thi, M.; Novak, A. *J. Mol. Struct.* **1987**, *161*, 1.
(119) Dimitriev, V. I.; Klanshek, M.; Latush, L. T.; Orel, B.; Rabkin, L. M.; Shagina, N. M. *Sov. Phys. Crystallogr.* **1986**, *31*, 410.
(120) Dimitriev, V. I.; Loshkarev, V. V.; Rabkin, L. M.; Shuvalov, L. A.; Yuzyuk, Yu. I. *Sov. Phys. Crystallogr.* **1986**, *31*, 673.
(121) Pham-Thi, M.; Colomban, Ph.; Novak, A.; Blinc, R. *Solid State Commun.* **1985**, *55*, 265.
(122) Mizeris, R.; Grigas, J.; Samulionis, V.; Skritski, V.; Baranov, A. I.; Shuvalov, L. A. *Phys. Status Solidi* **1988**, *110*, 429.
(123) Badot, J. C.; Colomban, Ph. *Solid State Ionics* **1989**, *35*, 143.
(124) Lushnikov, S. G.; Prokhorova, S. D.; Sinii, I. G.; Smolenskii, G. A. *Sov. Phys. Solid State* **1987**, *29*, 280.
(125) Shchepetil'nikov, B. V.; Baranov, A. I.; Shuvalov, L. A.; Dolbinia, V. A. *Sov. Phys. Solid State* **1990**, *32*, 142.
(126) Dilanyan, R. A.; Shekhtman, V. Sh. *Sov. Phys. Solid State* **1989**, *31*, 1313.
(127) Friesel, M.; Baranowski, B.; Lunden, A. *Solid State Ionics* **1989**, *35*, 85.
(128) Baranowski, B.; Friesel, M.; Lunden, A. *Physica* **1989**, *A156*, 353.
(129) Ponyatovskii, E. G.; Rashchupkin, V. I.; Sinitsyn, V. V.; Baranov, A. I.; Shuvalov, L. A.; Schagina, N. M. *JETP Lett.* **1985**, *41*, 139.
(130) Yokata, S. *J. Phys. Soc. Jpn.* **1982**, *51*, 1884.
(131) Mhiri, T.; Daoud, A.; Colomban, Ph. *Solid State Ionics* **1991**, *44*, 215.
(132) Colomban, Ph.; Pham-Thi, M.; Novak, A. *Solid State Ionics* **1987**, *24*, **193**.
(133) Baranov, A. I.; Sinitsyn, V. V.; Ponyatovskii, E. G.; Shuvalov, L. A *JETP Lett.* **1986**, *44*, 237.
(134) Friesel, M.; Lunden, A.; Baranowski, B. *Solid State Ionics* **1989**, *35*, 91.
(135) Henn, F. E. G.; Giuntini, J. C.; Zanchetta, J. V.; Granier, W.; Taha, A. *Solid State Ionics* **1990**, *42*, 29.
(136) Moskvich, Yu. N.; Sukhovskii, A. A.; Rozanov, O. V. *Sov. Phys. Solid State* **1984**, *26*, 21.
(137) Baranov, A. I.; Ponyatovskii, E. G.; Sinitsyn, V. V.; Fedosyuk, R. M.; Shuvalov, L. A. *Sov. Phys. Crystallogr.* **1985**, *30*, 653.
(138) Reddy, A. D.; Sathyanarayan, S. G.; Sastry, G. S. *Phys. Status Solidi A* **1982**, *73*, K41.
(139) Makarova, I. P. *Acta Crystallogr.* **1993**, *B49*, 11.
(140) Makarova, I. P.; Muradyan, L. A.; Rider, E. E.; Sarin, V. A.; Aleksandrova, I. P.; Simonov, V. I. *Sov. Phys. Crystallogr.* **1990**, *35*, 377.
(141) Denoyer, F.; Rozycki, A.; Parlinski, K.; More, M. *Phys. Rev.* **1989**, *B39*, 405.
(142) Rozycki, A.; Denoyer, F.; Novak, A. *J. Phys.* **1987**, *48*, 1553.
(143) Pasquier, B.; Le Calve, N.; Rozycki, A.; Novak, A. *J. Raman Spectrosc.* **1990**, *21*, 465.
(144) Toupry, N.; Poulet, H.; Le Postollec, M. *J. Raman. Spectrosc.* **1981**, *11*, 81.
(145) Baran, J.; Czapala, Z.; Ilczyazyn, M. M.; Ratajczak, H. *Acta Phys. Pol.* **1981**, *A59*, 753.
(146) Colomban, Ph.; Badot, J. C. *J. Phys.: Condens. Matter* **1992**, *4*, 5625.
(147) Krasikov, V. S.; Zherebtsova, L. I.; Zaitseva, M. P. *Sov. Phys. Solid State* **1981**, *23*, 163.
(148) Gesi, K.; Ozawa, K. *J. Phys. Soc. Jpn.* **1977**, *43*, 563.
(149) Gesi, K.; Ozawa, K. *J. Phys. Soc. Jpn.* **1975**, *38*, 459.
(150) Aleksandrova, I. P.; Colomban, Ph.; Denoyer, F.; Le Calve, N.; Novak, A.; Pasquier, B.; Rozycki, A. *Phys. Status Solidi A* **1989**, *114*, 531.
(151) Colomban, Ph.; Rozycki, A.; Novak, A. *Solid State Commun.* **1988**, *67*, 969.
(152) Czapla, Z. *Acta Phys. Pol.* **1982**, *A61*, 47.
(153) Gesi, K. *J. Phys. Soc. Jpn.* **1980**, *48*, 1399.
(154) Pawlowski, A.; Pawlaczyk, Cz.; Hilczer, B. *Solid State Ionics* **1990**, *44*, 17.
(155) Baranov, A. I.; Tregubchenko, A. V.; Shuvalov, L. A.; Shchagina, N. M. *Sov. Phys. Solid State* **1987**, *29*, 1448.
(156) Lukaszewicz, K.; Pietraszko, A.; Augustyniak, M. A. *Acta Crystallogr.* **1993**, *C49*, 430.
(157) Melnikov, B. V.; Antipin, M. Yu.; Baranov, A. I.; Tregubchenko, A. M.; Shuvalov, L. A.; Stuchkov, Yu. T. *Sov. Phys. Crystallogr.* **1991**, *36*, 488.
(158) Ichikawa, I. P.; Gustafsson, T.; Olovsson, I. *Acta Crystallogr.* **1992**, *C48*, 603.
(159) Makarova, I. P.; Shuvalov, L. A.; Simonov, V. I. *Ferroelectrics* **1988**, *79*, 111.
(160) Makarova, I. P.; Verin, I. A.; Shchagina, N. M. *Sov. Phys. Crystallogr.* **1986**, *31*, 105.
(161) Fortier, S.; Fraser, M. E.; Heyding, R. D. *Acta Crystallogr.* **1985**, *C41*, 1139.
(162) Baranov, A. I.; Makarova, I. P.; Muradyan, L. A.; Tregubchenko, A. V.; Shuvalov, L. A. Simonov, V. I. *Sov. Phys. Crystallogr.* **1987**, *32*, 400.
(163) Ichikawa, M.; Gustafsson, T.; Olovsson, I. *Acta Crystallogr.* **1992**, *B48*, 633.
(164) Merinov, B. V.; Bolatina, N. B.; Baranov, A. I.; Shuvalov, L. A. *Sov. Phys. Crystallogr.* **1991**, *36*, 639.
(165) Merinov, B. V.; Baranov, A. I.; Shuvalov, L. A. *Sov. Phys. Crystallogr.* **1990**, *35*, 200.
(166) Merinov, B. V.; Bolotina, N. B.; Baranov, A. I.; Shuvalov, L. A. *Sov. Phys. Crystallogr.* **1988**, *33*, 824.
(167) Belushkin, A. V.; Tomkinson, J.; Shuvalov, L. A. *J. Phys. II (France)* **1993**, *3*, 217.
(168) Adamic, D.; Dolinsek, J.; Blinc, R.; Shuvalov, L. A. *Phys. Rev.* **1990**, *B42*, 442.
(169) Mizeris, R.; Sueta, A.; Urbonavichus, V.; Grigas, I.; Shuvalov, L. A. *Sov. Phys. Crystallogr.* **1991**, *36*, 385.
(170) Komukae, M.; Osaka, T.; Kaneko, T.; Makita, Y. *J. Phys. Soc. Jpn.* **1985**, *54*, 3401.
(171) Osaka, T.; Makita, Y.; Gesi, K. *J. Phys. Soc. Jpn.* **1979**, *46*, 577 1979.
(172) Shchepetil'nikov, B. V.; Shuvalov, L. A.; Tregubchenko, A. V. *Sov. Phys. Solid State* **1992**, *34*, 236.
(173) Lushnikov, S. G.; Shuvalov, L. A. *Ferroelectrics* **1991**, *124*, 409.
(174) Shchepetil'nikov, B. V.; Baranov, A. I.; Shuvalov, L. A.; Shchagina, N. M. *Sov. Phys. Solid State* **1990**, *32*, 1676.
(175) Lushnikov, S. G.; Prokhorova, S. D.; Shuvalov, L. A. *Bull. Acad. Sci. USSR−Phys. Ser.* **1989**, *53*, 78.
(176) Ichikawa, M.; Motida, K.; Gustafsson, T.; Olovsson, I. *Solid State Commun.* **1990**, *76*, 547.
(177) Ichikwa, M.; Gustafsson, T.; Olovsson, I. *Solid State Commun.* **1991**, *78*, 547.
(178) Hilczer, B.; Pawlowski, A. *Ferroelectrics* **1990**, *104*, 383.
(179) Plakida, N. M.; Salejda, W. *Phys. Status Solidi B* **1988**, *148*, 473.
(180) Osaka, T.; Sato, T.; Makita, Y. *Ferroelectrics* **1984**, *55*, 283.
(181) Ichikawa, M. *J. Phys. Soc. Jpn.* **1979**, *47*, 681.
(182) Kumar, A.; Hashmi, S. A.; Chandra, S. *Bull. Mater. Sci.* **1992**, *15*, 191.
(183) Chandra, S.; Kumar, A. *J. Phys.: Condens. Matter* **1991**, *3*, 5271.
(184) Chandra, S.; Kumar, A. *Solid State Ionics* **1990**, *40/41*, 863.
(185) Chandra, S.; Hashmi, S. A. *J. Mater. Sci.* **1990**, *25*, 2459.
(186) Baranov, A. I.; Khiznichenko, V. P.; Shuvalov, L. A. *Ferroelectrics* **1989**, *100*, 135.

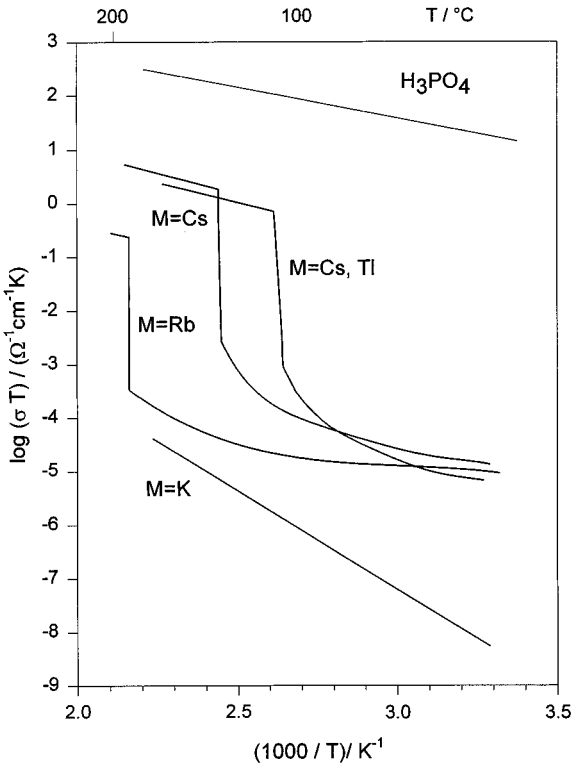

Figure 4. Proton conductivity of sulfates of composition $MHSO_4$ according to ref 103. The conductivity of anhydrous phosphoric acid is given for comparison.

found for acidic salts with large cations (e.g., Rb^+, Cs^+) (Figure 4).

Whereas $MHXO_4$ (M = Rb, Cs) exhibits fast proton-conducting phases for X = S and Se, only for the selenates of the $M_3H(XO_4)_2$ family have such phases been identified above phase transitions around 450 K. In most cases the high-temperature phase has tetragonal or rhombohedral symmetry, but for some compositions another transition into a slightly more conducting cubic phase at higher temperature and pressure is observed. Most compounds with high conductivity above so-called "superprotonic" phase transitions at elevated temperature have another ferroelastic phase transition at low temperature.

Within the KDP family, a transition into a proton-conducting phase is reported only for CsH_2PO_4 just below the decomposition temperature. Whether this is just an artifact due to the onset of decomposition is not yet clear.

There are many more related compositions for which "superprotonic" phase transitions have been reported in the meantime. Only references to the above-mentioned families, for which a comprehensive set of data is available, are included in Table 2.

Proton conductivity in hydrogen- or water-containing atmospheres is even reported for neutral sulfates and phosphates (e.g., Li_2SO_4[210] and $LaPO_4$[209]), which do not exhibit constitutional protons. Proton conductivity in oxide glasses containing large amounts of P_2O_5 has recently been reviewed by Abbe.[211]

All of the above-mentioned compounds have in common that the proton is coordinated to oxygen of the XO_4 tetrahedra. These are, so to say, solvating the proton just like the water does in water-containing systems. But when there are more basic groups available in the structure, the proton may also be coordinated to other moieties. This is, e.g., the case in the one-dimensional proton-conductor $LiN_2H_5SO_4$ where the conducting proton is part of the hydrazonium ion.[212]

3.3. High-Temperature Proton Conductors (Oxides, Hydroxides, Apatites). Just after proton conductivity in oxides was first suggested in 1964[213] Stotz and Wagner quantified the solubility of water in some oxides and its impact on transport properties.[214] The oxide, which was the first to be shown to be predominantly proton conducting, was acceptor-doped thoria for low p_{O_2} (high p_{H_2}) and temperatures above 1200 °C.[215] The systematic investigation of Takahashi and Iwahara on the ionic conductivity of compounds with the perovskite structure in 1980 revealed several materials with pure oxide ion, mixed oxide ion/proton and pure proton conductivity[216] in hydrogen- or water-containing atmospheres. Indium-doped $SrZrO_3$, which is the only proton-conducting oxide being commercialized as separator material in hydrogen probes (see section 6.2.2), was already reported in this early work. The highest proton conductivities, however, are observed in cerates, as first reported by Iwahara et al.[217] Table 3 provides

(187) Baranov, A. I.; Khiznichenko, V. P.; Sandler, V. A.; Shuvalov, L. A. *Ferroelectrics* **1988**, *81*, 183.
(188) Bronowska, W.; Pietrasko, A. *Solid State Commun.* **1990**, *76*, 293.
(189) Fukami, T. *Phys. Status Solidi A* **1990**, *122*, K117.
(190) Hagiwara, T.; Itoh, K.; Nakamura, E.; Komukae, M.; Makita, Y. *Acta Crystallogr.* **1984**, *C40*, 718.
(191) Suzuki, S.; Arai, K.; Sumita, M.; Makita, Y. *J. Phys. Soc. Jpn.* **1983**, *52*, 2394.
(192) Tibballs, J. E.; Zhong, W. L.; Nelmes, R. J. *J. Phys. C: Solid State Phys.* **1982**, *15*, 4431.
(193) Hay, W. J.; Nelmes, R. J. *J. Phys. C: Solid State Phys.* **1981**, *14*, 1043.
(194) Nelmes, R. J.; Choudhary, R. N. P. *Solid State Commun.* **1981**, *38*, 321.
(195) Goyal, P. S.; Chakravarthy, R.; Dasannacharya, B. A.; Kulshreshtha, S. K.; Sastry, M. S.; Tomkinson, J. *Phys. Status Solidi B* **1990**, *157*, 547.
(196) Shin, S.; Ishigame, M. *Phys. Rev.* **1988**, *B37*, 2718.
(197) Fillaux, F.; Marchon, B.; Novak, A. *Chem. Phys.* **1984**, *86*, 127.
(198) Orel, B.; Hadzi, D. *J. Mol. Struct.* **1973**, *18*, 495.
(199) Levstik, A.; Zeks, B.; Levstik, I.; Unruh, H. G.; Luther, G.; Roemer, H. *Phys. Rev.* **1983**, *B27*, 5706.
(200) Deguchi, K.; Nakamura, E.; Okaue, E.; Aramaki, N. *J. Phys. Soc. Jpn.* **1982**, *51*, 3575.
(201) Yasuda, N.; Fujimoto, S.; Okamoto, M.; M. Shimizu, M. *Phys. Rev.* **1979**, *B20*, 2755.
(202) Baranov, A. I.; Shuvalov, L. A.; Ryabkin, V. S.; Rashkovichi, L. N. *Sov. Phys. Crystallogr.* **1979**, *24*, 300.
(203) Levstik, A.; Blinc, R.; Kadoba, P.; Cizikov, S.; Levstik, I.; Filipic, C. *Solid State Commun.* **1975**, *16*, 1339.
(204) Baranowski, B.; Friesel, M.; Lunden, A. *Phys. Scr.* **1988**, *37*, 209.
(205) Nirsha, B. M.; Gudinitsa, E. N.; Fakeev, A. A.; Efremov, V. A.; Zhadanov, B. V.; Olikova, V. A. *Russ. J. Inorg. Chem.* **1982**, *27*, 770.
(206) Metcalfe, B.; Clark, J. B. *Thermochim. Acta* **1978**, *24*, 149.
(207) Rapoport, E.; Clark, J. B.; Richter, R. W. J. *Solid State Chem.* **1978**, *24*, 423.
(208) Loiacono, G. M.; Ladell, J.; Osborne, W. N.; Nicolosi, J. *Ferroelectrics* **1976**, *14*, 761.
(209) Norby, T.; Christiansen, N. *Solid State Ionics* **1995**, *77*, 240.
(210) Heed, B.; Zhu, B.; Mellander, B. E.; Lunden, A. *Solid State Ionics* **1991**, *46*, 121.
(211) Abbe, Y. *Phosphorous Lett.* **1994**, *20*, 3.
(212) Kreuer, K. D.; Weppner, W.; Rabenau, A. *Solid State Ionics* **1981**, *3/4*, 353.
(213) Forrat, F.; Dauge, G.; Trevoux, P. *Compt. Rend.* **1964**, *t259*, 2813.
(214) Stotz, S.; Wagner, C. *Ber. Bunsen-Ges. Phys. Chem.* **1966**, *70*, 781.
(215) Shores, D. A.; Rapp, R. A. *J. Electrochem. Soc.* **1972**, *119*, 300.
(216) Takahashi, T.; Iwahara, H. *Rev. Chim. Miner.* **1980**, *t17*, 243.
(217) Iwahara, H.; Esaka, T.; Uchida, H.; Maeda, N. *Solid State Ionics* **1981**, *3/4*, 359.
(218) Iwahara, H. In ref 19, p 122.

Table 2. Acidic Salts of Oxo Acids Which Have Attracted Major Interest and References to Some Properties Relevant to Their High Proton Conductivity

	$CsHXO_4$ (X = S, Se)	$MHXO_4$ (M = NH_4, Rb; X = S, Se)	$M_3H(SeO_4)_2$ (M = NH_4, Rb, Cs)	MH_2XO_4 (M = Rb, Cs; X = P, As)
transport	101−103 conductivity; 104−106 QNS, NMR	135−138	154, 155	182−187
structure	107−111	139−142	156−166	188−194
local dynamics	112−121	143−145	167−176	195−198
dielectric elastic properties, thermal expansion	122−126	146		199−203
phase diagram	127−129	147−149		204−208
phase transitions	130−134	150−153	177−181	204−208

Table 3. References to Proton-Conducting Cerates and Zirconates

	cerates based on $MCeO_3$ (M = Sr, Ba)	zirconates based on $MZrO_3$ (M = Ca, Sr, Ba)
defect formation and transport	222−245a	251−257
structure	246, 247	258−260
local dynamics	248−250	261

access to the comprehensive literature on proton-conducting cerates and zirconates which also includes the work on a single crystal of acceptor-doped $BaCeO_3$,[245a] $SrCeO_3$, and $SrZrO_3$.[255]

In the meantime proton conductivity in different families of oxides has been studied and recently reviewed from different points of view.[218−221]

Especially Norby et al. systematically studied proton conductivity in rare-earth oxides including La_2O_3 and Y_2O_3 within the framework of a consistent description of their defect chemistry.[262−267] Even single-crystal data are available on the rather low proton conductivities in acceptor-doped tantalates ($KTaO_3$[268−271]) and niobates ($LiNbO_3$[272−274]). Acceptor-doped titanates ($MTiO_3$, M = Sr, Ba) are also rather poor proton conductors owing to their low proton concentrations. But the diffusivity of protons in these compounds is extremely high, as demonstrated in a set of papers by Waser.[275−277] The contribution of protons to the conductivity of alumina[278] and zirconia[279] has also been studied. The proton conductivities of some representative oxides are shown in Figure 5.

(219) Iwahara, H. *Solid State Ionics* **1992**, *52*, 99.
(220) Fukatsu, N. *Nippon Kinzoku Gakkai Kaiho* **1990**, *29*, 612.
(221) Norby, T. *Solid State Ionics* **1990**, *40/41*, 857.
(222) Taniguchi, N.; Hatoh, K.; Niikura, J.; Gamo, T.; Iwahara, H. *Solid State Ionics* **1992**, *53−56*, 998.
(223) Yajima, T.; Iwahara, H.; Uchida, H. *Solid State Ionics* **1991**, *47*, 117.
(224) Yajima, T.; Iwahara, H. *Solid State Ionics* **1992**, *50*, 281.
(225) Yajima, T.; Iwahara, H. *Solid State Ionics* **1992**, *53−56*, 983.
(226) Yajima, T.; Iwahara, H.; Uchida, H.; Koide, K. Solid State Ionics **1990**, *40/41*, 914.
(227) Uchida, H.; Yoshikawa, H.; Iwahara, H. *Solid State Ionics* **1989**, *35*, 229.
(228) Nowick, A. S. *Solid State Ionics* **1995**, *77*, 137.
(229) Liu, J. F.; Nowick, A. S. *Solid State Ionics* **1992**, *50*, 131.
(230) Liu, J. F.; Nowick, A. S. *Mater. Res. Soc. Symp. Proc.* **1991**, *210*, 675.
(231) Scherban, T.; Nowick, A. S. *Solid State Ionics* **1989**, *35*, 189.
(232) Scherban, T.; Lee, W. K.; Nowick, A. S. *Solid State Ionics* **1988**, *28−30*, 585.
(233) Bonanos, N. *Solid State Ionics* **1992**, *53−56*, 967.
(234) Bonanos, N.; Ellis, B.; Knight, K. S.; Mahmood, M. N. *Solid State Ionics* **1989**, *35*, 179.
(235) Bonanos, N.; Ellis, B.; Mahmood, M. N. *Solid State Ionics* **1988**, *28−30*, 579.
(236) Slade, R. C. T.; Flint, S. D.; Singh, N. *J. Mater. Chem*. **1994**, 4, 509.
(237) Slade, R. C. T.; Singh, N. J. Mater. Chem. **1991**, *1*, 441.
(238) Baikov, Yu. M.; Shalkova, E. K. J. *Solid State Chem*. **1992**, *97*, 224 1992.
(239) Kreuer, K. D.; Schönherr, E.; Maier, J. *Solid State Ionics* **1994**, *70/71*, 278.
(240) Kreuer, K. D.; Fuchs, A.; Maier, J. *Solid State Ionics* **1995**, *77*, 157.
(241) Hempelmann, R.; Karmonik, Ch.; Matzke, Th.; Capadonia, M.; Stimming, U.; Spinger, T.; Adams, M. *Solid State Ionics* **1995**, *77*, 152.
(242) Zimmermann, L.; Bohn, H. G.; Schilling, W.; Syskakis, E. *Solid State Ionics* **1995**, *77*, 163.
(243) Schober, T.; Friedrich, J.; Condon, J. B. *Solid State Ionics* **1995**, *77*, 175.
(244) De Souza, R. A.; Kilner, J. A.; Steele, B. C. H. *Solid State Ionics* **1995**, *77*, 180.
(245) Ferreira, A. A.; Labrincha, J. A.; Frade, J. R. *Solid State Ionics* **1995**, *77*, 210. (a) Kreuer, K. D.; Dippel, Th.; Baikov, Yu. M.; Maier, J. *Solid State Ionics*, in press.
(246) Ranloev, J.; Nielsen, K. *J. Mater. Chem*. **1994**, *4*, 867.
(247) Knight, K. S.; Soar, M.; Bonanos, N. *J. Mater. Chem*. **1992**, *2*, 709.
(248) Scherban, T.; Baikov, Yu. M.; Shalkova, E. K. *Solid State Ionics* **1993**, *66*, 159.
(249) Kosacki, I.; Schoonman, J.; Balkanski, M. *Solid State Ionics* **1992**, *57*, 345.
(250) Scherban, T.; Villeneuve, R.; Abello, L.; Lucazeau, G. Solid State Commun. **1992**, 84, 341.
(251) Iwahara, H.; Yajima, T.; Hibino, T.; Ozaki, K.; Suzuki, H. *Solid State Ionics* **1993**, *61*, 65.
(252) Yajima, T.; Suzuki, H.; Yogo, T.; Iwahara, H. *Solid State Ionics* **1992**, *51*, 101.
(253) Hibino, T.; Mizutani, K.; Yajima, T.; Iwahara, H. *Solid State Ionics* **1992**, *57*, 303.
(254) Hibino, T.; Mizutani, K.; Yajima, T.; Iwahara, H. *Solid State Ionics* **1992**, *58*, 85.
(255) Shin, S.; Huang, H. H.; Ishigame, M.; Iwahara, H. *Solid State Ionics* **1990**, *40/41*, 910.
(256) Liang, K. C.; Lee, L. Y.; Nowick, A. S. *Mater. Res. Soc. Symp. Proc.* **1993**, *293*, 355.
(257) Labrincha, J. A.; Frade, J. R.; Marques, F. M. B. *Solid State Ionics* **1993**, *61*, 71.
(258) van Roosmalen, J. A. M.; van Vlaanderen, P.; Cordfunke, E. H. P. *J. Solid State Chem*. **1992**, *101*, 59.
(259) Ahtee, M.; Glazer, A. M.; Hewat, A. W. *Acta Crystallogr*. **1978**, *B34*, 752.
(260) Carlsson, L. *Acta Cryst*. **1967**, *23*, 901.
(261) Hibino, T.; Mizutani, K.; Yajima, T.; Iwahara, H. *Solid State Ionics* **1992**, *58*, 85.
(262) Norby, T.; Dyrlie, O.; Kofstad, P. *J. Am. Ceram. Soc.* **1992**, *75*, 1176.
(263) Norby, T.; Dyrlie, O.; Kofstad, P. *Solid State Ionics* **1992**, *53−56*, 446.
(264) Larring, Y.; Norby, T.; Kofstad, P. *Solid State Ionics* **1991**, *49*, 73.
(265) Norby, T.; Kofstad, P. *Solid State Ionics* **1986**, *20*, 169.
(266) Balakireva, V. B.; Gorelov, V. P.; Nevolina, O. A. *Neorg. Mater*. **1994**, *30*, 234.
(267) Balakireva, V. B.; Gorelov, V. P. *Solid State Ionics* **1989**, *36*, 217.
(268) Scherban, T.; Nowick, A. S.; Boatner, L. A.; Abraham, M. M. *Appl. Phys*. **1992**, *A55*, 324.
(269) Scherban, T.; Nowick, A. S. *Solid State Ionics* **1992**, *53−56*, 1004.
(270) Lee, W. K.; Nowick, A. S.; Boatner, L. A. *Adv. Ceram*. **1987**, *23*, 387.
(271) Liang, K. C.; Du, Y.; Nowick, A. S. S*olid State Ionics* **1994**, *69*, 117.
(272) Klauer, S.; Woehlecke, M.; Kapphan, S. *Phys. Rev*. **1992**, *B45*, 2786.
(273) Kovacs, L.; Polgar, K.; Capelletti, R.; Mora, C. *Phys. Status Solidi A* **1990**, *120*, 97.
(274) Groene, A.; Kapphan, S. *Ferroelectrics* **1992**, *125*, 307.
(275) Waser, R. *J. Am. Ceram. Soc.* **1988**, *71*, 58.
(276) Waser, R. *Z. Naturforsch*. **1987**, *42a*, 1357.
(277) Waser, R. *Ber. Bunsen-Ges. Phys. Chem*. **1986**, *90*, 1223.
(278) Norby, T.; Kofstad, P. *High Temp. High Pressures* **1988**, *20*, 345.
(279) Norby, T. *Zirconia 88, Proc. Int. Conf.* **1988**, 209.

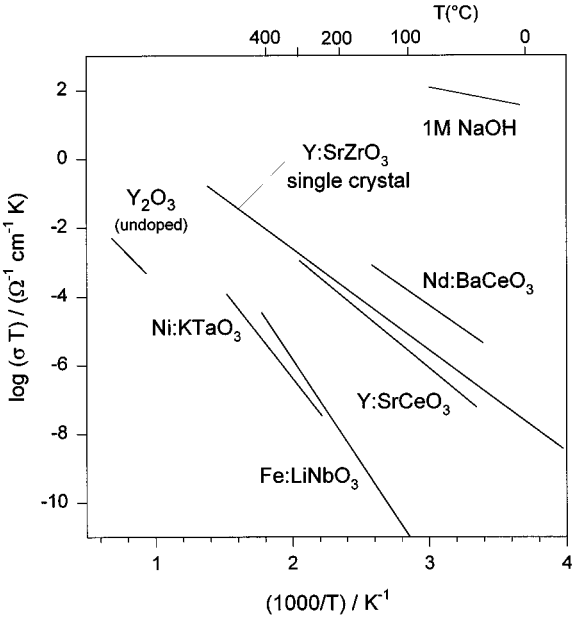

Figure 5. Proton conductivity of some acceptor doped oxides in water-containing atmospheres. The conductivity of a 1 M aqueous solution of NaOH is given for comparison. References are given in the text and Table 3.

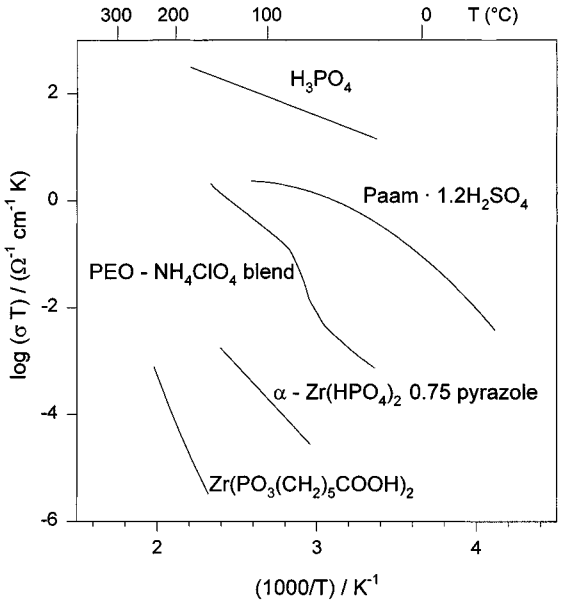

Figure 6. Proton conductivity of some representative mixed organic/inorganic compounds. References are given in the text.

As will be described later (section 5.1) the protonic defect in oxides corresponds to a hydroxyl ion on an oxygen site ($OH_O^{\bullet}$). It is, therefore, appropriate to also include hydroxides into this family of proton conductors. Proton conductivities have been reported for hydroxides of Na, K, Cs, Mg, and Y.[280−285] As in the case of sulfates (see Figure 4) high proton conductivity frequently occurs with first-order phase transitions. The data, however, are poorly reproducible and very sensitive to impurities such as CO_2 and H_2O.

Phosphates with the structure of apatite ($Ca_5(PO_4)_3$-OH) may retain structural hydroxyl ions up to very high temperature (>1000 °C) where some compounds with the apatite structure show appreciable proton conductivity as recently reviewed by Yamashita.[286]

3.4. Organic/Inorganic Systems. Acids like H_2SO_4 or H_3PO_4 form compounds in narrow composition ranges with organic molecules exhibiting basic groups, for example, H_2SO_4 with triethylenediamine ($C_6H_{12}N_2$) and hexamethylenetetramine ($C_6H_{12}N_4$) which leads to compounds for which moderate proton conductivity has been reported as early as 1976.[287]

The main activities, however, focused on blends of oxo acids with a variety of polymers. The abundance of data has recently been reviewed by Lassègues,[288] who states a blend of polyacrylamide and sulfuric acid (Paam·1.2H_2SO_4) to be the composition with the highest conductivity within this family of compounds (Figure 6). This is, however, still lower than that of the pure acid.

Blends of poly(ethylene oxide) (PEO) with ammonium salts have been stated to be proton conductors.[289,290] The conductivities compare to those of corresponding compositions with alkaline ions (Figure 6).

An interesting new chemistry is accessible by the intercalation of organic molecules such as heterocyclic bases, pyrazoles, imidazoles, and alkyls, into the lamellar structures of acidic phosphates and phosphonates.[291−293] Especially for large molecules with basic sites, this results in materials with significant proton conductivity (Figure 6).

4. Models of Proton Conductivity

During the past two decades most of the activities in the field of proton conductivity have been undertaken by the materials science community. The major motivation was to develop new proton-conducting materials suitable for applications in electrochemical cells (e.g., fuel cells, batteries, sensors; see section 6). For several proton-conducting compounds, structural and dynamical data clearly identify the principal proton-conduction mechanism (see section 2), but there was very little interest in a general and theoretical understanding of the underlying elementary transport steps.

However, there is a variety of valuable experimental data and comprehensive literature on proton-transfer reactions in chemistry providing guidelines for developing a theory of proton conductivity in condensed matter. In this section some characteristic aspects of such models will be outlined from a "bird's view", i.e., on a molecular level.

4.1. Hydrogen Bonding. As pointed out in section 2, the rates relevant for describing the two limiting proton-conduction mechanisms (vehicle and Grotthuss-

(280) El'kin, B. Sh. *Solid State Ionics* **1990**, *37*, 139.
(281) Yamamoto, O.; Takeda, Y.; Kanno, R.; Fushimi, M. *Solid State Ionics* **1985**, *17*, 107.
(282) Haas, K. H.; Schindewolf, U. *Ber. Bunsen-Ges. Phys. Chem.* **1983**, *87*, 346.
(283) Stephen, P. M. S.; Howe, A. T. *Solid State Ionics* **1980**, *1*, 461.
(284) Freund, F.; Wengler, H. *Ber. Bunsen-Ges. Phys. Chem.* **1980**, *84*, 866.
(285) Lechner, R. E.; Bleif, H. J.; Dachs, H.; Marx, R.; Stahn, M.; Anderson, I. *Solid State Ionics* **1991**, *46*, 25.
(286) Yamashita, K.; Kogyo, K. **1993**, *44*, 721.
(287) Takahashi, T.; Tanase, S.; Yamamoto, O.; Yamauchi, S. *J. Solid State Chem.* **1976**, *17*, 353.
(288) Lassègues, J. C. In ref 19, p 311.
(289) Maura, K. K.; Srivastava, N.; Hashmi, S. A.; Chandra, S. *J. Mater. Sci.* **1992**, *27*, 6357.
(290) Chandra, S.; Hashmi, S. A.; Prasad, G. *Solid State Ionics* **1990**, *40/41*, 651.
(291) Casciola, M.; Costantino, U.; Calevi, A. *Solid State Ionics* **1993**, *61*, 245.
(292) Casciola, M.; Chieli, S.; Costantino, U.; Peraio, A. *Solid State Ionics* **1991**, *46*, 53.
(293) Alberti, G.; Costantino, U.; Casciola, M.; Vivani, R.; Peraio, A. *Solid State Ionics* **1991**, *46*, 61.

type mechanisms) are the rates of diffusion (Γ_D) and reorganization (Γ_{reo}) of the proton "solvent" and the proton-transfer rate (Γ_{trans}). Before we examine the critical parameters controlling each rate, let us commence with some general considerations about hydrogen bonding. This kind of interaction is a common feature of most known proton conductors and appears to be the clue to a better understanding of the above addressed rates and their mutual dependences.

The hydrogen bond is a rather weak directional interaction. Its energy is only of the order of some kT ($\sim$0.1−0.6 eV) which is about 1 order of magnitude lower than the energy of other types of chemical bonds. This makes it extremely flexible and adaptable to its environment and sensitive to thermal fluctuations. In molecular liquids such as H_2O and NH_3, where hydrogen bonding is the predominant intermolecular interaction, this leads to transient short-range ordering with strong fluctuations in time and space. Although details of this situation are still unknown, this state between "order" and "disorder" has been described by the term "flickering cluster" already by Franks[294] for the local structure of liquid water.

Whereas the isolated dimer $H_5O_2^+$ finds its energetic minimum for a O/O separation of only 240 pm,[295,296] corresponding to a very strong symmetrical hydrogen bond, this bond is weakened due to the presence of additional hydrogen bonds in bulk water (see section 5.3). In the presence of other stronger ionic or covalent bonds, hydrogen bonds tend to fluctuate less. The proton donor/acceptor distance, which mainly determines the hydrogen-bond interaction, is then more confined by the stronger bonds of both proton donor and acceptor. The auxiliary hydrogen bonds have, so to say, to adopt to a structure, which is dominated by stronger interactions.

It is a striking observation that the compounds with the highest proton diffusivity are hydrogen-bonded liquids (e.g., dilute aqueous solutions of acids) or solids, in which weak or medium hydrogen-bond interactions are not or only slightly confined by the presence of other bond types. These are mostly soft materials such as heteropolyacid hydrates (e.g., $H_3PW_{12}O_{40}\cdot 29H_2O$) or acidic salts of oxo acids with big cations (e.g., $CsHSO_4$). For the further considerations it is therefore essential to include the hydrogen-bond fluctuations as well as the influence of the environment on its properties. This goes beyond approaches which attempt to explain proton conductivity just on a structural basis (e.g., refs 297 and 298).

4.2. Elements of Proton Conductivity. *4.2.1. Proton Transfer. 4.2.1.1. Proton Transfer as the Rate-Limiting Step.* One important aspect of the hydrogen bond is to provide a path for proton transfer from a proton donor to a proton acceptor. Besides its thermodynamic and geometrical properties, this aspect was recently referred to as the third fundamental property of the hydrogen bond.[299,300] For the few proton conductors with known rates of each transport step, the proton transfer along hydrogen bonds appears to limit the overall proton conductivity.

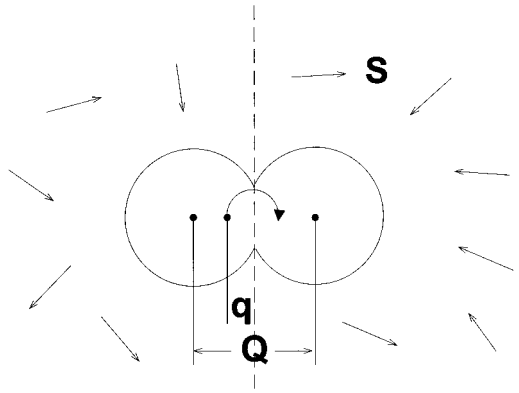

Figure 7. Coordinates determining proton-transfer reactions: **q**, the proton position with respect to the center of the hydrogen bond; **Q**, the proton donor/acceptor separation coordinate; **S**, the multi-dimensional solvent coordinate.

In the fast proton conductor $CsHSO_4$, e.g., dielectric absorption spectroscopy reveals a very high HSO_4^- reorientation rate of the order 10^{11} s^{-1}, whereas the proton-transfer rate is only in the 10^9 s^{-1} range (e.g., ref 123). From ^{17}O NMR of aqueous solutions of different pH the intermolecular proton transfer rate has been found to be only of the order of the molecular diffusion rate[301] (see also Figure 30). The conductivity of one of the first known solid fast proton conductors ($H_3OUO_2PO_4\cdot 3H_2O$, HUP[39]) was initially thought to occur via a Grotthuss-type mechanism. Indeed, the rather short oxygen separations and the disorder on the hydrogen-bond net (10 sites available for 9 protons[46]) seemed to favor this assumption. However, ^{18}O-tracer experiments showed that proton conductivity was controlled by the rate of molecular diffusion (vehicle mechanism), i.e., the intermolecular proton-transfer rate appeared to be even lower than the rate of molecular diffusion.[44] In the meantime, this is a general observation for proton conductivity in aqueous systems with a high concentration of excess protons.[302] These findings are in fundamental contrast to early suggestions that the extra proton of a H_3O^+ is rapidly exchanging with the water molecules of the first hydration sphere and that water reorientation is limiting the rate of proton conductivity in aqueous solutions.[303−305] Such considerations were inspired by the high de Broglie wavelength of the proton ($\sim$100 pm at 300 K) and the possibility of proton tunneling from the hydronium ion to an adjacent water molecule.

4.2.1.2. Static Proton-Transfer Potential. In the meantime, however, the potentials along the proton-transfer coordinate are better examined. For most known proton conductors the proton is coordinated to an oxygen and transfer occurs between adjacent oxygens as schematically illustrated in Figure 7, where the proton-transfer coordinate is denoted **q**.

(294) Frank, H. S. *Proc. R. Soc. London* **1958**, *A247*, 481.
(295) Scheiner, S. *J. Am. Chem. Soc.* **1981**, *103*, 315.
(296) Janoschek, R. *J. Mol. Struct.* **1994**, *321*, 45.
(297) Merinov, B. V.; Shuvalov, L. A. *Sov. Phys. Crystallogr.* **1992**, *37*, 211.
(298) Baranov, A. I.; Merinov, B. V.; Tregubchenko, A. V.; Khirznichenko, V. P.; Shuvalov, L. A.; Schagina, N. M. *Solid State Ionics* **1989**, *36*, 279.
(299) Maréchal, Y. *Proton Transfer in Hydrogen-Bonded Systems*; Bountis, T., Ed.; Plenum Press: New York, 1992; p 1.
(300) Maréchal, Y. *J. Mol. Liq.* **1991**, *48*, 253.
(301) Pfeifer, R.; Hertz, H. G. *Ber. Bunsen-Ges. Phys. Chem.* **1990**, *94*, 1349.
(302) Kreuer, K. D. In ref 19, p 474.
(303) Conway, B. E.; Bockris, J. O'M.; Linton, H. *J. Chem. Phys.* **1956**, *24*, 834.
(304) Eigen, M.; DeMaeyer, L. *Proc. R. Soc. London* **1958**, *A247*, 505.
(305) Eigen, M. *Angew. Chem.* **1963**, *75*, 489.

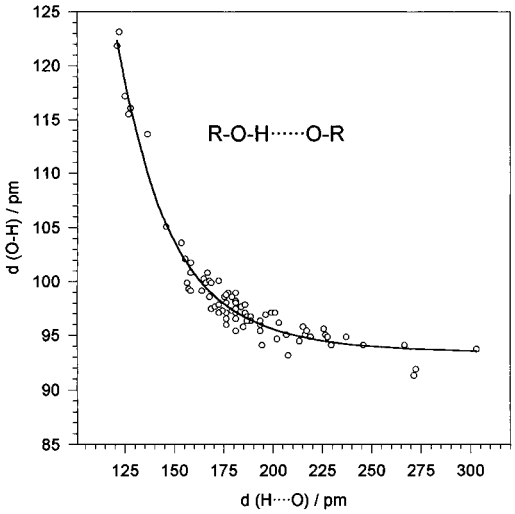

Figure 8. Bond distance relationship for hydrogen bonds of the type R−O−H···O−R in a variety of compounds.[309]

Let us first consider proton transfer while keeping the position of all other nuclei of the surroundings fixed. Only the electronic structures are allowed to respond to changes of the position of the proton along the proton-transfer coordinate **q** (Born−Oppenheimer approximation). A quantitative description of this situation is accessible by static high-level quantum chemical calculations which have been performed for a number of small clusters such as the oligomer $H_3O^+(H_2O)_n$.[306] The curvature of the potential surface in the vicinity of the proton equilibrium position may also be obtained from the frequency of the corresponding fundamental vibration (e.g., OH stretching). Spectroscopy of the overtones allows probing of the potential for higher energies.[307] Some qualitative features of the proton-transfer potential are obtained from elastic diffraction experiments, which reveal the average positions of protons in hydrogen bonds of periodic structures. For KDP (KH_2PO_4), for instance, the low-temperature structure exhibits a slightly split proton position indicating that the hydrogen bond potential for proton transfer is close to forming a single minimum for a proton donor/acceptor distance of ~248 pm (e.g., ref 308).

This observation corresponds to just one data point in Figure 8 showing the donor/proton versus the proton/acceptor distance for hydrogen bonds of the type RO−H···OR in a variety of compounds.[309] The data demonstrate (i) that the equilibrium position of the proton in a hydrogen bond for a given O/O separation is quite uniform for otherwise different environments (all data points lie close to one curve) and (ii) that the closest possible O/O separation is about 240 pm where the hydrogen bond becomes eventually symmetrical. This corresponds to a strong hydrogen bond contracting the O/O distance by about 40 pm.

Because of the relatively small scatter of these data, we may use the semiempirical potential given in ref 310 as a typical model potential for our first general considerations. The potential has been parameterized to a Lennard-Jones type potential by fitting the results

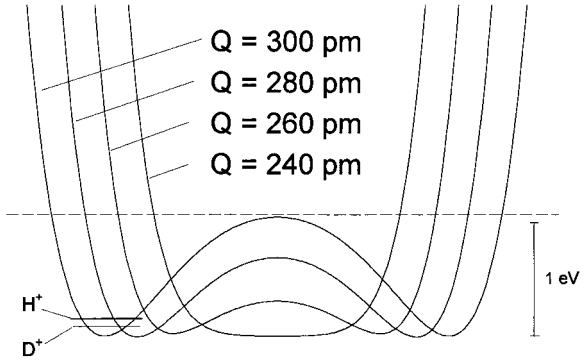

Figure 9. Semiempirical potential $E_Q(\mathbf{q})$ for proton transfer along hydrogen bonds of symmetrical configurations of the type R−O−H···O−R for different oxygen separations **Q** and full relaxation of the environment.[310] For one potential (Q = 300 pm) the H^+ and D^+ vibrational ground states and the transition state for proton (deuteron) transfer are indicated.

of quantum chemical calculations and experimental data. It is also in reasonable agreement with the bond distance relationship shown in Figure 8. Figure 9 shows this potential for various oxygen separations **Q**. For large distances it is a symmetrical double well with a barrier which successively decreases with decreasing oxygen separation. For separations below approximately 250 pm, it is eventually lower than the zero-point energy of the OH oscillator (~190 eV), i.e., the hydrogen bond becomes symmetrical, as already indicated by the relationship of Figure 8. The proton-transfer barrier reflects the fact that the proton suffers a depletion of electron density upon being transferred from the proton donor midway to the proton acceptor. For the largest oxygen separations this charge loss amounts to almost 0.1 electron,[295] but the proton is still embedded in a significant electron density in the transition state, i.e., it does not transfer through a completely "naked" state (see section 2). In fact, the electronic relaxation accompanying the transferring proton, smooths the effective transfer potential along **q**. For very short separations, the electron shells of donor and acceptor interpenetrate to such an extent that the barrier completely vanishes. It is worth mentioning, that any bending of the hydrogen bond leads to a further depletion of the electron density in the center of the bond and thus to some increase of the transfer barrier.[311]

The vibration of the proton in this potential (OH stretching) is quantized with a rather high energy separation corresponding to the low reduced mass of the oscillator. Therefore, the heights of the potential barriers in Figure 9 do not exactly relect the activation enthalpies for proton transfer across those barriers. As is also shown for one potential in Figure 9, the zero-point energy of the OH oscillator is about 190 meV above the bottom of the potential. Whereas this energy is about 60 meV higher than that of the OD oscillator, the energy difference successively decreases for the excited states because of the increasing flattening of the potential with increasing energy. Therefore, the transition-state energies of both oscillators (dashed line in Figure 9) are close to the energy of the top of the barrier for relatively high barriers. Consequently, the effective barrier for proton transfer is expected to be up to 60 meV lower than for deuteron transfer as already sug-

(306) Komatsuzaki, T.; Ohmine, I. *Chem. Phys.* **1994**, *180*, 239.
(307) Freund, F. In ref 19, p 138.
(308) McMahon, M. I.; Nelmes, R. J.; Kuhs, W. F.; Dorwarth, R.; Piltz, P. O.; Tun, Z. *Nature* **1990**, *348*, 317.
(309) Alig, H.; Lösel, J.; Trömel, M. *Z. Kristallogr.* **1994**, *209*, 18.
(310) Borgis, D.; Tarjus, G.; Azzouz, H. *J. Chem. Phys.* **1992**, *97*, 1390.

(311) Scheiner, S. *Acc. Chem. Res.* **1994**, *27*, 402.

gested by Bigeleisen.[312] This conclusion has later also been drawn for proton conductivity by Scherban, Liu, and Nowick (e.g., ref 232).

The attempt frequency for deuteron transfer is anticipated to be about $\sqrt{2}$ smaller than for proton transfer corresponding to the ratio of the frequencies of the two oscillators.

In any case, one might expect an increasing proton-transfer rate for a decreasing separation of proton donor and acceptor. This is observed in the very vew systems for which the prerequisite of a rigid, isotropic proton host is approximately fulfilled. But, as will be demonstrated in section 5, this does not hold for many proton conductors. There are compounds where proton transfer is rapid despite a large average proton donor/acceptor separation (e.g., in $BaCeO_3$-based compounds) as well as compounds where proton transfer is suppressed even in short hydrogen bonds (e.g., in the layer compound $H_3OUO_2AsO_4 \cdot 3H_2O$). Both observations are a result of the interaction of the proton with the dynamics of its nearest and next-nearest neighbors. This will be discussed in the next two sections.

*4.2.1.3. Influence of the Nearest Proton Environment (Oxygen Separation Coordinate **Q**).* We continue the discussion by including the effect of the nearest proton environment which is described by the one-dimensional coordinate **Q** representing the proton donor/acceptor separation (Figure 7). This already allows us to describe proton diffusivity in many compounds with low proton concentration such as certain oxides (see section 5.1).

The static or average oxygen separations $\mathbf{Q}_O$ of most good proton conductors, usually obtained from diffraction experiments, are generally higher than 260 pm which suggests asymmetric, medium, or weak hydrogen bonds.[313] In most cases, however, the corresponding transfer barriers in Figure 9 are even higher than the observed activation enthalpies of the total proton conductivity process.

One possible reason for this observation are the thermal fluctuations in the donor/acceptor separation coordinate **Q**, which may lower the effective barrier for proton transfer in the energy surface $E(\mathbf{q},\mathbf{Q})$. Of course, this potential remains symmetrical with respect to the middle of the hydrogen bond because of the inherent symmetry of the considered configuration.

Figure 10a−c shows three distinct ways to excite proton transfer in a potential $E(\mathbf{q},\mathbf{Q})$. In a rigid array of proton-donors and acceptors ($\mathbf{Q} = \mathbf{Q_O}$ = constant) the entire activation enthalpy is provided by the proton vibration (Figure 10a) and the attempt frequency is close to the donor/proton stretching frequency ($\sim 10^{14}$ s^{-1} for OH). Fluctuations in the proton donor/acceptor separation coordinate **Q**, however, may open proton-transfer paths with lower energy barriers. The corresponding transition states involve excitations in both coordinates **q** and **Q** (Figure 10b) or, as the other limiting case, only in **Q** (Figure 10c). The latter proton transfer is "adiabatic" in the sense that no excitation of the proton-transfer coordinate **q** is involved (usually the term "adiabatic" is used for a different case, i.e., when the proton environment is energetically completely relaxed at any instant of the proton transfer). The proton is, so to say, pushed half way by the donor before it is pulled the remaining distance by the acceptor, thus

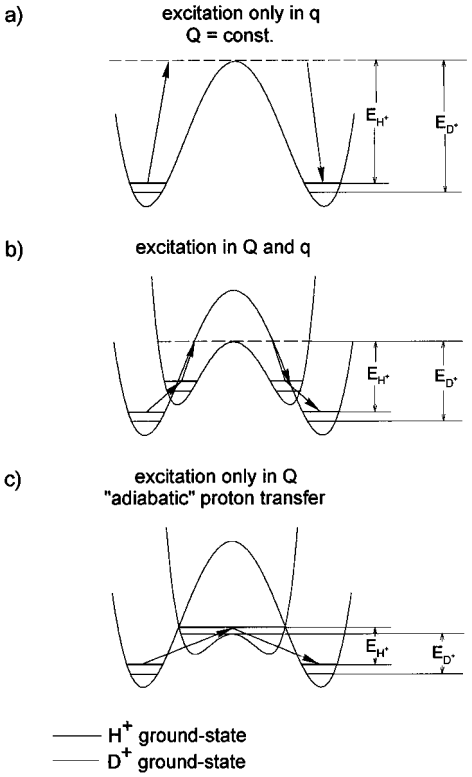

Figure 10. Different cases of proton transfer in the potential $E(\mathbf{q},\mathbf{Q})$. The transition states are indicated as dashed lines.

completing proton transfer. The oscillating proton remains in its vibrational ground state which is superimposed on this process. Therefore, a large part of the zero-point energy difference between the OH and OD oscillators is maintained in the transition state, which leads to a drastic decrease of the H/D isotopic effect for proton transfer (Figure 10c).[240] In the "adiabatic" limit, also the attempt frequency of proton transfer has decreased from that of the OH stretching mode to the frequency of the proton donor/acceptor oscillation which is usually one to two orders of magnitudes lower (10^{12}–10^{13} s^{-1}) depending on the masses of the involved moieties.

To what extent fluctuations in **q** and **Q** contribute to proton transfer in a given system depends on the relative "softness" of the two coordinates.

This is demonstrated in the contour maps of $E(\mathbf{q},\mathbf{Q}) = E_{\mathbf{Q}}(\mathbf{q}) + E(\mathbf{Q})$ (Figure 11). $E_{\mathbf{Q}}(\mathbf{q})$ is the model potential shown in Figure 9 and $E(\mathbf{Q})$ is expanded by second-, third-, and twelfth-order terms. The second-order (harmonic) coefficient is chosen according to a zero-point frequency of 10^{13} s^{-1}, which is a typical vibrational frequency of an oxygen in an oxide lattice. The twelfth-order coefficient prevents proton donor and acceptor from approaching significantly closer than 240 pm (see also Figure 8) and the third-order coefficient introduces the anharmonicity ("softness") into the potential. Only the latter is varied and expressed in terms of the corresponding thermal expansion coefficient α for convenience.

For the harmonic donor/acceptor vibration ($\alpha = 0$), the transition state of proton transfer involves only a small reduction of the donor/acceptor distance, and the transition-state energy (0.95 eV) is only slightly reduced compared to the static barrier (1.05 eV). With increasing "softening" of **Q** (up to $\alpha = 4 \times 10^{-6}$ K^{-1}), the transition-state energy remains almost unchanged, but

(312) Biegeleisen, J. *J. Chem. Phys.* **1949**, *17*, 675.
(313) Novak, A. *Struct. Bonding* **1974**, *18*, 177.

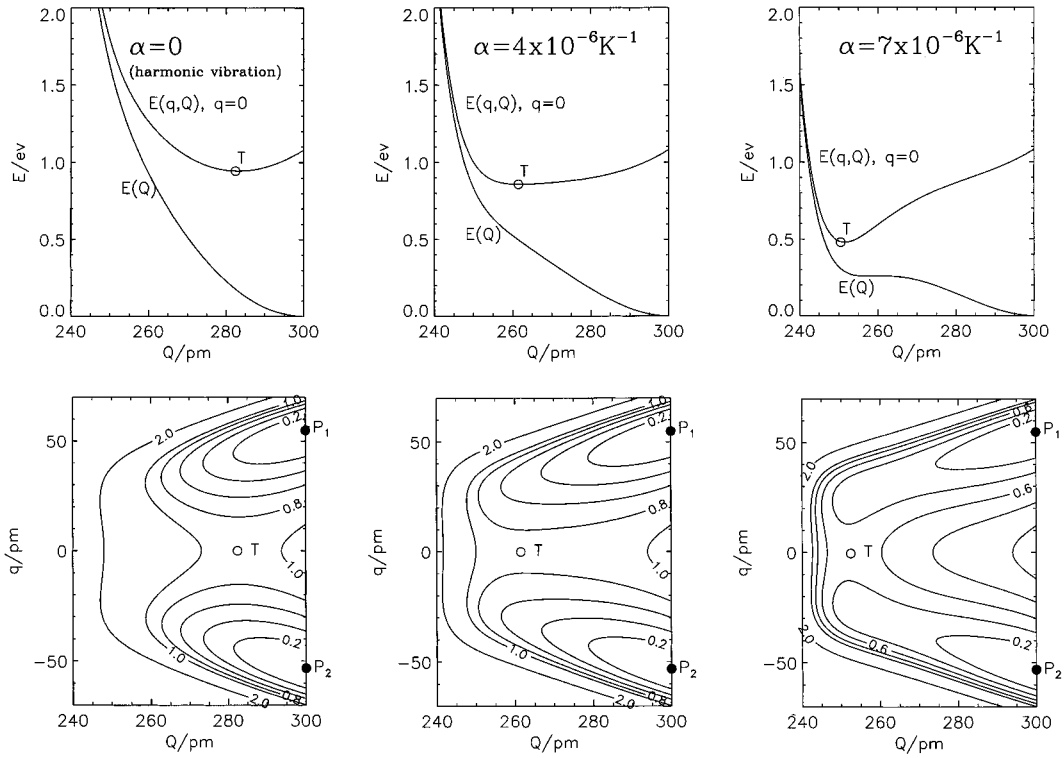

Figure 11. Model potential $E(\mathbf{q},\mathbf{Q})$ for different anharmonicities of the proton donor/acceptor vibration (anharmonicities are expressed in terms of the thermal expansion coefficient α and the contour unit is electronvolt). The transition states for proton transfer are indicated by T and the equilibrium positions of the proton by P_1 and P_2.

the position of the transition state in the **q**/**Q** plane shifts to smaller donor/acceptor separations **Q**. In other words, the partition of the vibrational excitation of proton donor and acceptor involved in the excitation of proton transfer is successively increased at the expense of the excitation in **q**. But further "softening" of **Q** ($a > 4 \times 10^{-6}$ K^{-1}) eventually leads to a significant decrease of the energy of the transition state, whereas its position remains almost unchanged just above **Q** = 240 pm, where the barrier along **q** disappears. That is the situation where no excitation in **q** is involved in proton transfer. Only excitations in the donor/acceptor separation coordinate **Q** is involved in the transition state which leads to a decrease of the proton transfer attempt frequency to that of the donor/acceptor vibration, as already pointed out above. Often this frequency is similar to the attempt frequency for the diffusion of the proton donor/proton complex as a whole, thus nicely demonstrating the relation between Grotthuss and vehicle mechanism (see also section 2).

The situation is summarized in Figure 12, showing the H- and D-transfer rates between fixed, harmonically, and anharmonically vibrating donors and acceptors as a function of temperature.[240] The effect of "softening" the donor/acceptor separation coordinate **Q** is to decrease the activation barrier, the attempt frequency, and the H/D isotope effect.

Of course, the use of a simple proton donor/acceptor vibration may illustrate only some principal features of proton transfer. Not only proton-conducting liquids but also solids generally show strong anharmonicities of the host species and, therefore, complex fluctuations of the proton donor/acceptor separation due to strong vibrational coupling, rather than periodic oscillations dominated by just one normal mode (see also Figures 14 and 24).

*4.2.1.4. Influence of the Next-Nearest Environment (Solvent Coordinate **S**).* Let us include all species of the

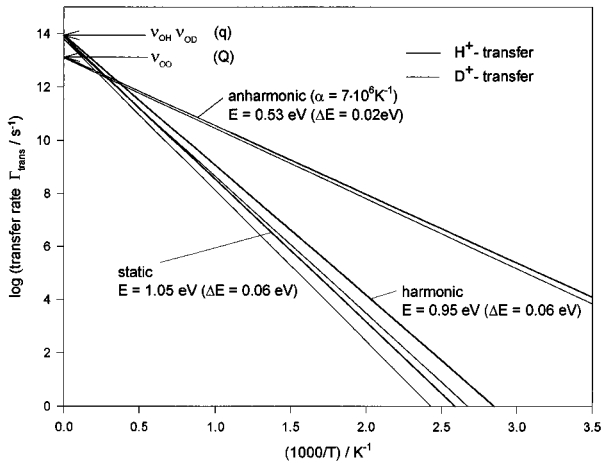

Figure 12. Modeled proton- and deuteron-transfer rates between static, harmonically, and anharmonically vibrating donors and acceptors.[240] The activation enthalpies (E) and their isotope effects (ΔE) are indicated.

next-nearest environment of the proton, i.e., all species beyond the proton donor and acceptor, into the solvent (Figure 7). This is necessary for describing proton conductivity in compounds with high dielectric constants in particular with high proton densities such as aqueous systems (see section 5.3).

In contrast to **Q** which is, for a linear hydrogen bond, just a scalar quantity, i.e., the modulus of the separation vector of two species, the much higher number of positional coordinates of the solvent species may be described only by a multidimensional coordinate **S** where the dependence of the proton-transfer potential on **S** is represented by a higher rank tensor. **S** may disturb the symmetry of the proton-transfer potential by polarizing the hydrogen bond, i.e., the two possible sites in the hydrogen bond become inequivalent. As for **Q**, we consider a time-independent, static part $\mathbf{S}_O$,

representing the average solvent configuration and the solvent fluctuations. Because of the much higher variety of possible species and positions, the solvent effects may be very different for different systems. They become particularly relevant to systems with high proton concentrations, where solvent effects are dominated by proton/proton interactions. The following considerations are only thought to illustrate principal cases. In section 5 the situation is quantified for acid aqueous solutions as a typical example for strong solvent interactions.

4.2.1.4.1. Proton Self-Localization and Solvent-Induced Proton Transfer. Let us first consider an isotropic solvent, where the effect of $\mathbf{S}_O$ does not disturb the symmetry of the average proton-transfer potential along the hydrogen bond. As already recognized by Zundel, the proton can easily be displaced within the hydrogen bond in an electric field, the "protonic" polarizability being about 2 orders of magnitude higher than usual electronic polarizabilities.[314−316]

This has two important implications for the proton-transfer potential in the presence of a polar solvent, especially when hydrogen bonds are mutually involved in solvent interactions: (i) the solvent accommodates to the position of the proton in the hydrogen bond which leads to an energetic stabilization of this particular position, i.e., the proton "digs" its own potential well, it is self-localized; (ii) the proton-transfer potential responds to solvent fluctuations which may even lead to solvent-induced proton-transfer events. The distribution of protons over the different hydrogen-bond sites may, therefore, be discussed as a result of the competition between enthalpy and entropy.

$E_{\mathbf{Q}}(\mathbf{q},\mathbf{S})$ is illustrated in Figure 13. For the average solvent coordinate, $\mathbf{S} = \mathbf{S}_O$, the proton-transfer potential is symmetrical. But the longer the proton resides oscillating in one of the equivalent wells, the more this site stabilizes at the expense of the other by the solvent relaxation. The proton is energetically stabilized on one of the two sites of the hydrogen bond corresponding to the self-localization energy ΔE_{loc}. At any finite temperature, however, this self-localization energy is competing with the entropy of the whole system, in particular the configurational and vibrational entropy of the protons and the solvent. As for the coordinate $\mathbf{Q}$, a soft solvent coordinate $\mathbf{S}$ may open proton-transfer paths with low transition-state energies $\Delta E_{\mathrm{HT}} = \Delta E(\mathbf{q}) + \Delta E(\mathbf{S})$ where $\Delta E(\mathbf{S}) \lesssim {}^1/_2\Delta E_{\mathrm{loc}}$ (Figure 13). In an isotropic solvent the transition state corresponds to a symmetrical solvent configuration with respect to the center of the hydrogen bond and a symmetrical proton-transfer potential $E_{\mathbf{Q},\mathbf{S}_O}(q)$.

In any case, solvent interactions decrease the rate of proton transfer for two reasons: (i) the activation enthalpy ΔE_{HT} increases by the amount equal to the solvent activation energy $\Delta E(\mathbf{S})$, which mainly depends on the degree of interaction and the time the proton resides on one position, i.e., the rate of proton-transfer compared to that of solvent relaxation; (ii) the attempt frequency of proton transfer is expected to decrease to the rate of solvent fluctuations, which is generally lower than $\sim 10^{12}$ s^{-1}.

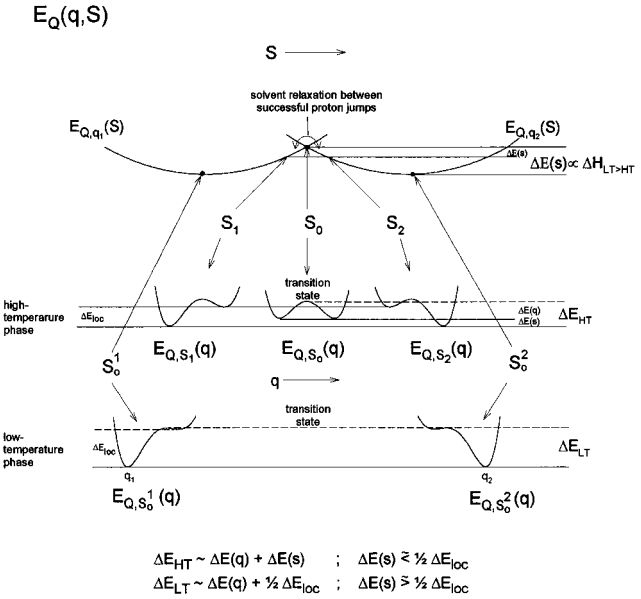

Figure 13. Proton transfer and proton ordering in the presence of proton/solvent interactions: Schematic representation of the proton transfer potential $E_{\mathbf{Q}}(\mathbf{q},\mathbf{S})$ for fluctuations of $\mathbf{S}$ around an isotropic solvent coordinate $\mathbf{S}_O$ (high-temperature phase) and anisotropic solvent coordinate $\mathbf{S}_O^1$ or $\mathbf{S}_O^2$ (low-temperature phase, see text). The proton donor/acceptor separation coordinate $\mathbf{Q}$ is taken as fixed as opposed to the configuration illustrated in Figure 15b.

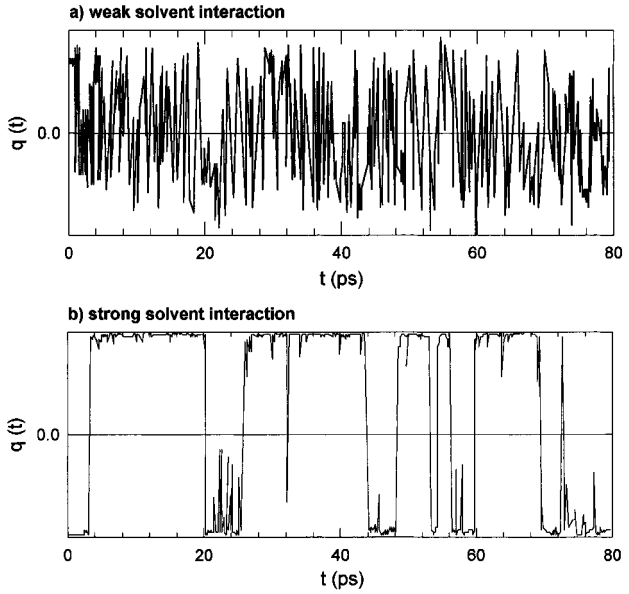

Figure 14. Modeled proton motion in hydrogen bonds experiencing different solvent interaction.[310] The system passes from a more "oscillative" (a) to a more "reactive" regime (b) for increasing solvent interaction, thus suppressing the effective rate of proton transfer.

Owing to the high anharmonicities and the corresponding vibrational coupling in good proton conductors, these fluctuations and the resulting motion of the proton in real space may be very complex. This becomes apparent in the results of a MD simulation of a model system with strong hydrogen bonding,[310] showing that proton transfer passes from a more "oscillative" (Figure 14a) to a more "reactive" regime (Figure 14b) for an increasing solvent interaction. This simulation has been carried out for a constant $\mathbf{Q}$. But the effects of the fluctuations in $\mathbf{Q}$ are always superimposed on the solvent effects, where $\Delta E(\mathbf{Q})$ may also depend on the

(314) Zundel, G.; Eckert, M. *J. Mol. Struct. (THEOCHEM)* **1989**, *200*, 73.
(315) Eckert, M.; Zundel, G. *J. Phys. Chem.* **1987**, *91*, 5170.
(316) Janoschek, R.; Weidemann, E. G.; Zundel, G. *J. Chem. Soc., Faraday Trans.* **1973**, *2*, 69, 771.

solvent coordinate **S** as a result of multiparticle interactions.

General expressions for the potential surface $E(\mathbf{q},\mathbf{Q},\mathbf{S})$ or even the Gibbs energy surface $G(\mathbf{q},\mathbf{Q},\mathbf{S})$ are not available so far. But at least their solvent contribution $E_{\mathbf{q},\mathbf{Q}}(\mathbf{S})$ describing the creation of a symmetrical solvent coordinate **S** may be formulated in close analogy to corresponding expressions of the theory of polarons[317] and the Marcus theory of electron transfer.[318] Because of the high proton density in many proton conductors, such approaches must be supplemented by cooperative effects as a result of mutual hydrogen-bond polarization. This leads to the ordering of protons below so-called "superprotonic" phase transitions, which will be treated in the next section.

4.2.1.4.2. Proton-Transfer and "Superprotonic" Phase Transitions. In Figure 13 the energy $\Delta E(\mathbf{S})$ required to produce a symmetrical solvent configuration $\mathbf{S}_O$ is lower than about half the self-localization energy ΔE_{loc}.

But with a decreasing rate of proton transfer, i.e., with decreasing temperature, an increasing relaxation time between proton jumps is provided for the solvent to accommodate to the position of the proton. Thus the long-range part of the solvent interaction becomes successively accessible, i.e., $\Delta E(\mathbf{S})$ increases more than ΔE_{loc} until $\Delta E(\mathbf{S}) > {}^1/_2\Delta E_{loc}$. This means that less activation energy is required for proton transfer in its unmodulated asymmetrical transfer potential compared to transfer in a symmetrical potential corresponding to an activated symmetrical solvent configuration. But as the proton prefers to reside on one of the two positions in this polarized hydrogen bond, the solvent is provided with sufficient time to almost completely accommodate to this preferred proton position. When the solvent interaction is mainly due to proton/proton interactions (high proton density), i.e., to the mutual polarization of hydrogen bonds, this leads to a first-order phase transition, where ordering of the whole hydrogen-bond network is established. Then, $\Delta E(\mathbf{S}) \gg {}^1/_2\Delta E_{loc}$ and the solvent interaction extends to more than nearest-neighbor interaction, i.e., longer range interactions, which mainly contribute to $\Delta E(\mathbf{S})$ compared to ΔE_{loc}, determine the average structure. This is probably the reason why in fast conducting phases no significant correlation of proton transfers are observed. As soon as correlation extends to more than transfer in neighboring hydrogen bonds, the system responds with a macroscopic proton ordering in a first-order phase transition (e.g., the "superprotonic" phase transition of $CsHSO_4$). The proton-transfer potentials $E^1_{\mathbf{S}_O}(q)$ and $E^2_{\mathbf{S}_O}(q)$ in the low-temperature phase are also illustrated in Figure 13. As opposed to the high-temperature phase where the self-localization is transient, giving an additional contribution to the activation enthalpy of proton transfer only, the self-localization in the low-temperature phase becomes static in a frustrated structure corresponding to one of the two equivalent solvent configurations $\mathbf{S}^1_O$ and $\mathbf{S}^2_O$.

The relative energy stabilization of the whole system with respect to the high-temperature phase is raised at the expense of a loss of entropy, i.e., the phase transition is endothermic. To a good approximation this entropy is often just the difference of the configurational entropy of the hydrogen bond network ΔS_{config} of the two phases (see section 5.2). The phase transition temperature is then $T_{LT>HT} \sim \Delta E(\mathbf{S})/\Delta \mathbf{S}_{config}$ (see Figure 13). Therefore, such phase transitions are observed only in systems with small solvent interactions. This is, in particular, the case when the protons are well separated, e.g., by big anions, which themselves are only poorly polarizable thus giving no significant extra solvent effect. Compounds with strong proton/proton interactions frequently decompose or melt before the transition temperature is reached. Examples of superprotonic phase transitions will be provided in section 5.2.

Of course, hydrogen bonding is relevant only for structure and dynamics in the absence of other stronger interactions. These may produce anisotropic structures which do not transform into disordered phases. Especially when the structure is polar, the resulting electric fields may bias hydrogen bonds to such an extent that proton transfer is practically suppressed by the static solvent effect. This is relevant in particular for polar layered compounds and for aqueous adsorbates on polar surfaces.

4.2.1.5. Proton Tunneling versus Hopping. So far, we have just considered hopping of the proton, either being assisted or suppressed by the interaction with its environment. All motions are taken as classical except for the energy quantization of the OH (OD) stretching mode which may give rise to a minor H/D isotope effect for the proton-transfer rate.

We cannot rule out resonant proton tunneling effects, a priori, because of the low proton mass and the relatively narrow potential barriers in the considered systems (see Figure 9). But the requirements for tunneling through barriers are rather rigorous. For given barrier dimensions the tunneling matrix element has a very narrow maximum (i) in the case of energy conservation, i.e., states of identical energy are available on both sides of the barrier and (ii) the Frank−Condon approximation is valid, i.e., the positional and vibrational coordinates of all neighboring species do not change during the tunneling process (e.g., ref 319).

For the structure of proton systems in their energetic minimum ($T = 0$ K), the first requirement is expected to be violated because of the self-localization of the proton, inducing asymmetry into the hydrogen-bond potential with respect to proton tunneling (see Figures 13 and 29). This has contributions not only from the relaxation of the positional and vibrational coordinates of the solvent but also from the electronic relaxation, especially of the valence electrons of the proton donor and acceptor. The latter is not relevant for classical motions, because the Born−Oppenheimer approximation may be assumed, i.e., the classical motion of all nuclei is adiabatic with respect to the electronic relaxation, which is not necessarily the case for tunneling.

With increasing temperature, the thermal fluctuations of the proton environment may occasionally compensate for the proton self-localization in thermally activated coincident configurations, where the energy levels of neighboring potential wells become temporarily degenerate, thus increasing the proton tunneling probability. This process of incoherent phonon-assisted tunneling is still thermally activated because of the

(317) Fröhlich, H. *Adv. Phys.* **1954**, *3*, 325.
(318) Marcus, R. A. *J. Chem. Phys.* **1956**, *24*, 966.
(319) Lewis, E. S. In *Proton-Transfer Reactions*; Caldin, E., Gold, V., Eds.; Chapman and Hall: New York, 1975; p 317.

thermal activation of the involved phonons.[320] This proton transfer mechanism has only been confirmed by the extremely large H/D isotope effect for hydrogen diffusion in some metals.[321,322] In proton conductors, however, the H/D isotope effect hardly exceeds a value of 5 even at low temperature, which may simply be explained by the difference of zero-point energies (see section 4.2.1.3) rather than by proton tunneling.

Obviously, the dynamics involved in proton-transfer and structural reorganization, which are both required for fast proton conductivity, produce sufficient incoherence, such that classical hopping dominates proton tunneling processes at reasonably high temperature. This makes sense when one considers that proton conductors are usually much softer than metals showing proton tunneling. As already pointed out in section 4.2.1.3, proton transfer in very good proton conductors probably occurs almost barrierless ("adiabatic" limit), where the concept of tunneling does not make sense anymore. Of course, such transfers may include tunneling through some remaining barrier, however, with a tunneling matrix element close to unity and no significant mass dependence.

On the other hand, in systems where proton transfer does not lead to proton conductivity, i.e., in the absence of fast structural reorganization, large H/D effects at low temperature are very common. They can exceed a factor of 100 as in the case of benzoic acid dimers[323] and thioindigo,[324] which is a clear indication for resonant proton tunneling.

Some authors have claimed the appearance of proton tunneling also for proton conduction phenomena, e.g., in hydrated proteins[325] and perchloric acid.[326]

Also coherent tunneling, i.e., simultaneous tunneling of the proton and the perturbation of its environment (self-localization) may be considered. But only in metals at very low temperature is this indicated to occur on a local scale in two-level systems (e.g., niobium with traces of oxygen as a host for hydrogen[327]).

4.2.2. Structural Reorganization: Reorientation, Rotation, Diffusion, and Cooperative Phenomena. The remaining modes which have been considered as elements of proton-conduction processes are diffusion of large structural entities, and structural reorganization comprising rotation or just reorientation modes. These are either a physical part of the proton migration path (Γ_D, Γ_{reo} in Figure 2) or they are elements of the structural reorganization going along with the migration of protons (Γ^S_{reo} in Figure 2).

High rates of such modes are not in accordance with the breaking of any directional chemical bond except weak hydrogen bonding. It is, therefore, not surprising that the species involved in fast proton-conduction processes are either just weakly hydrogen bonded or they show reorientation around covalent σ-bonds, which gives no contribution to the activation barrier. As opposed to the effect on the rate of proton transfer, a strengthening of the hydrogen bonding stabilizes the position and orientation of the considered species and therefore leads to a suppression of the rates of all modes requiring bending or rupturing of such bonds. An electric field at the position of the considered species may be generated by Coulomb interactions, especially in polar, anisotropic media or at surfaces and interfaces. Since the structural reorganization accompanying the migration of the proton charge occurs along with a change of the electrical moment, this interaction also suppresses the rate of structural reorganization.

As well as the proton-transfer mode, also the rates of diffusion, rotation, and reorientation are expected to depend on fluctuations of the positional coordinates of the environment. The energy of the central hydrogen bond in, e.g., the $H_5O_2^+$ dimer, which is closely related to the reorientation barrier, depends nonlinearly on the oxygen separation[328,329] (see also Figure 16). Therefore, not only the rate of proton transfer but also the rate of breaking the central hydrogen bond is expected to be affected by fluctuations of the oxygen separation in real systems. This is very sensitive to the coupling with the environment because of the weakness of the hydrogen-bond interaction. This coupling mediates the energy transfer between neighboring hydrogen bonds, which is required to obey energy conservation for the whole system, when the energy of the considered bond, i.e., the donor/acceptor separation, changes. Because of the nonlinear distance/energy relationship an increased partition of short bonds is expected to coexist with an increased partition of long hydrogen bonds for a given volume. There is still a debate about "random network" and "cluster" models, especially for the hydrogen-bonded structure of water (e.g., ref 330), but some dynamical patterning of hydrogen-bonded networks are favored by the above considerations. This might cause an additional energy contribution to the activation enthalpy and entropy contribution to the preexponential factor of the rate of structural reorganization. Of course, this effect should be successively dominated by thermal excitations which may be a reason for the non-Arrhenius behavior of transport properties in weakly hydrogen-bonded networks such as liquid water (see section 5.3).

The limiting cases of the described patterning as a result of the coupling between hydrogen bonds are schematically illustrated in Figure 15. Figure 15a shows the totally disordered situation with a high number of equivalent proton sites between evenly distributed proton donors and acceptors, and Figure 15b the perfectly ordered state where the number of sites is reduced to the number of protons, i.e., the site occupancy is unity (see also Figure 23). As already described in section 4.2.1.4.2, this ordering as a result of proton/proton interaction comprises the preferential occupancy of one site with respect to the other in one hydrogen bond, and the ordering of the hydrogen-bond orientation with respect to that of neighboring bonds. But, in addition, also the heavy host species tend to

(320) Flynn, C. P.; Stoneham, A. M. *Phys. Rev.* **1970**, *B1*, 3966.
(321) Völkl, J.; Alefeld, G. In *Diffusion in Solids, Recent Developments*; Nowick, A. S., Burton, L. J. J., Eds.; Academic Press: New York, 1975; p 231.
(322) Messer, R.; Blessing, A.; Dais, S.; Höpfel, D.; Majer, G.; Schmidt, C.; Seeger, A.; Zag, W.; Lässer, R. *Z. Phys. Chem. N. F.* **1986**, *Suppl.-H.2*, 61.
(323) Rambaud, C.; Oppenländer, A.; Pierre, M.; Trommsdorff, H. P.; Vial, J. C. *Chem. Phys.* **1989**, *136*, 335.
(324) Clemens, J. M.; Hochstrasser, R. M.; Trommsdorff, H. P. *J. Chem. Phys.* **1984**, *80*, 1744.
(325) Careri, G.; Consolini, G. *Ber. Bunsen-Ges. Phys. Chem.* **1991**, *95*, 376.
(326) Cappadonia, M.; Kornyshev, A. A.; Krause, S.; Kuzuetsov, M.; Stimming, U. *Solid State Ionics* **1995**, *77*, 65.
(327) Wipf, H.; Steinbinder, D.; Neumaier, K.; Gutsmiedl, P.; Magerl, A.; Dianoux, A. J. *Europhys. Lett.* **1987**, *4*, 1379.
(328) Janoschek, R.; Widemann, E. G.; Zundel, G. *J. Am. Chem. Soc.* **1972**, *94*, 2387.
(329) Scheiner, S. *Int. J. Quantum. Chem.* **1980**, *7*, 199.
(330) Belch, A. C.; Rice, S. A.; Sceats, M. G. *Chem. Phys. Lett.* **1981**, *77*, 455.

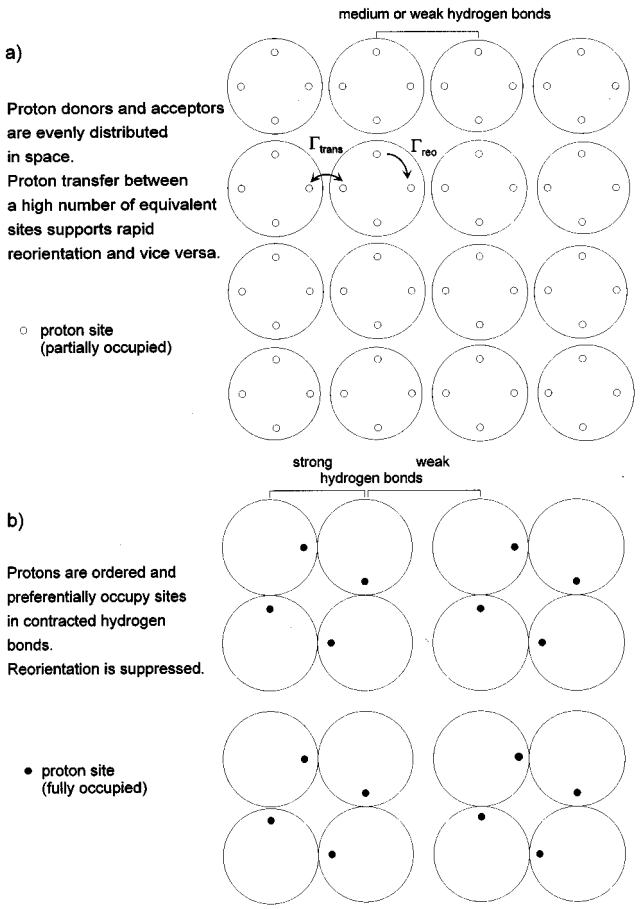

Figure 15. Schematic illustration of the patterning of the heavy particles in hydrogen-bonded networks as a result of proton ordering (see Figure 13) and energy transfer between hydrogen bonds (see text). Only the two limiting cases (a) complete disorder and (b) perfect order are illustrated.

order gaining energy by the contraction of hydrogen bonds within the "cluster" (these can be dimers, chains, ribbons, layers, or other structural units) and the elongation of hydrogen bonds between such structural units of ordered phases.

Above so-called "superprotonic" phase transitions the average structure is closer to that of Figure 15a, possibly with some dynamical patterning due to short-range coupling. The random distribution of protons leads to a transient accumulation and depletion of proton charge on all sites, which are thus on average only partially occupied. This self-dissociation is essential for the appearance of proton conductivity.

When the coupling extends to the whole crystal, an ordered phase close to the structure of Figure 15b is formed (see also section 4.2.1.4.2). But at any finite temperature this structure has some translational and reorientational defects (see also section 5.2), which still allow some structural reorganization besides some proton transfer. It is obvious that the onset of proton-transfer (Γ_{trans}) and proton-donor and -acceptor reorientation (Γ_{reo}) are mutually dependent and, therefore, frequently appear simultaneously with order/disorder phase transitions.

In short, at low temperature there is long-range ordering with some discrete point defects, which may cause some residual conductivity, whereas at high temperature structural disorder possibly with some dynamical patterning (ordering) goes along with high proton conductivity. Both states may be separated by a phase transition.

Cooperativity is also important for the diffusion of species involved in proton transport. This is particularly relevant for proton conductors where proton transport is related to the dynamics of small molecules such as H_2O and NH_3. This diffusion may be an element of a vehicle mechanism or be involved in proton-transfer reactions as part of a Grotthuss mechanism (see section 5.3.2). In aqueous solution, e.g., the activation enthalpy of H_2O (H_3O^+) diffusion at room temperature is even smaller than the average energy of a single hydrogen bond (~170 meV compared to ~200 meV). The dynamical patterning of the hydrogen-bonded structure may provide this low-energy molecular diffusion path (see also section 5.3). Besides the energy distribution between bonds also the accessible free volume has to be considered for diffusion processes. This includes "bottleneck" considerations which are particularly relevant for the diffusion in solids (e.g., ref 331).

Several authors have envisaged the concept of solitons as a collective excitation to explain proton conductivity (e.g., ref 332). This idea is probably stimulated by the old concept of extended Grotthuss chains still present in many textbooks of physical chemistry. In fact, there is no experimental confirmation for correlation effects comprising more than two transfer events in accordance with the considerations in section 4.2.1.4.

4.3. Proton Conductivity: A Complex Process. To establish fast proton transport over macroscopic distances, all elements of the transport process have to gear like the cog wheels of a transmission at sufficiently high rate in order to produce a fast uninterrupted proton-transport trajectory. But the elementary reactions may depend on the interactions with the environment in a conflicting way.

Short, strong hydrogen bonding favors intrabond proton transfer but suppresses the rates of diffusion, rotation, and reorientation of the involved species, whereas the opposite is true for weak hydrogen bonding. This is demonstrated in Figure 16 which shows the static barrier for proton transfer and the hydrogen-bond energy as a function of the oxygen separation. The latter is closely related to the activation enthalpy of molecular rotation involving breaking of the central hydrogen bond of the H_2O/H_3O^+ dimer as a function of the oxygen separation. Only for medium hydrogen bonds is the barrier for both modes reasonably low. Indeed, good proton-conducting phases usually show only medium or sometimes even weak hydrogen bonding as demonstrated by comparing hydrogen-bond lengths in good and poor proton-conducting sulfates (Figure 23). Of course, this conflicting situation is diminished to some extent by the fluctuations of the donor/acceptor separation which become apparent as high Debye–Waller factors (temperature factors) of the donor and acceptor species (see also Figure 20). The systems then pass through configurations where hydrogen bonds are compressed, thus assisting proton transfer, and configurations where hydrogen bonds are weakened which assists structural reorganization.

In fact, the highest proton conductivities are observed in liquids (see all figures in section 2) and fast proton-

(331) Kreuer, K. D.; Weppner, W.; Rabenau, A. *Mater. Res. Bull.* **1982**, 17, 501.

(332) Salvin, A. V.; Zolotaryuk, A. V. *Phys. Rev.* **1991**, *A44*, 8167.

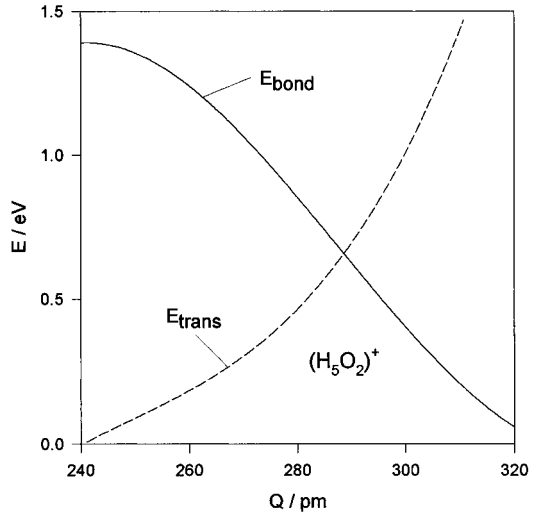

Figure 16. Hydrogen-bond energy E_{bond} and barrier for adiabatic proton transfer E_{trans} for the dimer $(H_5O_2)^+$ as a function of the proton donor/acceptor separation **Q** obtained from ab initio calculations.[295]

conducting solids show liquidlike dynamics of the species involved in the conduction process.

At low temperature the translational modes are usually excluded from that dynamics, i.e., the conductivity is Grotthuss-type. But with increasing temperature the progressive elongation and breaking of hydrogen bonds may (i) suppress proton transfer and (ii) release the translational degrees of freedom, i.e., there is a gradual transition from Grotthuss to vehicle-type conductivity.

The situation becomes even more complex if solvent effects are included. On one hand the modes involved in the solvent rearrangement (diffusion, rotation, reorientation) contribute to the self-localization of the proton at one side of the hydrogen bond; on the other hand they are also a necessary part of the proton diffusion trajectory (see Figure 2). This is probably the reason some compounds, where the proton is associated with big, rigid anions and nonpolar materials with a low dielectric constant, are among the best proton conductors. Rigid anions give only small contributions to the solvent effect because of their small dielectric polarizability, and they efficiently separate neighboring hydrogen bonds by their large size, thus diminishing the mutual polarization of neighboring hydrogen bonds. The proton disorder provides the isotropic environment which minimizes the barriers for the reorientation of these anions which, in turn, averages solvent effects with respect to proton transfer, thus supporting Grotthuss-type conduction (Figure 15a). Therefore, proton disordering and fast reorientation modes frequently set on together at "superprotonic" phase transitions.

The electrostatic contribution to this scenario reflects the dielectric response as a function of frequency and space. On one hand the necessary structure reorganization along the proton diffusion path contributes to the local dielectric response, which, on the other hand, induces solvent effects on proton transfer when it has contributions below the proton-transfer frequency. In fast proton conductors, however, this effect is small, because structural reorganization is much faster than proton transfer (see section 4.2.1), i.e., the protons "see" an isotropic solvent on the time scale of the proton transfer. Of course, any static polarization or low-frequency dielectric response of the environment along the proton diffusion path tends to suppress the transport rate. Therefore, the optimum scenario for fast proton conductivity with respect to the dielectric properties is a large high-frequency dielectric constant and little contributions at low frequency ($\epsilon_O - \epsilon_\infty$) of the proton diffusion path embedded in a nonpolar environment characterized by covalent rather than ionic interactions.

4.4. Simulation of Proton Conductivity. The above-addressed two aspects give just a flavor of the complexity of the interactions. It is the very nature of proton conductivity that many particles, mutually interacting on different time scales, are involved. Therefore, there have been only few attempts at a full simulation of proton conductivity.

The initial crude approaches are static lattice simulations, where the positions of all nuclei except the proton are taken as fixed. Energy minimization then suggests a proton diffusion path in the rigid array of host species. Only electrostatic interactions are considered in a simulation of proton conductivity in some perovskite-type oxides.[333] Somewhat better results are obtained from static high-level quantum chemical calculations. The results describe better the effect of covalency, e.g., in $BaCeO_3$-based compounds, where the CeO_6 octahedron contains strong covalent bonds. Considering the strong coupling of the proton dynamics to that of its environment, the static calculations produce by far too high activation barriers. In addition they lose any entropic effect.

More sophisticated simulations, therefore, also include the dynamics of all species. If the system is predominently ionic, classical MD simulations are useful. The equations of motion for all particles are solved for forces obtained from the superposition of pair potentials. These are frequently described by a short-range, repulsive Buckingham term and a long-range Coulomb term. The corresponding parameters are either chosen such that the equilibrium structure is reproduced, or they are fitted to spectroscopic data. The potential of the proton in the hydrogen bond can be obtained only experimentally or by quantum chemical calculations. Such simulations are realistic only when the dynamics of the host are dominated by ionic interactions, i.e., the hydrogen-bond interaction, which cannot be precisely described by Coulomb interactions only, is just following the dynamics of the host and not vice versa. This is the framework of a first classical MD simulation of proton conductivity in $CsHSO_4$ advanced by Münch et al.[334] (see section 5.2).

But if the dynamics of the system are influenced by directional interactions, i.e., covalent and hydrogen bonding, quantum chemical ab initio MD simulations provide a higher level of sophistication. For such simulations, the forces are directly calculated from the electronic structure with the Hellmann−Feynman theorem. With these forces the equations of classical motion are then solved in the usual way.

Especially when the system is dominated by hydrogen-bond interactions, the quality of the quantum chemical part of the simulation highly depends on its self-

(333) Mitsui, A.; Miyayama; Yangagida, H. *Solid State Ionics* **1987**, *22*, 213.
(334) Münch, W.; Kreuer, K. D.; Traub, U.; Maier, J. *Solid State Ionics* **1995**, *77*, 10.

consistency. In Car−Parrinello type simulations[335,336] this is achieved by applying local density functional (LDF) with gradient correction for the wave functions of the valence electrons, which are expanded as a series of plane waves (the core electrons are usually described by a pseudopotential). At the moment, this method is unfortunately limited to the treatment of few valence electrons and the simulation of short times (some picoseconds). It has been successfully applied to the simulation of proton transfer in liquid water with one excess proton[337] (see also section 5.3).

Many proton-conducting compounds, however, contain heavy atoms involved in covalent bonds. These compounds can be calculated using different quantum chemical methods. In particular, the quantum molecular dynamics technique developed by Seifert et al.[338] using a LCAO scheme with LDF seems a reasonable approach for simulating the dynamics of the heavy particles, but hydrogen-bond features are not yet well described by this technique. It is currently being further developed for the simulation of proton conductivity in cerates by Münch et al.[339] (see also cover page of this issue).

The applicability of simulations always depends on whether the appropriate physical model is chosen. If this is the case, they may even reach a level where some predictive character is achieved because of the exclusive advantage to vary relevant parameters independently (e.g., the mass, size, charge, and polarizability of species). The simultaneous application of appropriate simulation techniques and experiments provides an interesting route to a deeper understanding of proton-conduction processes and the development of new proton-conducting materials.

5. Compounds and Conduction Mechanisms

Section 4 provides some insight into the complexity of interactions in proton-conduction phenomena. There is no compound for which the whole set of data of relevant modes and interactions is available. But the similarities in the macroscopic phenomenology suggest that the underlying proton-transport processes on a molecular scale are also related among compounds of one family. It is, therefore, reasonable to compile relevant data from different compounds in order to form a "puzzle" describing the principal situation for each family of compounds.

These will be treated in the order of increasing complexity of the transport mechanism. It appears as an anachronism that aqueous media, for which proton conductivity is known since the early days of physical chemistry, show the most complex proton-transport processes, whereas proton conductivity of relatively "modern" materials, such as oxides, can be interpreted more easily. As opposed to the order in section 3, we therefore start with oxides followed by compounds based on oxo acids before the transport processes in aqueous media will be treated.

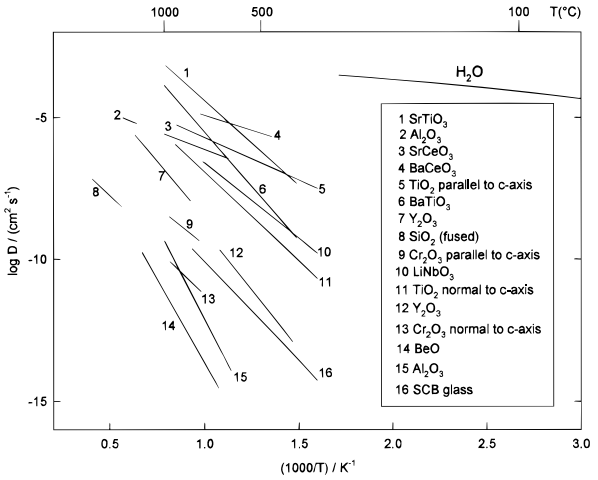

Figure 17. Diffusivity of protonic defects (OH_O^*) in a variety of oxides.[221,239] The self-diffusion coefficient of water is given for comparison.

5.1. Oxides. Oxides are the family of compounds for which proton conductivity was established most recently. This was probably due to the low concentration of protonic defects ($OH_O^\bullet$) which corresponds to a hydroxyl ion on an oxygen site) in most oxides under normal conditions. But as can be seen from Figure 17 high diffusivities of protonic defects in oxides are a widespread phenomenon at elevated temperature.

At these temperatures the weak hydrogen-bond interaction is not expected to have a significant influence on the average position and dynamics of the heavy host species. These are rather dominated by the much stronger ionic and covalent interactions in high melting oxides. Because of the low proton concentration, solvent effects as a consequence of proton/proton interaction may be neglected. The high covalency and the corresponding low dielectric constant of oxides with high proton diffusivities[229] also suggest that there are only minor solvent effects arising from the displacement of other charged species in such oxides. This is, in particular, valid for $BaCeO_3$-based compounds in which the oxygen is involved in rather covalent Ce−O interactions. The problem may, therefore, be reduced to the coupling of the proton to the dynamics of its two intimate nearest oxygens, i.e., it may approximately be described on the basis of fluctuations of the oxygen separation coordinate **Q**. A recent quantum chemical calculation has identified the equilibrium site of the proton between two adjacent oxygens in perovskite-type oxides.[340]

The principal proton conduction mechanism involves proton transfer between adjacent OH^- and O^{2-} and OH^- reorientation (Grotthuss mechanism) rather than OH^- diffusion as sometimes emphasized.[223,235,341]

This has been directly proven for $BaCeO_3$-based compounds and some rare-earth sesquioxides. For the first, the ^{18}O-tracer diffusion coefficient is found to be more than 3 orders of magnitude smaller than is necessary to explain the diffusivity of the protonic defect via hydroxyl ion migration.[239] For the latter, the results of EMF experiments in oxygen, hydrogen, and water concentration gradients are consistent only with the

(335) Car, R.; Parrinello, M. *Phys. Rev. Lett.* **1985**, *55*, 2471.
(336) Laasonen, K.; Pasquarello, A.; Car, R.; Lee, C.; Vanderbilt, D. *Phys. Rev.* **1993**, *B47*, 10142.
(337) Tuckerman, M.; Laasonen, K.; Sprik, M.; Parrinello, M. *J. Phys. Chem.* **1995**, *99*, 5749.
(338) Blaudeck, P.; Frauenheim, Th.; Porezag, D.; Seifert, G.; Fromm, E. *J. Phys: Condens. Matter* **1992**, *4*, 6389.
(339) Münch, W.; Seifert, G.; Kreuer, K. D.; Maier, J. *Solid State Ionics*, in press.
(340) Cherry, M.; Islam, M. S.; Gale, J. D.; Catlow, C. R. A. *Solid State Ionics* **1995**, *77*, 207.
(341) Iwahara, H.; Uchida, H.; Morimoto, K. *J. Electrochem. Soc.* **1990**, *137*, 462.

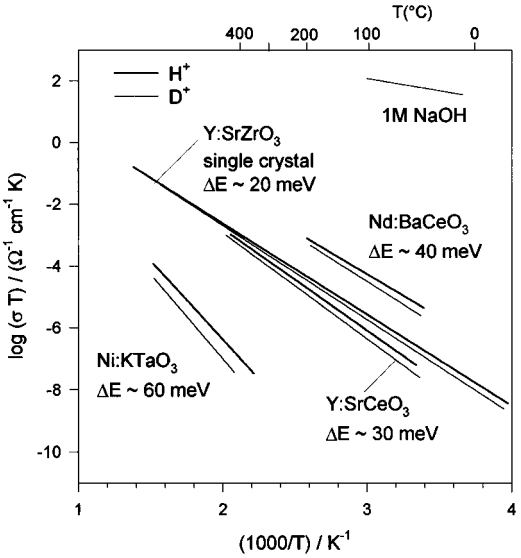

Figure 18. H/D isotope effect of proton conductivity in some perovskite-type oxides.[240] The differences of the activation enthalpies are indicated.

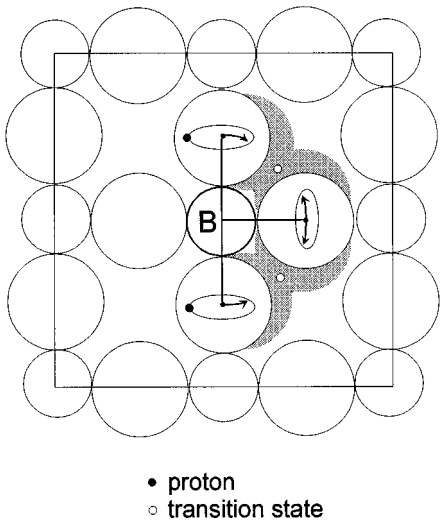

Figure 19. Schematic illustration of proton diffusivity in perovskite-type oxides (ABO_3) involving O−B−OH bending and rapid rotation around the B−OH bond.

migration of protons (e.g., ref 262). But also for other oxides, Grotthuss-type mechanisms are more likely to occur than the migration of hydroxyl ions for simple structural reasons. Most known proton-conducting oxides exhibit the perovskite, antifluorite, the cubic c-type rare-earth sesquioxides or rutile structure. These are closely packed with respect to oxygen, allowing oxygen and hydroxyl ions to migrate only via vacancies ($V_O^{\bullet\bullet}$) which does not allow for diffusivities as high as those observed for protonic defects.[239]

Let us take $BaCeO_3$ as an example of a proton host. This has a perovskite structure (~440 pm corresponding to an oxygen separation of 312 pm) and a set of Raman bands at around 330 cm^{-1} (10^{13} s^{-1}), which has been assigned to the O−Ce−O bending mode.[249,250] Mainly this mode is expected to determine the oxygen-separation coordinate **Q**. The high thermal expansion coefficient of about 7×10^{-6} K^{-1},[342] however, suggests significant anharmonicities and, therefore, also a softening of the O−Ce−O bending mode for higher excitations. This allows some displacement of the hydroxyl ion from the oxygen site toward a neighboring oxygen as a result of the OH···O hydrogen-bond interaction. This effect, however, is omitted in the calculation of the contour map in Figure 11 ($\alpha = 7 \times 10^{-6}$) for which the parameters of $BaCeO_3$ have been chosen. It shows a saddle point with an energy of about 0.5 eV which is very close to the activation enthalpy of proton conductivity shown in Figure 18 together with the H/D isotope effect and the conductivities in other perovskite-type oxides. The coincidence between the activation enthalpies of proton transfer and conductivity and the appearance of a H/D isotope effect support the assumption that proton transfer rather than OH^- reorientation is rate limiting for proton conductivity. The barrier for OH^- reorientation around the Ce−O bond should mainly be determined by the hydrogen-bond interaction with the nearest oxygen. Owing to the large average oxygen separation, this bond can hardly build up a barrier. This is also demonstrated by recent LCAO calculations which find barriers lower than 50 meV.[343] The coincidence of the conductivity attempt frequency and that of the O−Ce−O bending mode support the idea that the local oxygen dynamics "triggers" proton conductivity and that entropic effects do not contribute significantly to the preexponential factor.

Low preexponential factors for proton conductivity in cerates have also been explained by the presence of a certain fraction of "immobile" protons.[232,248] For this, however, no further evidence is given.

Figure 19 schematically illustrates proton conductivity in $BaCeO_3$ involving O−Ce−O bending and rapid rotation of the OH^- around the Ce−OH bond. This mechanism has recently been supported by the results of a quantum molecular dynamics simulation of a protonic defect in $BaCeO_3$[339] (see also cover page of this issue). The simulation reveals a rapid rotation of the proton around the oxygen positions ($\tau = 10^{12}$ s^{-1}), whereas proton transfer between neighboring oxygens, which is assisted by extended oxygen vibrations, is a relatively rare event.

For this mechanism, the situation in $BaCeO_3$ is almost ideal. The perovskite structure is characterized by high coordination numbers for both types of cation (12 for the A site and 6 for the B site) and crystallographic mirror planes between adjacent oxide ions which all have the same site symmetry. The first leads to rather low cation/anion bond strengths corresponding to soft bending modes, and the second to a "solvation" coordinate **S** being symmetrical with respect to all hydrogen bond centers in the time average. In addition, the average oxygen separation is large, allowing a high degree of anharmonicity in the oxygen vibration. However, one should keep in mind that the observed anharmonicities may also have contributions from the nonlinear oxygen polarizability responsible for the ferroelectric phase transitions observed in other oxides with the perovskite structure. The low static dielectric constant ($\epsilon_O = 20$[229]), reflecting the high covalency of $BaCeO_3$, is probably the reason for the small effects from fluctuations in the "solvent" coordinate **S** in this oxide.

Indeed, the highest proton diffusivities are observed for perovskite-type structures (Figure 17). Any reduction of the symmetry, coordination number, and oxygen separation tends to reduce proton diffusivity. In such cases, the influence of the static part of the solvent coordinate $\mathbf{S}_O$ on the proton-transfer potential has to be included. This also includes the interaction of other

(342) Kreuer, K. D., unpublished result.
(343) Münch, W., private communication.

charged defects, such as the negatively charged cation substitutional defects (e.g., RE'_{Ce}) with the proton.[241]

Especially for proton conductivity in pure hydroxides, solvent effects arising from strong proton/proton interactions are expected to dominate proton-transfer reactions. This is probably the reason proton conductivity in oxides shows a simple Arrhenius behavior over a temperature range of several hundred kelvin whereas the conductivity in hydroxides sets on with so-called "superprotonic" phase transitions as in acidic salts of oxo acids.

Let us finally consider the concentration of protonic charge carriers in oxides. These are not a constitutional part of the oxide structure, and their concentration may vary by several orders of magnitude depending on the host and the composition of the surrounding atmosphere. Beside the diffusivity of protonic defects, it is, therefore, the other important parameter determining proton conductivity in oxides.

In most cases protonic defects are incorporated into oxides according to:

$$H_2O + V_O^{\bullet\bullet} + O_O^x = 2OH_O^{\bullet} \quad \text{(equilibrium constant } K = K_3/K_2) \quad (1)$$

i.e., the concentration of protonic defects ($OH_O^{\bullet}$) competes with that of oxygen ion vacancies ($V_O^{\bullet\bullet}$). The reaction may be split into the formation of oxygen ion vacancies:

$$O_O^x + 2h^{\bullet} = V_O^{\bullet\bullet} + {}^1/_2O_2 \quad \text{(equilibrium constant } K_2) \quad (2)$$

and the formation of protonic defects:

$${}^1/_2H_2O + h^{\bullet} + O_O^x = OH_O^{\bullet} + {}^1/_4O_2 \quad \text{(equilibrium constant } K_3) \quad (3)$$

Together with the internal reaction:

$$0 = h^{\bullet} + e^- \quad \text{(equilibrium constant } K_1) \quad (4)$$

and the electroneutrality condition:

$$[h^{\bullet}] + 2[V_O^{\bullet\bullet}] + [OH_O^{\bullet}] - [e^-] = [RE'_{Ce}] \quad (5)$$

the concentrations of all defects are fixed for a given gas composition (p_{O_2}, p_{H_2O}, (p_{H_2})). When the concentration of electronic charge carriers ($h^{\bullet}$, e^-) is neglected ($K_1 \ll$), the solution for the concentration of protonic defects is:

$$[OH_O^{\bullet}](p_{H_2O}) = (K/4)p_{H_2O}\left(\sqrt{1 + (8[RE'_{Ce}]/Kp_{H_2O})} - 1\right) \quad (6)$$

For low p_{H_2O} this corresponds to Sievert's law:

$$[OH_O^{\bullet}](p_{H_2O}) = \sqrt{K/2[RE'_{Ce}]}\sqrt{p_{H_2O}} \quad (7)$$

and for high p_{H_2O}, $[OH_O^{\bullet}]$ approaches the concentration of the cationic dopant $[RE'_{Ce}]$. This approach assumes an ideal solution for all defects. In real oxides, the expressions for the water solubility must be corrected by an activity coefficient smaller than 1, which has been suggested to reflect the reduced water solubility as a result of the relaxation of the oxygen ion vacancy environment.[245a]

As reaction 2 is endothermic and reaction 3 exothermic, the first reaction is shifted to the right, the second reaction to the left with increasing temperature, i.e., the concentration of oxygen ion vacancies increases at the expense of that of protonic defects. As the diffusivity of protonic defects is preceding that of oxygen diffusion with temperature, also the corresponding concentration of protonic defects dominate at low, and that of oxygen ion vacancies at high temperature.

Larring and Norby have assumed that the enthalpy change of reaction 3 does not differ very much for different oxides, in contrast to that of reaction 2, which is thus anticipated to mainly determine the relative enthalpy change of reaction 1 for different oxides. As reaction 2 is expected to depend on the stability of the oxide, the enthalpy of reaction 1 should also reflect the stability of the host. Indeed, a correlation between the equilibrium constant of reaction 1 and the molar volume for chemically related oxides has been found.[344] Loosely packed oxides release their protonic defects (water) at lower temperature than closely packed structures.

This leads to a conflicting situation with respect to proton conductivity at high temperature. Whereas loosely packed structures usually have a high thermal expansion coefficient reflecting extended, anharmonic oxygen vibrations, which supports proton diffusivity, the thermodynamic stability of the charge carriers is restricted to moderate temperatures and high water partial pressures.

The assumption that the enthalpy of reaction 3 is independent of the oxide host is valid only for oxides with similar acid/base properties. Of course, the defect $OH_O^{\bullet}$ is expected to be more stable in basic oxides compared to acidic oxides.[245a]

Indeed, the highest dissociative water solubilities have been observed for basic oxides. For example, loosely packed $BaCeO_3$-based compounds dissolve more water than corresponding $SrCeO_3$-based compounds at moderate temperature (<600 °C), but they release this water at lower temperature at the expense of the formation of oxygen ion vacancies. ZrO_2-based oxygen ion conductors are fairly loosely packed; they are amphoteric and, therefore, dissolve very little water.[214,279]

One should also bear in mind that oxygen ion vacancies and protonic defects compete with electronic holes ($h^{\bullet}$). The highest degrees of hydration are therefore expected for closely packed, basic oxides with high ionicity (bandgap), i.e., low equilibrium constants K_1 and K_2 and a high constant K_3.

5.2. Compounds Based on Oxo Acids. Chemical bonding in this family of compounds is more complex. For example in $CsHSO_4$, hydrogen bonding (−O−H···O−), Coulomb interaction (Cs^+/HSO_4^-), and covalent bonding (S−O) determine structure and dynamics.

There is no doubt about the principal proton conduction mechanism: Proton transfer between oxygen of neighboring tetrahedra (XO_4) and the local dynamics of such tetrahedra are elements in Grotthuss-type conduction mechanisms. This appears plausible for solid salts, but even in liquid phosphoric acid this has been shown to be the dominant conduction process.[96] Rapid proton transfer between the pairs $H_4PO_4^+/H_3PO_4$ and $H_3PO_4/H_2PO_4^-$ is involved in almost 98% of the total conductivity, the remaining 2% arising from the "normal" hydrodynamic diffusion of charged species originating from the self-dissociation of the rather viscous liquid.

(344) Larring, Y.; Norby, T. *Solid State Ionics* **1995**, *77*, 147.

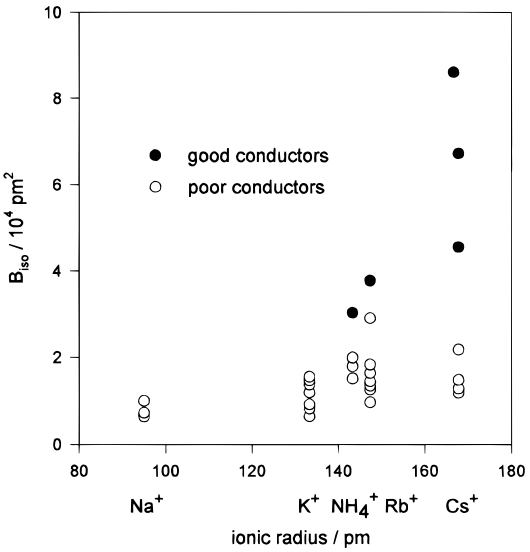

Figure 20. Debye−Waller factor of sulfur of good and poor proton-conducting sulfates of the type $MHSO_4$ as a function of the cation radius (data from different sources).

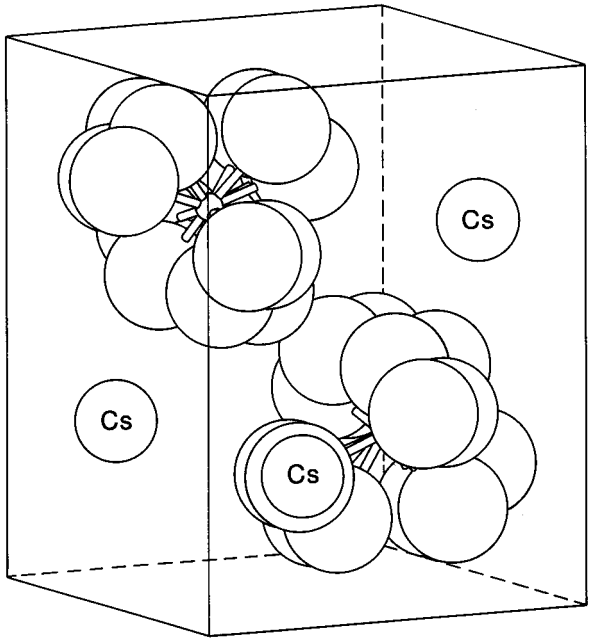

Figure 21. Four different orientations of two sulfate tetrahedra of the high-temperature phase of $CsHSO_4$ as revealed from a neutron diffraction experiment.[107] These are assumed to mimic the dynamical reorientational disorder (see text). The cesium sites are also indicated.

Although no translational motion of complex proton containing species is involved, the local dynamics of the tetrahedra is essential for proton conductivity. This comprises extended tetrahedra vibration and libration modes as is shown in Figures 20 and 21. The distinctly higher sulfur Debye−Waller factors of good proton-conducting phases as opposed to those of poorly conducting phases of acidic sulfates are shown in Figure 20. Tetrahedra librations are also shown by diffraction experiments and vibrational spectroscopy.[104,107,112,120,121] For instance, neutron diffraction experiments on the high-temperature phase of $CsDSO_4$ reveal the four different tetrahedra orientations shown in Figure 21 which probably just mimic the dynamical orientational disorder of the tetrahedra.[107]

Vibration and libration are the elements of the "tumbling" dynamics of the tetrahedra in such phases.

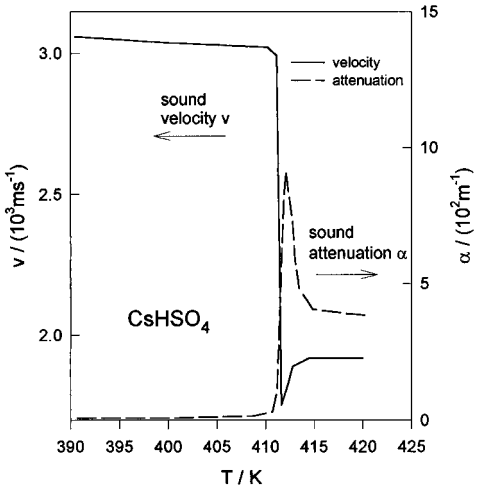

Figure 22. Changes of the sound velocity and sound attenuation at the "superprotonic" phase transition of $CsHSO_4$ at 412 K.[122]

These are sometimes denoted "plastic"[345] because the weak structural tetrahedra confinement reflects the weak bonding. It is a striking observation that such phases only appear for salts with big cations as Rb^+, Cs^+, and Tl^+ (Figure 4). Similar to the case of oxides, big cations require either high coordination numbers or large anion separations. This lowers the cation/anion and anion/anion bond strengths thus promoting the anion (tetrahedron) and cation dynamics. Indeed, extended dynamics of the tetrahedra are always accompanied by similar dynamics of the cations. In addition, big cations separate the structural protons more effectively, thus diminishing solvent effects arising from proton/proton interaction. Consequently, acidic salts of oxo acids transform into plastic phases at lower temperature for bigger cations (Figure 4).

In acidic salts of oxo acids the proton conducting plastic phases appear with endothermic first-order improper ferroelastic phase transitions, which anticipate a great deal of the enthalpy and entropy difference with respect to the molten state ($\Delta H = 5.52$ kJ mol^{-1}, $\Delta S = 13.3$ J mol^{-1} K^{-1} for the transition of $CsHSO_4$ at ~412 K compared to $\Delta H = 13.2$ kJ mol^{-1} and $\Delta S = 27.2$ J mol^{-1} K^{-1} for the melting at 484 K).[134] The tetrahedra dynamics are close to that of a liquid except for the diffusional degrees of freedom. This becomes greatly apparent in the drastic decrease of the sound velocity and increase of the sound attenuation (Figure 22)[122] in accordance with the sulfate decoupling, i.e., the breaking down of the static solvent effect and the onset of proton translocation upon transformation into the high-temperature phase of $CsHSO_4$.

Similar transitions into plastic phases are observed for neutral sulfates,[346] which also show proton conductivity when protonic species are dissolved as minority defects.[209,210] Therefore, the principal dynamical features of acidic compounds may be simulated without taking into account the hydrogen-bond interactions explicitly. This appears to be reasonable when considering the average hydrogen bond length in good conducting phases shown in Figure 23 together with that of poor conductors. This is generally higher than 260

(345) Timmermans, J. *Bull. Soc. Chim. Belg.* **1935**, *44*, 17.
(346) Lunden, A.; Thomas, J. In *High Conductivity Solid Ionic Conductors*; Takahashi, T., Ed.; World Publishing Co.: Singapore, 1988; p 45.

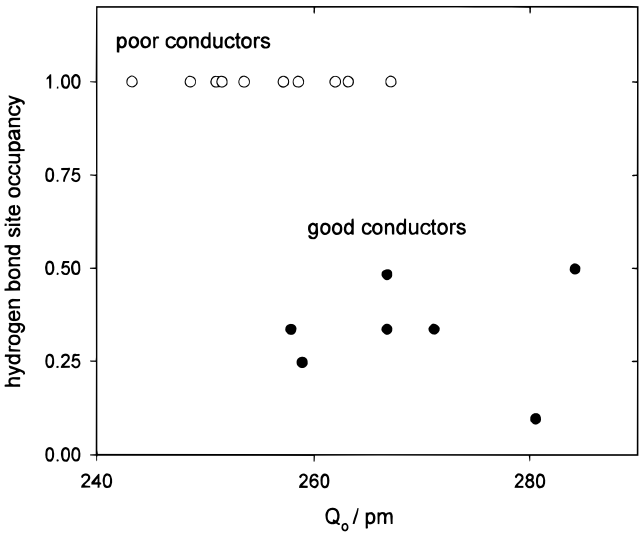

Figure 23. Static hydrogen-bond lengths ($\mathbf{Q}_O$) and hydrogen-bond occupancies for good and poor proton conducting phases of sulfates of the type $MHSO_4$ (data are taken from different sources; see Table 2).

pm, corresponding to only medium or weak hydrogen-bond interaction.[313] As a rough approximation one might, therefore, consider the hydrogen bonding as being confined by the stronger ionic interactions.

This is the framework of a recent MD simulation of the high-temperature phase of $CsHSO_4$,[334] treating the host dynamics just on the basis of the potential surface $E(\mathbf{q},\mathbf{Q})$, i.e., neglecting any solvent effect. Figure 24 shows the observed distance between oxygens of neighboring tetrahedra and how the corresponding configurations evolve with time. Figure 24a demonstrates the situation where one oxygen is approaching that of a neighboring tetrahedron while another oxygen is separating from that oxygen, i.e., the orientation of one tetrahedron flips with respect to the other. Figure 24b demonstrates that the oxygen of neighboring tetrahedra may approach closer than $Q = 245$ pm, where the potential surface $E(\mathbf{q},\mathbf{Q})$ shows a transition state for proton transfer. The simulation rates of tetrahedra reorientation ($\sim 10^{11}$ s^{-1}) and the estimated proton-transfer rate ($\sim 10^{9}$ s^{-1}) are surprisingly close to the experimental values.[104,112,119,121] Once the rate-limiting proton transfer occurs, it is suggested to be adiabatic without any significant H/D isotope effect.

But this is not observed experimentally. Distinct isotope effects are found in the preexponential factor and the activation enthalpy of the high-temperature phase of $CsHSO_4$,[101] which are even more pronounced in the low-temperature phase (Figure 25). But in contrast to the situation in oxides, these effects are most probably due to differences in the dynamics of the tetrahedra rather than in the excitation of the protons compared to deuterons. This is already suggested by the total activation enthalpy of proton conductivity ($\sim$0.27 eV) being slightly lower than the separation of ground and first excited state of the OH oscillator. For liquid phosphoric acid this assumption has already been proven by the H/D isotope effect for diffusion shown in Figure 26. The application of the PFG-NMR technique allowed the separate measurement of proton and deuteron diffusion in the same environment with respect to the isotopic composition.[347] Both diffusion coefficients are almost identical, suggesting that (i) proton and deuteron transfer occurs close to the "adiabatic" limit and (ii) that the total isotope effect mainly reflects the effect of the isotopic composition on the solvent dynamics. This is consistent with the observation that the viscosity of phosphoric acid increases with increasing deuteron content.[348]

The idea that proton transfer is predominantly an "adiabatic" process also in the solid state of good proton conductors, is supported by the preexponential factors of both proton conductivity and diffusion in the high-temperature phase of $CsHSO_4$.[347] It corresponds to an attempt frequency of 1.6×10^{12} s^{-1} (54 cm^{-1}) which is very close to the frequency of the external HSO_4^- vibrations (58−170 cm^{-1}).[118]

Since protons in such compounds are coordinated with rather big and rigid XO_4 tetrahedra, "solvent" effects are expected to be small except for some remaining proton/proton interaction (see section 4.2.1.4). This is manifested in (i) the appearance of "superprotonic" phase transitions (Figure 4), i.e., order/disorder transitions with respect to the distribution of the protons within the hydrogen bond network, and (ii) in a small correlation of proton transfers in adjacent hydrogen bonds between the pairs $H_4PO_4^+/H_3PO_4$ and $H_3PO_4/H_2PO_4^-$ in phosphoric acid.[96] In this particular case, correlated jumps contribute to the total proton diffusion coefficient, but the effects of charge displacement just cancel out, i.e., there is no contribution to proton conductivity. As with the appearance of proton mobility, also the creation of protonic charge carriers is a result of proton transfer. But the latter is reactive in nature, i.e., it requires a change of the Gibbs free energy, which also has contributions from solvent effects. In phosphoric acid, e.g., about 5% of the molecules are dissociated according to $2H_3PO_4 \rightarrow H_4PO_4^+ + H_2PO_4^-$,[96] which is much higher than the fraction of 0.1 ppm dissociated water molecules in pure water, for which solvent effects are much stronger (see section 5.3). Whereas the proton density in water is higher than in phosphoric acid, the proton density in salts like $CsHSO_4$ is lower suggesting even lower contributions of proton/proton interactions to the solvent effect and, therefore a higher degree of dissociation in the high-temperature phase. For $CsHSO_4$ a complete dissociation, i.e., a random distribution of the protons over all sulfate oxygens corresponds to fractions of 31.6%, 42.2%, 21.5%, 4.3%, and 0.4% of unprotonated sulfates and sulfates with one, two, three, and four protons respectively. To what extent solvent effects lead to deviations from this proton distribution is not yet clear. But the high entropy change associated with the "superprotonic" transformation (e.g., ref 134) suggests a high degree of dissociation.

In blends of oxo acids and polymers the highest proton conductivities are observed for weak hydrogen-bond interaction between acid and polymer host suggesting a transport mechanism similar to that of pure oxo acids.

In short, in proton conducting compounds based on oxo acids, XO_4 tetrahedra, so to say, act as a solvent for the proton, which approximately follows the "tumbling" dynamics of these tetrahedra.

5.3. Water-Containing Systems. The largest variety of known proton-conducting systems contain water. This not only reflects the unique properties of water but

(347) Dippel, Th.; Hainovsky, N. G.; Kreuer, K. D.; Münch, W.; Maier, J. *Ferroelectrics* **1995**, *167*, 59.
(348) Greenwood, N. N.; Thompson, A. *J. Chem. Soc.* **1959**, 3485.

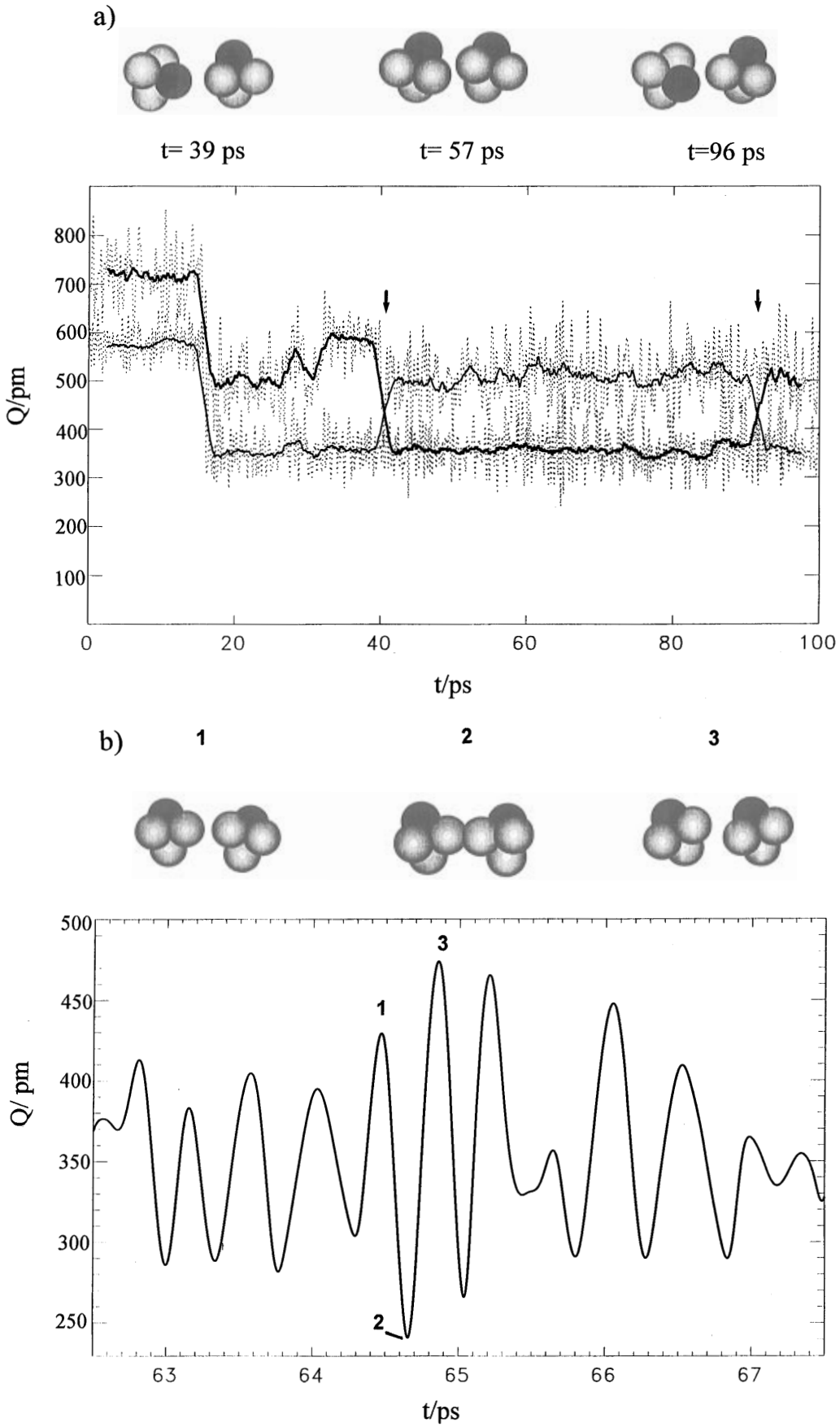

Figure 24. Oxygen−oxygen separation $Q(t)$ for two oxygens of one tetrahedron relative to an oxygen of a neighboring tetrahedron as revealed from an MD simulation of the high-temperature phase of $CsHSO_4$:[334] (a) Tetrahedra reorientation events indicated by arrows result in the interchange of the two oxygen atoms in the nearest-neighbor position. Three selected configurations of the sulfate tetrahedra are shown on top where one oxygen atom is marked to indicate the tetrahedra orientation. (b) In configuration 2 the oxygen−oxygen separation Q is transiently smaller than 250 pm thus allowing barrierless proton transfer.

also its omnipresence on this planet. Despite many activities since the early days of physical chemistry, a consistent description of proton conductivity in such systems is hardly available.

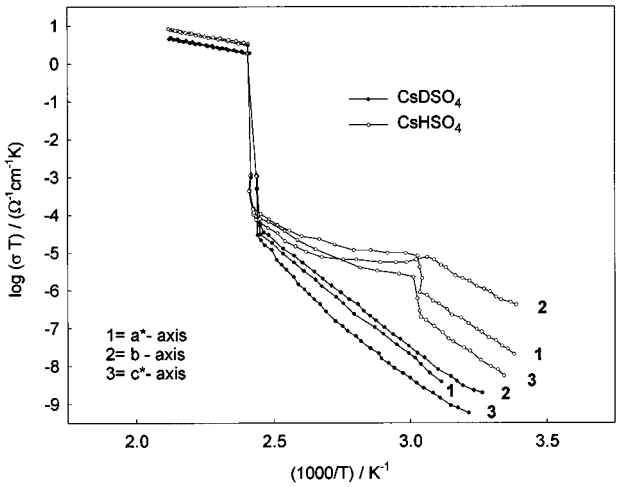

Figure 25. H/D isotope effect of the conductivity of $CsHSO_4$ for different crystallographic directions.[101]

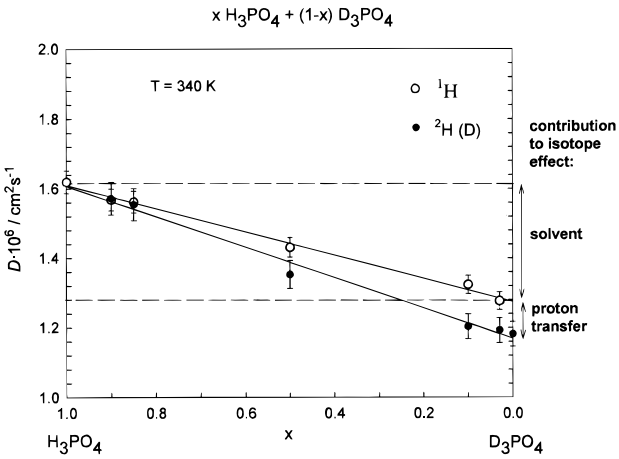

Figure 26. H/D isotope effect of diffusion of ^1H and ^2H (D) in mixtures of H_3PO_4 and D_3PO_4.[347]

Although pure water consists of only two different elements, its structure and dynamics are very complex.[349] The predominant intermolecular interaction is hydrogen bonding with an average energy of only ~200 meV/bond. This weak interaction is very sensitive to fluctuations in pure water and, additionally, to static perturbations in water-containing systems. Because of the high density of protons and the high anharmonicity of their potentials, there is some interaction leading to solvent effects. These comprise a rather high number of species and can, therefore, be described completely only on a rather long time scale in the microwave range, where significant collective excitations are observed for aqueous hydrogen-bonded networks (e.g., refs 350 and 351). Comparable proton transfer, molecular diffusion, and reorientation rates is another consequence of that coupling. The complex scenario leads to the abundant variety in the phenomenology of proton transport in aqueous systems. Whereas pure water and ice are rather poor proton conductors under usual conditions, aqueous solutions of strong acids and solid acidic hydrates show the highest proton conductivities reported so far.

Historically, the first ideas about proton conductivity in aqueous solutions were stimulated by considerations about the electrolytic decomposition of water in 1806. Van Grotthuss postulated chains of water dipoles along which electricity is transported.[24] One fundamental step, which is part of any suggested proton-conduction mechanism, had already been described by several authors at the beginning of this century.[352−354] They recognized that intermolecular proton transfer can lead to a charge transport at a rate exceeding that of other charged species, which simply diffuse within the hydrodynamic domain. The first formal theory was attempted by Hückel in 1928[355] at a time when the existence of a discrete H_3O^+ ion had already been suggested. Hückel treated this species as a dipole and tried to calculate its reorientational rate into positions favorable for proton transfer to neighboring water molecules. A first quantum mechanical theory of intermolecular proton transfer was presented by Bernal and Fowler in 1933[356] putting the old concept of Grotthuss chains into a modern dress. The water reorientation was treated like that of a structureless liquidlike argon. The anticipated strong H/D isotope effect of the conductivity, however, could not be confirmed.[357] In the mid-1950s Conway, Bockris, and Linton[303] as well as Eigen and DeMaeyer[304,305] focused on the question of the rate-limiting step. In their historical papers, they agree that classical proton transfer is slow, proton tunneling is much faster, and the rotation of hydrogen-bonded water molecules near the H_3O^+ ion is the rate-determining reaction. More recent contributions by Halle and Karlström[358] and Hertz et al.[359] show, from quite different viewpoints, the solvent to be an indispensible element in Grotthuss-type proton transport.

Our present understanding of proton transport in aqueous media still comprises the same elements, but, as will be discussed in the following, they are put together into a somewhat different "puzzle". For this, we will first consider the formation of protonic charge carriers and then their diffusivity in different environments.

5.3.1. Formation of Protonic Charge Carriers. In pure water and ice there is a rather strict association of two protons with one sp^3-hybridized oxygen thus forming neutral water molecules. For the distribution of protons in the network of the asymmetric hydrogen bonds in ice, this has been expressed as one of the two Bernal−Fowler rules.[360] Of course, at any finite temperature, this rule is broken to some extent, i.e., protons are transferred within hydrogen bonds:

$$2H_2O = H_3O^+ + OH^- \qquad (8)$$

i.e., charged protonic defects with respect to the perfect state are intrinsically formed as a consequence of water self-dissociation. But, in contrast to, e.g., pure H_3PO_4, where about 5% of the molecules are dissociated, the ionic product of the small water molecule is only $[H_3O^+][OH^-] = 10^{-14}$ under standard conditions. In ice,

(349) Franks, F. Ed. *The Physics and Physical Chemistry of Water*; Plenum Press: New York, 1972; Vols. 1−4.
(350) Collie, C. H.; Hasted, J. B.; Ritson, D. M. *Proc. Phys. Soc.* **1948**, *60*, 145.
(351) Lane, J. A.; Saxton, J. A. *Proc. R. Soc. Lond.* **1952**, *A213*, 400.
(352) Dempwolff. *Phys. Z.* **1904**, *5*, 637.
(353) Tijmstra, S. *Z. Elektrochem.* **1905**, *11*, 249.
(354) Danneel, H. *Z. Elektrochem.* **1905**, *11*, 249.
(355) Hückel, E. *Z. Elektrochem.* **1928**, *34*, 546.
(356) Bernal, J. D.; Fowler, R. H. *J. Chem. Phys.* **1933**, *1*, 515.
(357) Gierer, A. *Z. Naturforsch.* **1950**, *5a*, 581.
(358) Halle, B.; Karlström, G. *J. Chem. Soc. Faraday Trans 2* **1983**, *79*, 1047.
(359) Hertz, H. G.; Braun, B. M.; Müller, K. J.; Maurer, R. *J. Chem. Educ.* **1987**, *64*, 777.
(360) Bernal, J. D, Fowle, R. H. *J. Chem. Phys.* **1933**, *1*, 515.

close to the melting point, it is only 2 orders of magnitude smaller with an activation enthalpy of 0.98 eV and approximately no barrier between perfect and defect state.[361] The self-dissociation increases with increasing temperature. For the liquid state it has been measured up to 1000 °C, where water is still not completely dissociated.[362,363] This is in interesting contrast to compounds such as $CsHSO_4$, where the reorientational disorder and the full dissociation of the compound set on simultaneously at a first-order phase transition. Obviously, proton disorder in water is suppressed by strong solvent effects and the stability of the sp^3 hybrid which highly favor an ordered distribution of protons in space.

Under increasing pressure, however, the hydrogen bonds are successively compressed which leads to a reduction of solvent effects (see also Figure 29). This is probably the main reason for the considerable decrease of the enthalpy of reaction 8 and the corresponding increase of the ionic product. At room temperature, e.g., the ionic product increases from 10^{-14} at ambient pressure to about 10^{-10} at 1 GPa, where water solidifies forming ice VI.[362,363]

Under high pressure and temperature, the charge-carrier concentration in pure water may resemble that of a rather concentrated aqueous solution of a strong acid, however, with an equal concentration of protons and hydroxyl ions.

Apart from this intrinsic self-dissociation of water and ice, dissolved acids donate protons into the water solvent to a degree which is determined by the pK_A of the acid, as is commonly known. Speaking in terms of defect chemistry, this may be considered a homogeneous extrinsic doping as opposed to heterogeneous doping which is restricted to interfaces, separating different phases.[364] This is relevant for water at surfaces (e.g., in partical hydrates or at biological membranes) or in the cavities of porous materials such as zeolites. Owing to specific interactions with protons, such interfaces may stabilize or destabilize protons depending on their acid/base properties. This leads to the formation of a space charge with an increased charge-carrier concentration within twice the Debye length of the aqueous phase. Such electrified interfaces are the reason for diverse phenomena like the stability of colloids[365] or the response of a pH-FET.[366]

5.3.2. Mobility of Protonic Charge Carriers. The equivalent proton conductivity in aqueous solution is significantly higher than that of any other ion.[367] It tentatively marks the upper limit for the conductivity of such systems and any interaction of the water molecules with the environment (e.g., in a solid hydrate, a particle hydrate, a polymer or biological membrane) may be regarded as a destructive perturbation with respect to proton diffusivity in water. Let us, therefore, start our considerations with dilute acidic aqueous solutions.

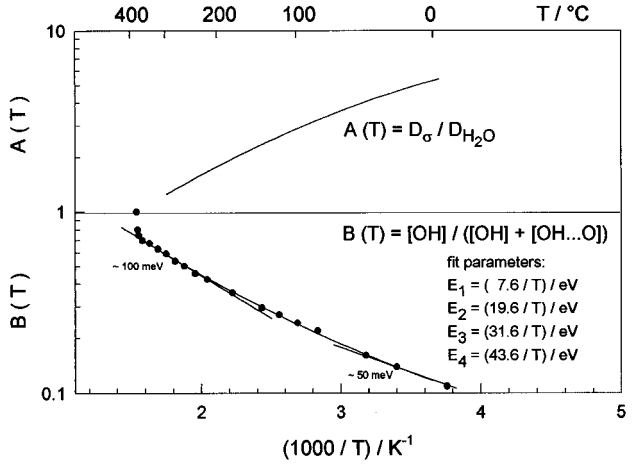

Figure 27. Fraction of broken hydrogen bonds B for pure water as a function of temperature as obtained by IR spectroscopy[368] including a fit to the data using four energies (E_1–E_4) for successively breaking the four possible hydrogen bonds of a molecule and the ratio $A = D_\sigma/D_{H_2O}$ for the limiting equivalent conductivity (diffusivity) of protons in water.

For these, the predominant intermolecular interaction is hydrogen bonding. Upon melting of ice, almost 90% of the hydrogen bonds remain intact in the liquid state. During further heating this hydrogen bonding successively disappears, but there is still some association left even at the critical point. The temperature dependence of the fraction of broken hydrogen bonds in water is shown in Figure 27.[368,369] The apparent activation enthalpy around room temperature (~50 meV) is significantly lower than the average energy of a hydrogen bond at that temperature (~200 meV), indicating some energy transfer into neighboring bonds when a hydrogen bond is weakened or broken. This may also explain the increase of the apparent activation enthalpy which amounts to ~100 meV below the critical point. Figure 27 also shows a fit to the data with four energies (E_1–E_4) for successively breaking the four possible hydrogen bonds of one molecule, where all energies are assumed to linearly decrease with temperature.[370]

Bond-length fluctuations have actually been investigated in a recent ab initio MD simulation of liquid water with one excess proton.[28,29] This proton is either found as part of a H_3O^+ acting as a proton donor in three rather strong hydrogen bonds with three neighboring water molecules thus forming the primary hydration sphere of a $(H_9O_4)^+$, or midway between two water molecules thus forming an $(H_5O_2)^+$. The three hydrogen bonds of the former are slightly contracted ($\mathbf{Q}_O \sim 260$ pm) compared to those in pure water where the central hydrogen bond of the dimer is the only contracted bond ($\mathbf{Q}_O \sim 250$ pm). The two structures are found to be part of the same fluctuating complex. Elongation (weakening) of two of the three hydrogen bonds of the $(H_9O_4)^+$ structure and contraction (tightening) of the third leads to the transformation into the $(H_5O_2)^+$ dimer and vice versa (Figure 28). Which of the three hydrogen bonds contracts depends on the asymmetry of the second hydration sphere. This rapid fluctuation, which is related to the oxygen vibration in water[28,29] ($\tau \sim 0.2$ ps) does not produce any significant charge separation, i.e.,

(361) Hobbs, P. V. *Ice Physics*; Clarendon Press: Oxford, 1974.
(362) Holzapfel, W.; Frank, E. U. *Ber. Bunsen-Ges.* **1966**, *70*, 1105.
(363) Holzapfel, W. *J. Chem. Phys.* **1969**, *50*, 4424.
(364) Maier, J. *J. Electrochem. Soc.* **1987**, *134*, 1524.
(365) Healy, T. W.; White, L. R. *Adv. Colloid Interface Sci.* **1978**, *9*, 303.
(366) Bousse, L.; DeRooij, N. F.; Bergveld, P. *Surf. Sci.* **1983**, *135*, 479.
(367) Kortüm, G. *Lehrbuch der Elektrochemie*; Verlag Chemie: Weinheim, 1972.
(368) Luck, W. A. P. *Ber. Bunsen-Ges.* **1965**, *69*, 626.
(369) Kohl, W.; Lindner, H. A.; Franck, E. U. *Ber. Bunsen-Ges. Phys. Chem.* **1991**, *95*, 1586.
(370) Fujita, Y.; Kawa, S. I. *Chem. Phys. Lett.* **1989**, *159*, 184.

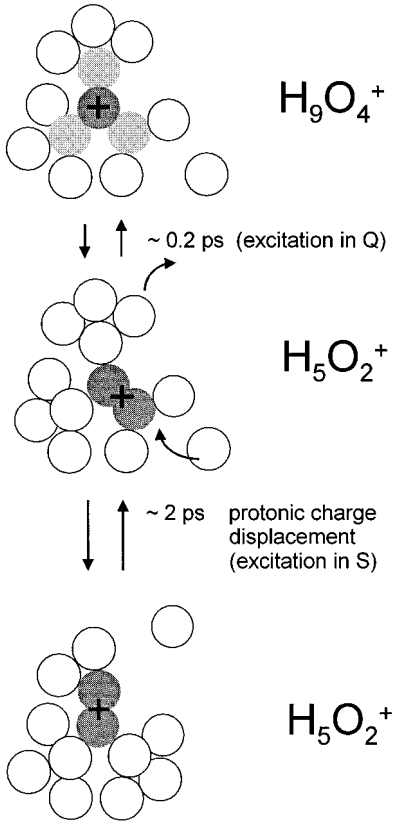

Figure 28. Proton diffusivity as revealed by an ab initio MD simulation.[28,29] Rapid fluctuation between $[H_9O_4]^+$ and $[H_5O_2]^+$ complexes related to fluctuations in the oxygen separation coordinate **Q** does not produce a significant charge separation. This is less frequently induced by changes of the coordination in the second hydration sphere (fluctuation in **S**).

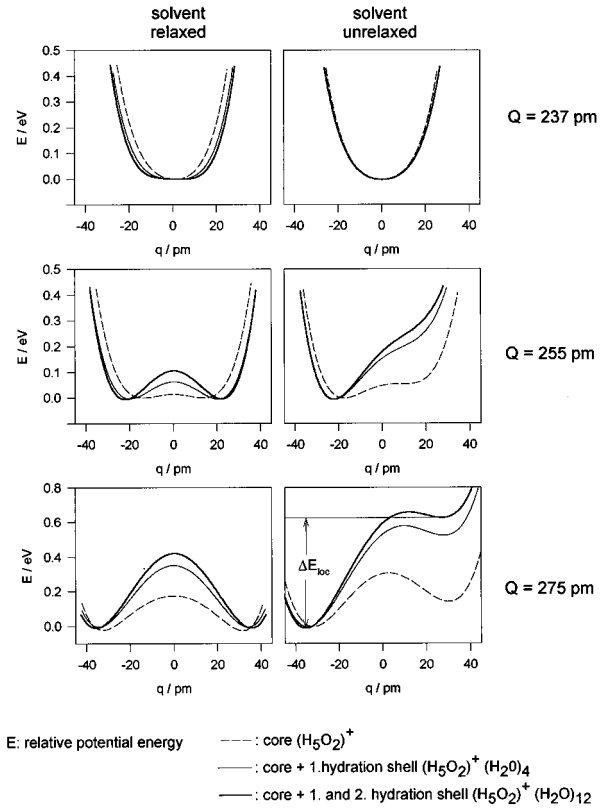

Figure 29. Proton-transfer potentials for differently hydrated $(H_5O_2)^+$ complexes and different oxygen separations with and without solvent relaxation as revealed from a static high-level quantum chemical calculation.[306]

electroneutrality is maintained even on a local scale. A net displacement of charge is found to be a comparatively rare event ($\tau \sim 2$ ps). It is observed when one of the long hydrogen bonds of the H_3O^+ ion contracts at the expense of the former short bond, thus forming a dimer with another neighbor. This process is induced by changes in the coordination within the second hydration sphere, which passes through a symmetrical configuration in the transition state of the proton-transfer event (see also Figure 13) before the solvent starts to accommodate to the new proton position thus forming another asymmetrical configuration confining the new position of the fluctuating $H_9O_4^+/H_5O_2^+$ complex. Owing to the short central hydrogen bond in the dimer, this transition state has no barrier in contrast to the situation in Figure 13. Therefore, effects from proton tunneling may be neglected.

Although the translocation of a single protonic defect is established by small displacements of several protons, including solvent protons, the translocation length is only of the order of one molecular separation. There is particularly no indication for cooperative proton transfers along extended hydrogen bond chains in accordance with the considerations in section 4.2.1.4.

The fluctuations between $(H_9O_4)^+$ and $(H_5O_2)^+$ are induced by fluctuations in an oxygen separation coordinate **Q** whereas successful proton transfer requires an excitation in the solvent coordinate **S**. Therefore, successful proton displacement is slower than frequently assumed. The proton diffusivity in water is actually only comparable to that in H_3PO_4,[96] a liquid with a much higher viscosity but smaller solvent effects. The strong effect of the solvent on the proton transfer potential is demonstrated by a recent high-level static quantum chemical calculation on the oligomer H_3O^+-$(H_2O)_{14}$.[306] Figure 29 shows the proton-transfer potential with and without solvent relaxation for different numbers of hydration spheres, i.e., for successively building up the first and second hydration sphere around the core complex $(H_5O_2)^+$. Except for very short oxygen separations in the core, the transfer barrier has major contributions from the interaction of the proton with the first and second hydration sphere. Therefore, also the symmetry of the proton-transfer potential is very sensitive to the position of the solvent species, as can be seen by comparing the potential for a relaxed and unrelaxed solvent. The proton self-localization (ΔE_{loc}) increases tremendously with increasing oxygen separation (compare the potentials for different **Q** in Figure 29). In the case of acidic aqueous solutions, however, proton transfer occurs in short hydrogen bonds (**Q** $\sim$ 250 pm) corresponding to small self-localization energies.

The transfer rate modeled by the MD simulation is of the order of that found experimentally by ^{17}O NMR.[301] This is shown in Figure 30 for the pairs H_3O^+/H_2O together with the rate of molecular diffusion. All rates fall into a very narrow range supporting the strong coupling of proton transfer to the hydrodynamics of the solvent. Water diffusion into and out of the second hydration sphere may change its coordination and thus induce protonic charge displacement in the center of the complex. The coincidence between Γ_D and Γ_{trans} has already been recognized earlier by Kreuer,[371] thus

(371) Kreuer, K. D. In ref 19, p 474.

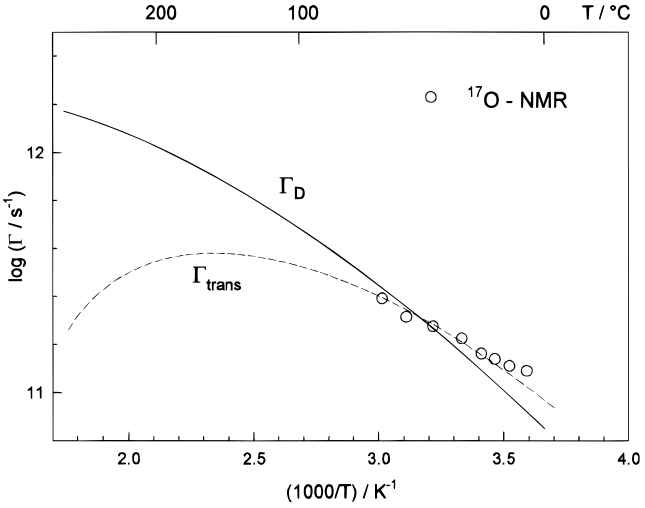

Figure 30. Proton-transfer rate between H_3O^+ and H_2O in water as revealed from ^{17}O NMR[301] and molecular diffusion rate of pure water calculated from the water self-diffusion coefficient.[372−374]

stimulating a first rough sketch of "structure diffusion triggered by molecular diffusion".

A single proton-transfer event, however, appears to be a process involving several molecules. It is, therefore, not surprising that there is no indication of concerted proton transfer along extended Grotthuss chains, which are generally presented in textbooks of physical chemistry.

The high molecular diffusion coefficient also leads to a proton conductivity contribution arising from the simple diffusion of charged complexes (e.g., H_3O^+, $H_5O_2^+$, $H_9O_4^+$) as a whole (vehicle mechanism). Of course, this diffusion of species being part of a hydrogen-bonded network must also be a highly cooperative process. At room temperature the apparent activation enthalpy is only 170 meV.[27,372−374] According to the fit presented in Figure 27, this exactly equals the energy required to break the first two of the four possible hydrogen bonds of a water molecule including the linear temperature dependence. The water diffusion coefficient in pure water can, therefore be expressed in the form

$$D = D_0 \exp(-(H/kT)^2) \qquad (9)$$

where $D_0 = 9.04 \times 10^{-4}$ cm^2 s^{-1} and $H = 49.4$ meV.

So far, there is no model available which provides a physical explanation of this striking observation. But the parameters seem to reflect (i) the linear temperature dependence of the average hydrogen-bond energy, indicating that hydrogen-bond breaking is involved in the diffusion process and (ii) the IR absorption at 79 cm^{-1},[375] which is revealed from D_0 and might, therefore, be identified as the attempt frequency of molecular diffusion.

The water diffusion coefficient D_{H_2O} is shown in Figure 31a together with that calculated from the proton diffusivity by the Nernst−Einstein relationship D_σ. At

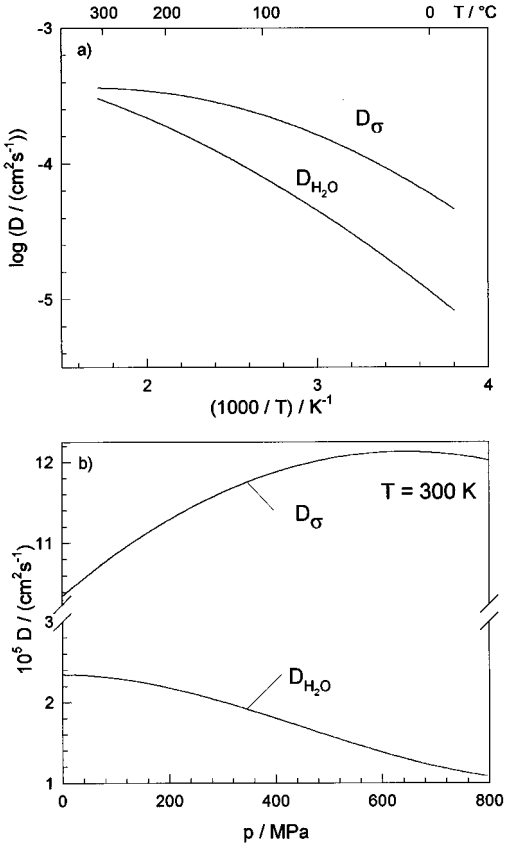

Figure 31. Proton diffusion coefficient in water as revealed from the equivalent proton conductivity D_σ and the self-diffusion coefficient D_{H_2O}: (a) as a function of temperature;[372−374] (b) as a function of pressure.[376−378]

room temperature the ratio $A = D_\sigma/D_{H_2O} = 4.5$, indicating that structure diffusion (Grotthuss mechanism) is more effective than protonic charge transport via molecular diffusion. With increasing temperature, however, the two diffusion coefficients merge together, i.e., proton conductivity in dilute aqueous solutions of acids is successively controlled by molecular diffusion. According to this observation, proton transfer seems to be virtually completely suppressed for temperatures above 300 °C although there is still considerable hydrogen bonding left (Figure 27). Another interesting observation is that the temperature dependence of $A = D_\sigma/D_{H_2O}$ almost resembles that of the fraction of broken hydrogen bonds $B = [O-H]/([O-H] + [O-H\cdots O])$ (Figure 27). Any model on water diffusion should be in accordance with these observations.

Whereas molecular diffusion successively dominates intermolecular proton transfer with increasing temperature, the opposite is true for the application of pressure. Although the molecular diffusion coefficient D_{H_2O} decreases with increasing pressure for pressures beyond ~0.1 GPa,[376,377] proton conductivity slightly increases up to a pressure of about 0.6 GPa before this also starts to decrease[378] (Figure 31). The increasing ratio A suggests that the proton-transfer mode becomes more effective under pressure in accordance with the self-localization energy decreasing with decreasing oxygen separation (Figure 29). Indeed, the activation enthalpy

(372) Krynicki, K.; Green, Ch. D.; Sawyer, D. W. *Faraday Discuss. Chem. Soc.* **1978**, *66*, 199.
(373) Harris, K. R.; Woolf, L. A. *J. Chem. Soc. Faraday Trans. 1* **1980**, *76*, 377.
(374) Hausser, R.; Maier, G.; Noack, F. *Z. Naturforsch.* **1966**, *211*, 1410.
(375) Walrafen, G. E. In ref 349, Vol. 1, p 151.
(376) Benedek, G. D.; Purcell, E. M. *J. Chem. Phys.* **1954**, *22*, 2003.
(377) Hertz, H. G.; Rädle, C. *Z. Phys. Chem.* **1969**, *68*, 324.
(378) Franck, E. U.; Hartmann, D.; Hensel, F. *Discuss. Faraday. Soc.* **1965**, *39*, 200.

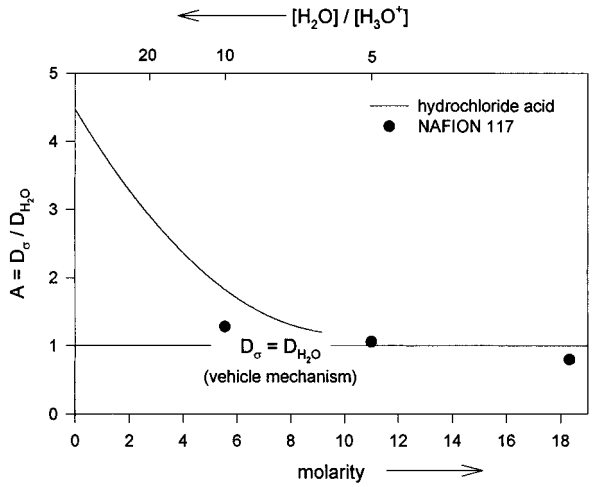

Figure 32. Ratio $A = D_\sigma/D_{H_2O}$ for aqueous solution of hydrochloric acid[27] and the hydrated polymer Nafion[91] as a function of the $[H_2O]/[H_3O^+]$ ratio.

of proton diffusivity also decreases under pressure.

The temperature and pressure dependence of A suggest that the coincidence of the rates of proton transfer and molecular diffusion is just a singularity for water under ambient conditions. In ice, the molecular diffusion is practically suppressed. The reorientation of water molecules, requiring an activation enthalpy of 0.68 eV[35] creates D-defects (two protons in one hydrogen bond) and L-defects (an empty hydrogen bond) thus violating the second Bernal−Fowler rule. Together with the highly activated translational defects creating protonic charge carriers (see section 5.3.2) this allows for the moderate proton conductivity in ice (Figure 3).

When the number of protonic charge carriers is increased in aqueous systems, proton transfer is progressively suppressed, i.e., protons preferentially diffuse as part of bigger species. This is probably due to increasing static solvent effects, i.e., an increasing biasing of hydrogen bonds originating from the presence of foreign ions.

The ratio $A = D_\sigma/D_{H_2O}$ for aqueous solutions of hydrochloric acid of different molarity is shown in Figure 32. It approaches unity (vehicle mechanism) for $[H_2O]/[H_3O^+] \sim 3$ corresponding to primary hydration of the hydronium ion.

Although the macroscopic water diffusion coefficient in the hydrated proton conducting polymer Nafion is distinctly lower than in solution, the ratio A lies close to the same line (Figure 32). Obviously, the dynamics on a molecular scale are similar to that in solution, where the macroscopic transport is reduced by the phase separated microstructure of Nafion.[91] This rather nonpolar polymer (the perfluorinated backbone has a very low dielectric constant) simply acts as an acidifying "container" for water without significantly interfering with the local water dynamics. In fact, the heat of water sublimation is almost identical with that of liquid water.[379]

Generally speaking, acidified water in a nonpolar host maintains its characteristic local structure and dynamics, i.e., its proton-transport properties are retained on a molecular scale. This observation may also be of particular relevance for proton transport in aqueous regions of certain biological structures.

(379) Escoubes, M.; Pineri, M. In ref 88, p 9.

In a polar host, however, a static solvent effect is induced into the water of hydration which shows up as an increased heat of hydration. This leads to a suppression of intermolecular proton transfer and molecular diffusion remains the only effective path for diffusion of protonic charge carriers. In particular, this holds for anisotropic, polar environments, like the layer structure $H_3OUO_2AsO_4 \cdot 3H_2O$, which is the solid proton conductor for which the vehicle mechanism was first established.[44] For the same reason, also proton transport along the particle surfaces of particle hydrates is anticipated to rely exclusively on molecular diffusion.

6. Applications

6.1. Proton Transport in Biological Systems. Nature was definitely the first to extensively "apply" proton transport. Most biochemical reactions are very sensitive to pH changes and proton transport serves as a vital route to cell pH stabilization.[380] Whereas information is generally transferred via metal ions in biological systems, all processes which convert energy from one form into another involve protonation and deprotonation reactions mediated by proton conductivity.[381] As the most prominent example, the role of proton conductivity in the formation of ATP (adenosine triphosphate) during photosynthesis should be briefly described. According to Mitchell's chemiosmotic theory,[382,383] a proton concentration gradient across a membrane can be utilized by a proton consumer (H^+ ATP synthase) to produce ATP, the universal storage device for energy required in every metabolic process of life.

This process has been extensively studied on the inner membrane of mitochondria and on the purple membrane of halobacteria which contain bacteriorhodopsin as the only trans-membrane protein (e.g., refs 384−386). This consists of a single polypeptide chain of 248 amino acids traversing the phospholipid bilayer. Photons are absorbed by a chromophore, the "antenna" retinal which is covalently linked via a protonated Schiff's base to lysin-216 of the protein moiety (Figure 33). During the photochemical cycle[385] one proton is vectorially translocated across the trans-membrane protein, thus creating a proton gradient between the cytoplasmotic and the extracellular side of the membrane. The structure of this "proton pump" down to the molecular level has been revealed by Dencher et al.[384] and the vibrational dynamics of the proton in all intermediates has been studied by Zundel.[387] Bacteriorhodopsin is shown as the insert of Figure 33, where hydrogen bonds are indicated by dashed lines and constitutional water molecules by dotted spheres. These form two hydrogen-bonded chains linked to the photoactive center, thus forming a possible pathway for proton transfer through the membrane. The

(380) Williams, R. J. P. *Annu. Rev. Biophys., Biophys. Chem.* **1988**, *17*, 71.
(381) Voet, D.; Voet, J. G. *Biochemistry*, John Willey & Sons: New York.
(382) Mitchell, P. *Nature* **1961**, *191*, 144.
(383) Nagle, J. F.; Tristram-Nagle, S. *J. Membr. Biol.* **1983**, *74*, 1.
(384) Dencher, N. A.; Heberle, J.; Büldt, G.; Höltje, H. D.; Höltje, M. In *Membrane Proteins: Structures Interactions and Models* Pullman, A.; et al., Eds., Kluwer Academic Publisher: 1992; p 69.
(385) Heberle, J.; Dencher, N. A. In *Proton Transfer in Hydrogen-Bonded Systems* Bountis, T., Ed.; Plenum Press: New York, 1992; p 187.
(386) Heberle, J.; Dencher, N. A. *Proc. Natl. Acad. Sci. U.S.A.* **1992**, *89*, 5996.
(387) Zundel, G. *J. Mol. Struct.* **1994**, *322*, 33.

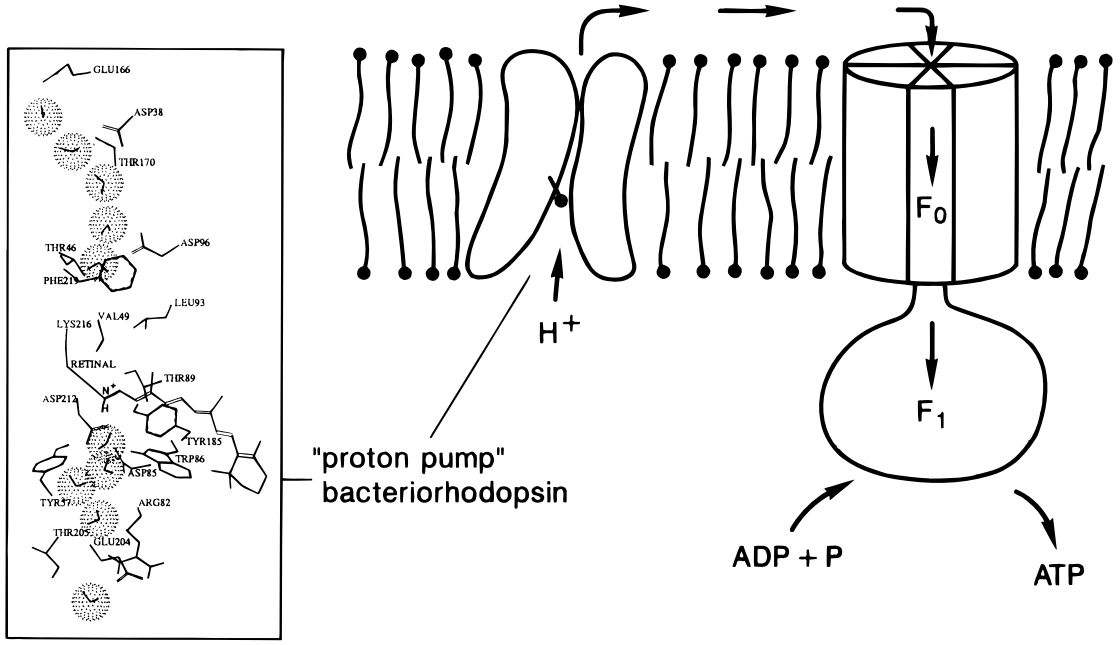

Figure 33. Schematic representation of the proton flux during the production of ATP. The molecular structure of the "proton pump" bacteriorhodopsin[384] is shown as insert (the author thanks N. A. Dencher for providing the drawing of the structure of bacteriorhodopsin).

proton mobility along the trans-membrane protein is significantly lower than in pure water with a total activation enthalpy of 0.52 eV.[388] Whether this energy corresponds to excitations in the water chain only or whether some conformational change of the protein backbone is involved in the proton translocation is not clear yet. The one-dimensional character of the water chains confined in the protein suggests the absence of strong solvent effects, which are typical for bulk water (see section 5.3.2). Whether this allows for collective proton-transfer phenomena along the chains is not yet clear however.

A change of the protein pK_A releases the proton at the cytoplasmotic side of the membrane.[381] Figure 33 also shows the protein complex F_0F_1 which is located in a different area of the membrane. F_0 provides another passive proton "channel" which allows the utilization of the proton activity gradient in the production of ATP at the enzymatic center of F_1 (e.g., refs 389 and 390). Details of the proton diffusion path along F_0 are still unknown. Most experimental results are in favor of the presence of polar groups (probably carboxyl groups) along the interior of F_0[381] which is hydrated to form a water "wire" similar to that of gramicidin.[391] Proton transport along that "wire" appears to be very sensitive to conformational changes of the surrounding proteins.[392]

There is an ongoing discussion as to whether protons reach F_0 through the intracellular aqueous bulk phase (delocalized theory) or whether their motion is restricted to the membrane surface (localized theory).[393,394] The latter has already been suggested by Haines,[395] and a recent picosecond-to-microsecond spectroscopic study seems to confirm this hypothesis. Heberle et al.[396] measured a highly retarded proton release from the purple membrane of halobacterium salinarium, whereas proton transport along the membrane surface was found to be much faster. This transport could be modelled assuming a diffusion coefficient of 3.4×10^{-7} cm^2 s^{-1}, which is even lower than the diffusion coefficient of water absorbed within a stack of purple membranes ($D = 4 \times 10^{-6}$ cm^2 s^{-1}).[397] This suggests that protonic charge transport along this membrane may occur via molecular diffusion (vehicle mechanism). This assumption is supported by the striking observation that many biological functions are dependent on the absorption of at least one monolayer of water.[398,399] But it has also been suggested that protons propagate along a hydrogen-bond net formed between the polar head groups and the first water layer.[387,394] The high buffer capacity of such surfaces,[400] which originates from the protonation/deprotonation capability of amino acids as well as the lipid head groups, may influence the effective concentration of protonic charge carriers in the aqueous near membrane region thus also affecting the proton flux.

It is interesting to note, that the principal scenario of proton transport in Nafion, one of the technologically most relevant membrane materials, almost resembles the situation of biological membranes (see also section 3.1). Acidic, hydrophilic headgroups ($-SO_3H$) on a hydrophobic backbone act as binding sites for water providing the environment for the efficient diffusivity of protons.

6.2. Technological Applications. Contrary to the central role of proton transport in life processes, energy

(388) Oesterhelt, D.; Tittor, J. *Trends Biochem. Sci.* **1989**, *14*, 57.
(389) Abrahams, J. P.; Leslie, A. G. W.; Lutter, R.; Walker, J. E. *Nature* **1994**, *370*, 621.
(390) Cross, R. L. *Nature* **1994**, *370*, 594.
(391) Akeson, M.; Deamer, D. W. *J. Biophys.* **1991**, *60*, 101.
(392) Monticello, R. A.; Brusilow, W. S. A. *J. Bacteriol.* **1994**, *176*, 1383.
(393) Antonenko, Y. N.; Kovbasnjuk, O. N.; Yaguzhinsky, L. S. *Biochim. Biophys. Acta* **1993**, *1150*, 45.
(394) Teissie, J.; Gabriel, G.; Prats, M. *TIBS* **1993**, *18*, 243.
(395) Haines, T. H. *Proc. Natl. Acad. Sci. U.S.A.* **1983**, *80*, 160.
(396) Heberle, J.; Riesle, J.; Thiedemann, G.; Oesterhelt, D.; Dencher, N. A. *Nature* **1994**, *370*, 379.
(397) Lechner, R. E.; Dencher, N. A.; Fitter, J.; Dippel, Th. *Solid State Ionics* **1994**, *70/71*, 296.
(398) Rupley, J. A.; Careri, G. *Adv. Protein Chem.* **1991**, *41*, 37.
(399) Settles, M.; Doster, W.; Kremer, F.; Post, F.; Schirmacher, W. *Philos. Mag.* **1992**, *B65*, 861 1992.
(400) Grzesiek, S.; Dencher, N. A. *Biophys. J.* **1986**, *50*, 265.

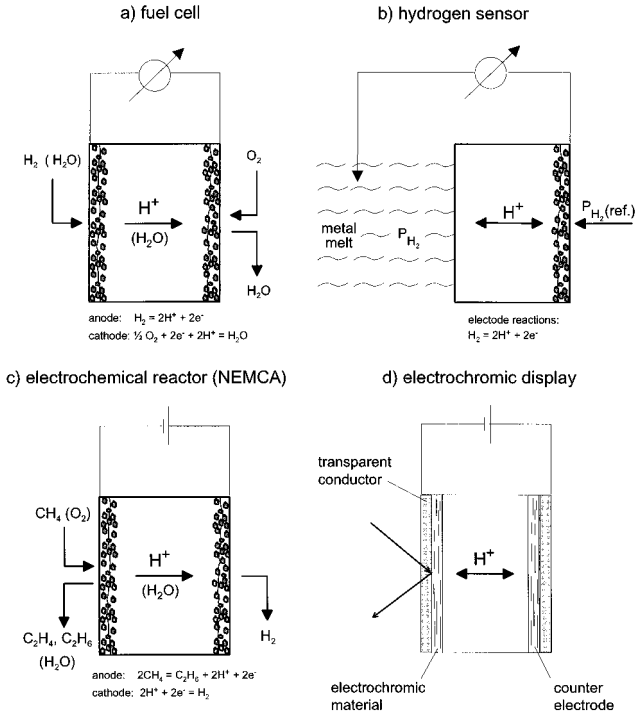

Figure 34. Schematic illustration of the application of proton conductors as separator material of electrochemical cells: (a) fuel (electrolysis) cell, (b) electrochemical hydrogen sensor, (c) electrochemical reactor, and (d) electrochromic display.

conversion and signal (information) transfer in most technological applications rely on electronic conductivity, either in metals or semiconductors. Since the early days of the industrial revolution, there have always been devices which depend on proton transport. Most conventional batteries rely on the proton conductivity of the corresponding aqueous electrolyte and at least some mixed conductivity (protonic and electronic) in the active electrode masses. So do many conventional gas sensors operating around room temperature. Even large-scale fuel cells with a power output in the MW range benefit from the high proton conductivity of phosphoric acid. Besides these traditional applications the progressive availability of solid proton-conducting materials stimulated the utilization of proton conduction in a variety of devices for energy conversion, chemical sensing, the production of chemicals, and electrochromic displays (Figure 34a−d).

It is the very nature of research that concepts are suggested regardless of their feasibility in a technological application such as the bizarre suggestion of ice-based devices.[401] In the following some selected concepts, which might potentially be applied in the near future, will be briefly presented.

6.2.1. Fuel and Electrolysis Cells. Stimulated by the aggravation of the legislative pollution control in most industrialized nations, activities in the development of batteries and fuel cells, i.e., devices directly converting chemical into electrical energy, have increased. It is the aim to avoid combustion processes with their inherent limits of thermodynamic efficiencies and their production of hazardous gases such as NO_x and CO.

The principal of hydrogen fuel cells based on proton-conducting separators is schematically illustrated in Figure 34a. Dry or wet hydrogen is fed in at the anode and pure oxygen or simply air at the cathode depending on whether proton transport in the separator is associated with water transport or not (see section 5.3). If the redox reactions taking place at the triple contacts of separator, gas phase, and the corresponding anode or cathode are reversible and there is no ohmic drop in the electrolyte (open-circuit conditions), the reversible potential difference E across the electrochemical cell directly corresponds to the Gibbs free energy of the overall reaction ($E = -\Delta G_r/zF$). Therefore, the energy efficiency for a reversibly operating fuel cell may be lower or higher than 100% depending on whether the reaction is accompanied by a negative or positive entropy change. Of course, in any real system under load there are irreversible losses due to electrode overpotentials and ohmic drops across the electrolyte. For state-of-the-art reports the reader is referred to refs 402 and 403.

Currently, the most investigated fuel-cell systems are proton-exchange membrane (PEM) based hydrogen fuel cells especially for transportation systems. So far, only hydrated perfluorinated ion-exchange membranes in their protonic form such as Nafion (see section 5.3) exhibit sufficient chemical, electrochemical and morphological stability for operation over several thousand hours under fuel cell conditions (temperatures up to 90 °C and energy densities up to 2 W cm^{-2}).[402,403] However, there are also activities to develop new proton conducting polymers, e.g., based on polyaromatic high-performance polymers. The water management in the hydrated electrolyte and within the heterogeneous gas electrodes as well as sufficient electrode reaction rates at the limited operation temperature are still problems of this type of fuel cell.[402,403]

At the operation temperature (∼70−90 °C), which is limited by the stability of the membrane, only rather pure hydrogen (CO < 10 ppm) can be used as a fuel and only noble metals as electrode materials. Hydrogen may be produced by reforming methanol on board, but there are also attempts to directly feed methanol to a fuel cell. This, however, requires a somewhat higher operation temperature (∼130 °C) and thus more stable membranes. Therefore, attempts are being made to substitute $-SO_3H$ as the acidic functional group by other groups (e.g., −COOH, $-PO_3H$) which are less sensitive to hydrolysis but also have a higher pK_A. The required morphological stability is hoped to be achieved by cross-linking and control of the polymer microstructure. Polymer-bonded particle hydrates based on tin mordenite, i.e., composite materials, reveal another interesting route to electrolyte materials for direct methanol fuel cells.[405,406] PEM fuel cells have been successfully applied in spacecraft and submarines. Their use in mass products, such as buses and cars, is currently being explored by several companies.

(401) Ryzhkin, I. A. In ref 19, p 523.

(402) Hirschenhofer, J. H.; Stauffer, D. B.; Engleman, R. R. *Fuel Cells, A Hanbbook*; U.S. Department of Energy, Gilbert/Commonwealth, Inc., 1994.
(403) *Proc. Fuel Cell Seminar*, San Diego Courtesy Associates, Inc., 1994.
(404) Zawodzinski, T. A.; Springer, T. E.; Davey, J.; Jestel, R.; Lopez, C.; Valerio, J.; Gottesfeld, S. *J. Electrochem. Soc.* **1993**, *140*, 1981.
(405) Lundsgaad, J. S.; Yde-Adersen, S.; Kjaer, J.; Knudsen, N. A.; Skou, E. *Proc. Electrochem. Soc.* **1992**, *92−14*, 131.
(406) Rao, N.; Andersen, T. P.; Ge, P. *Solid State Ionics* **1994**, *72*, 334.

Another fuel-cell technology under consideration is based on proton-conducting oxide ceramics.[407,408] Compared to solid oxide fuel cells (SOFC), they have the potential advantage that the fuel (e.g., H_2) is not polluted with the product of the electrochemical reaction (e.g., H_2O), and no electrochemical incorporation of oxygen into the electrolyte associated with high overpotentials is required. As opposed to PEM fuel cells the high operation temperature (500−800 °C) allows the use of electrode materials other than noble metals. However, the achieved current densities essentially limited by the proton conductivity of the electrolyte, are about one order of magnitude lower than for PEM fuel cells.

In addition, there are materials problems, which seem to be inherently associated with the high proton conductivity. As pointed out in section 5.1, high water solubility and high diffusivity of protonic defects is expected for basic oxides with high oxygen anharmonicity. High basicity, however, leads to thermodynamic instability toward reaction with acidic gases such as CO_2, SO_x, and NO_x which are present in air and most technical gases. High anharmonicities lead to high thermal expansion coefficients, which diminish the thermal shock resistance of the material. The oxides with the highest proton conductivity observed so far are $BaCeO_3$-based compounds. These are thermodynamically unstable against CO_2 under fuel-cell conditions[409] and their high thermal expansion coefficient ($\alpha \sim 7 \times 10^{-6}$ K^{-1}) leads to the formation of microcracks upon thermal cycling. Segregation and even phase separation have been shown to be another problem for $BaCeO_3$-based ceramics.[410] Thin film technologies of more stable but less conductive oxides may lead to a compromise between proton conductivity and stability within the requirements of fuel cells. In this respect, less basic niobates such as $Sr_3(Ca_{1+x}Nb_{2-x})O_{9-\delta}$ may be of particular interest. For these Nowick and Yang Du have recently reported high water solubilities and proton mobilities.[411]

The function of any fuel cell may be reversed in such a way that it operates, e.g., as an electrolysis or hydrogen isotope separation cell.[412] In many commercial electrolyzers, proton conducting polymer membranes are used as separators. Also H_3O β-aluminas have been suggested as separator materials.[413]

6.2.2. Electrochemical Sensors. Many sensors relying on acid/base reactions have a proton conductor as a separator.

In close analogy to the well-known oxygen probe based on yttria-stabilized zirconia, a potentiometric sensor for measuring hydrogen activities in aluminum melts based on indium-doped $CaZrO_3$ has been developed[414] and commercialized (Figure 34b).

Of course, any protonation/deprotonation reaction accompanying a change of the hydrogen activity may principally be utilized in similar sensors operating in the potentiometric, amperometric, or even more complex mode. The use of catalytically active electrodes may provide the desired selectivity for a given reaction.

Thus, sensors based on proton-conducting oxides have been suggested for the sensing of humidity,[415,416] of alkanes (methane, ethane, propane),[417] for alcohols (e.g., ethanol)[418] and even of CO_2.[419] They have recently been reviewed by Iwahara.[420]

Whereas such sensors operate at elevated temperature, a variety of sensors based on water-containing electrolytes operating at room temperature have been proposed. Sensors for CO, NH_3, O_2, H_2O_2, and even glucose, using hydrated antimony oxide as electrolyte have been reviewed by Miura and Yamazoe.[421] The coating of electrodes by hydrated proton-conducting polymers is also very popular. These have been used, e.g., in sensors utilizing enzymes for the detection of glucose[422−424] or cholesterol[425] or simply oxygen.[426]

Sensors based on "pellicular" zirconium phosphate have been tested for the detection of CO,[427] O_2,[428] and, of course, for H_2.[429] Sensors based on acid zirconium, phosphates, and phosphonates have recently been reviewed by Alberti, Casciola, and Palombari.[430]

Similar to the case for conventional electrochemical sensors, the development of electrocatalytically active electrode materials and their adaptation to particular applications will be a major part of the development of new sensors based on proton conductors. Especially the use of solid proton conductors provides access to reactions only taking place at sufficient rate at high temperature.

6.2.3. Electrochemical Reactors. It is near at hand to use proton-conducting separators to electrochemically "pump" hydrogen into or out of a reactor thus influencing or even controlling hydrogenation and dehydrogenation reactions.[431]

As schematically demonstrated by Figure 34c, ethane is converted into ethylene by dehydrogenation in a reactor using perovskite-type oxides as a proton conductor.[432,433] One may even "pump" out hydrogen from methane (CH_4) which eventually leads to the formation

(407) Iwahara, H.; Yajima, T.; Hibino, T.; Ushida, H. *J. Electrochem. Soc.* **1993**, *140*, 1687.
(408) Bonanos, N.; Ellis, B.; Mahmood, M. N. *Solid State Ionics* **1991**, *44*, 305.
(409) Scholten, M. J.; Schoonman, J.; van Mietenburg, J. C.; Oonk, H. A. J. *Solid State Ionics* **1993**, *61*, 83.
(410) Kreuer, K. D.; Schönherr, E.; Maier, J. *Proc. 14th Riso Intern. Symp. on Materials Science Roskilde* **1993**, 297.
(411) Iwahara, H. In ref 19, p 511.
(412) Nicholson, P. S. In ref 19, p 499.
(413) Munshi, M. Z. A.; Nicholson, P. S. *Solid State Ionics* **1990**, *42*, 63.
(414) Yajima, T.; Koide, K.; Fukatsu, N.; Ohashi, T.; Iwahara, H. *Sensors Actuators* **1993**, *B13−14*, 697.
(415) Yajima, T.; Iwahara, H.; Koide, K.; Yamamoto, K. *Sensors Actuators* **1991**, *B5*, 145.
(416) Iwahara, H. *Kagaku Kogyo* **1993**, *44*, 846.
(417) Iwahara, H.; Hibino, T. *Proc. Electrochem. Soc.* **1993**, *93−7*, 464.
(418) Hibino, T.; Iwahara, H. *Chem. Lett.* **1992**, 1225.
(419) Hibino, T.; Iwahara, H. *Chem. Lett.* **1992**, 1221.
(420) Iwahara, H. *Solid State Ionics* **1995**, *77*, 289.
(421) Miura, N.; Yamazoe, N. *Solid State Ionics* **1992**, *53−56*, 975.
(422) Wang, J. *Talanta* **1994**, *41*, 857.
(423) Moatti-Sirat, D.; Poitout, V.; Thome, V.; Gangnerau, M. N.; Zhang, Y.; Hu, Y.; Wilson, G. S. Lemonnier, F.; Klein, J. C.; Reach, G. *Diabetologia* **1994**, *37*, 610.
(424) Moussy, F.; Jakeway, S.; Harrison, D.; Rajotte, R. V. *Anal. Chem.* **1994**, *66*, 3882.
(425) Jin, L. T.; Zhao, G. Z.; Fang, Y. Z. Chin, *J. Chem.* **1994**, *12*, 343 1994.
(426) Kuwata, S.; Miura, N.; Yamazoe, N. *Chem. Lett.* **1988**, 1197.
(427) Alberti, G.; Casciola, M.; Palombari, R. *Solid State Ionics* **1993**, *61*, 241.
(428) Alberti, G.; Casciola, M.; Palombari, R. *Solid State Ionics* **1992**, *52*, 291.
(429) De Angelis, L.; Maimone, A.; Modica, L.; Alberti, G.; Palombari, R. *Sensors Actuators* **1990**, *B1*, 121.
(430) Alberti, G.; Casciola, M.; Palombari, R. *Elektrokhimiya* **1993**, *29*, 1436.
(431) Chowdari, B. V. R., ed.: *Solid State Ionics: Materials and Applications*; World Science: Singapore, 1992; p 247.
(432) Iwahara, H.; Esaka, T.; Uchida, H.; Yamauchi, T.; Ogaki, K. Solid State Ionics **1986**, *18/19*,1003.
(433) Hibino, T.; S. Hamakawa, S.; H. Iwahara, H. *J. Chem. Soc. Jpn.* **1993**, 238.

of C_2 compounds (C_2H_4, C_2H_6).[434−437] The reaction rate has been suggested to be limited by the abstraction of hydrogen from methane to form methyl radicals as precursors of C_2 compounds.[438] The rate of such reactions are usually not faradaic, i.e., it does not equal the protonic current through the separator. In many cases the reaction rate even exceeds the protonic current significantly. As indicated by the acronyn NEMCA (nonfaradaic electrochemical modification of catalytic activity) this effect is ascribed to the modification of the catalytic activity of the electrode, at which the reaction takes place. In such cases not only the proton conductor but also other chemical agents (e.g., oxygen) in the reactor gas act as a sink for hydrogen. The effect of the protonic current is to lower the energy of unfavored intermediates rather than acting as a sink for protons as one of the reaction products. In fact, it is not the protonic current directly affecting the reaction rate but the corresponding anodic overpotential (e.g., ref 449) which is exponentially enhancing the reaction rate. This behavior is reminescent of the Tafel behavior, i.e., the approximation of the Butler−Volmer equation for high electrode overpotentials (>100 mV) (e.g., ref 439), thus underlining the similarities of electrochemistry and heterogeneous catalysis.[440]

NEMCA effects observed so far in dehydrogenation reactions using proton conductors are rather small compared to that of the oxidation reactions via oxygen "pumping" using solid oxide ion conductors, for which NEMCA was observed first.[441]

6.2.4. Electrochromic Devices. There have been extensive activities in the development of electrochromic devices (displays, windows, mirrors) based on solid fast ionic conductors also including proton conductors, which have recently been reviewed by Bohnke.[442]

Figure 34d schematically represents an electrochromic display which is essentially a reversible hydrogen "pump" allowing electrochemical hydrogenization and dehydrogenization of an electrochromic layer, which responds with coloration and bleaching, respectively.

For the cathodic electrochromic material, metal organic compounds such as rare-earth phthalocyanines[443−445] or inorganic hydrogen intercalation compounds such as WO_3 and MoO_3 are widely used. Especially in electrochromic windows the latter are frequently used with another electrochromic material as counterelectrode which show anodic coloration such as Prussian blue,[446] iridium oxide,[447] or polyaniline.[448] As a proton-conducting separator, mostly hydrated materials (see section 3.1.) were employed initially. They allow for high proton conductivities and good contacts between the separator and the electrochromic layer. Although irreversible changes of the electrochromic layer under the respective water activities (e.g., hydration, dissolution) did limit the long-term stability initially, today more advanced systems allow for more than 10^7 cycles and a lifetime of more than 5 years.[449]

The use of water free electrolytes with high proton conductivity, such as the blend Paam·$1.2H_2SO_4$[447] offer another interesting way to overcome the problem of irreversible side reactions.

Other microdevices currently being developed are supercapacitors[450−452] and all solid-state batteries.[453,454]

Acknowledgment. The author thanks A. Fuchs and U. Traub for making the layout and M. Bernasconi, Y. Kershaw, M. Münch, and H. J. Schlüter for reading the proofs.

CM950192A

(434) Hamakawa, S.; Hibino, T.; Iwahara, H. *J. Electrochem. Soc.* **1993**, *140*, 459.
(435) Eng, D.; Stoukides, M. *Catal. Rev.-Sci. Eng.* ***1991***, *33*, 375.
(436) Chiang, P. H.; Eng, D.; Stoukides, M. *Solid State Ionics* **1993**, *61*, 99.
(437) Chiang, P. H.; Eng, D.; Stoukides, M. *Solid State Ionics* **1994**, *67*, 179.
(438) Chiang, P. H.; Eng, D.; Panagiotis, P.; Stoukides, M. *Solid State Ionics* **1995**, *77*, 305.
(439) Bockris, J. O'M.; Reddy, A. K. N. *Modern Electrochemistry*; Plenum Press: New York, 1970.
(440) Vayenas, C. G.; Bebelis, S.; Yentekakis, I. V.; Lintz, H. G. *Catal. Today.* **1992**, *11*, 303.
(441) Stoukides, M.; Vayenas, C. G. *J. Catal.* **1981**, *70*, 137.
(442) Bohnke, O. In ref 19, p 551.
(443) Moskalev, P. N.; Kirin, I. S. *Opt. Spektrosk.* **1970**, *29*, 414.
(444) Nicholson, M. M.; Pizarello, F. A. *J. Electrochem. Soc.* **1981**, *128*, 1740.
(445) Samuels, A. F.; Pujare, N. U. *J. Electrochem. Soc.* **1986**, *133*, 1065.
(446) Ho, K. C.; Rukavina, T. G.; Greenberg, C. B. *J. Electrochem. Soc.* **1994**, *141*, 2061.
(447) Rodriguez, D.; Jegat, C.; Trinquet, O.; Grondin, J.; Lassegues, J. C *Solid State Ionics* **1993**, *61*, 195.
(448) Akhtar, M.; Weakliem, H. A. *Proc. Electrochem. Soc.* **1990**, *90−2*, 232.
(449) Vaivars, G.; Kleperis, J.; Lusis, A. *Solid State Ionics* **1993**, *61*, 317.
(450) Colomban, Ph.; Pham-Thi, M. In ref 19, p 567.
(451) Lassègues, J. C.; Grodin, J.; Becker, T.; Hernandez, M. *Solid State Ionics* **1995**, *77*, 311.
(452) Sarangapani, S.; Forchione, J.; Griffith, A.; LaConti, A. B.; Baldwin, R. *J. Power Sources* **1991**, *36*, 341.
(453) Guitton, J.; Poinsignon, C.; Sanchez, J. Y. In ref 19, p 539.
(454) Kuriyama, N.; Sakai, T.; Miyamura, H.; Ishikawa, H. *Solid State Ionics* **1992**, *53*, 688.